The following manuscript was unavailable at time of publication.

IEA - FULL FUEL CYCLE STUDY

Dr. Perry Bergman
U.S. Department of Energy
Pittsburgh Energy Technology Center
P.O. Box 10940, M.S. 922-247A
Pittsburgh, PA 15236

Please contact author(s) for a copy of this paper.

THE USE OF FLUE GAS FOR THE GROWTH OF MICROALGAL BIOMASS

KATHRYN G. ZEILER
KIRAN L. KADAM
DANA A. HEACOX
DAVID W. KERBAUGH
JOHN J. SHEEHAN

NATIONAL RENEWABLE ENERGY LABORATORY
1617 COLE BLVD., GOLDEN, CO 80401

ABSTRACT - Capture and utilization of carbon dioxide (CO_2) by microalgae is a promising technology to help reduce emissions from fossil fuel-fired power plants. Microalgae are of particular interest because of their rapid growth rates and tolerance to varying environmental conditions. Laboratory work is directed toward investigating the effects of simulated flue gas on microalgae, while engineering studies have focused on the economics of the technology. One strain of a green algae, *Monoraphidium minutum* , has shown excellent tolerance and growth when exposed to simulated flue gas which meets the requirements of the 1990 Clean Air Act Amendments (1990 CAAA). Biomass concentrations of ~2g/L have been measured in batch culture. Several other microalgae have also shown tolerance to simulated flue gas; however, the growth of these strains is not equivalent to that observed for *M. minutum*. Coupling the production of biodiesel or other microalgae-derived commodity chemicals with the use of flue gas carbon dioxide is potentially a zero-cost method of reducing the amount of carbon dioxide contributed to the atmosphere by fossil fuel-fired power plants. We have identified two major biological performance parameters which can provide sufficient improvement in this technology to render it cost-competitive with other existing CO_2 mitigation technologies. These are algal growth rate and lipid content. An updated economic analysis shows that growth rate is the more important of the two, and should be the focus of near term research activities. The long term goal of achieving zero cost will require other, non-biological, improvements in the process.

INTRODUCTION - Anthropogenic emissions of CO_2 are estimated to be 2×10^{10} metric tons/y, primarily from combustion of fossil fuels. In addition, the increasing global population pushes the demand for economical energy sources higher every year. Contrasted with its potential for harm is the value of CO_2. It is the source of carbon for photosynthesis, without which there would not be life on earth as we know it today. Carbon dioxide is a valuable resource for many of man's activities including enhanced oil and gas recovery, urea production, and food processing and beverage carbonation[1]. These activities and others of similar nature, however, can use only a very small percentage of the total CO_2 emissions from fossil fuel combustion.

Using CO_2 from fossil fuel combustion as a feedstock for photosynthetic microorganisms can provide a large sink for carbon assimilation. Microalgae are the most productive CO_2 users, with yields of biomass per acre threefold to fivefold greater than those from typical crop plant acreage[2]. Earlier studies[3-5] have discussed the potential applications of power plant flue gas to microalgal farming. Experimental data are needed to determine the feasibility of this technology. The work presented here discusses the current efforts at the National Renewable Energy Laboratory (NREL) toward deployment of this technology.

Research at NREL on microalgal technology has two major focuses. The culture studies described in this paper represent the work we are doing to develop technology for CO_2 trapping from power plant flue gas. The second, and related work, involves the development of genetically engineered algae capable of producing high levels of lipids for use in the production of biodiesel. The success of this technology depends on good coordination between these two efforts. This work is a good example of leveraged research between the Fossil Energy side of DOE and its Renewable Energy counterpart.

CULTURE STUDIES - Initial studies were carried out using a green alga, *Monoraphidium minutum* (NREL Strain Monor02). Particular emphasis was placed on the gas delivery apparatus, as efficient dosing of the flue gas is crucial to successful growth. Mass culture facilities typically provide CO_2 "on demand" as determined by pH of the culture. Appropriate dosing allows efficient utilization of the introduced carbon; which is important because the efficiency of CO_2 utilization will have a significant impact on process economics. Previous studies showed that exposing cultures to continuous dosing with simulated flue gas resulted in no evidence of growth or viability of the culture[6]. The experiments described here examine the effect of simulated flue gas containing 1990 CAAA levels of sulfur and nitrogen oxides on culture growth and biomass accumulation as a measure of carbon assimilation. The simulated flue gas contained 0.015% NO, 0.02% SO_2, 5% O_2, 13.6% CO_2, with the balance N_2. The control gas contained 13.6% CO_2, 5% O_2, with the balance N_2. Cultures were inoculated at $\geq 10^5$ cells/mL into a final culture volume of 300 mL (10% artificial sea water[7]). Light was provided continuously by Cool White® fluorescent bulbs at an intensity of ~200 uE $m^{-2}s^{-1}$. The cultures were continuously stirred with a magnetic stirrer at 150 rpm and the temperature was maintained at 25°C.

In the initial experiments, the cultures were exposed to either simulated flue gas or control gas delivered in three equal doses during an 8-h period each day. The flow rate in these studies was 60 mL/min at STP. Rate of growth, biomass accumulation, chlorophyll concentration, and pH were measured. In subsequent work the dosing rate was changed to determine if the carbon delivery scheme was limiting culture growth. The same total amount of carbon was delivered; however, the flow rate was decreased to 15 mL/min (at STP) in 2-min intervals 55 times during the 24-h period. Unlike the continuous sparging results, the two schemes for intermittent dosing of flue gas result in reasonable (and equivalent) growth. Figure 1 illustrates that there was no significant change in the rate of growth or total number of cells compared to the initial delivery schedule, suggesting that, over this range of flow rates, instantaneous carbon delivery rate is not limiting.

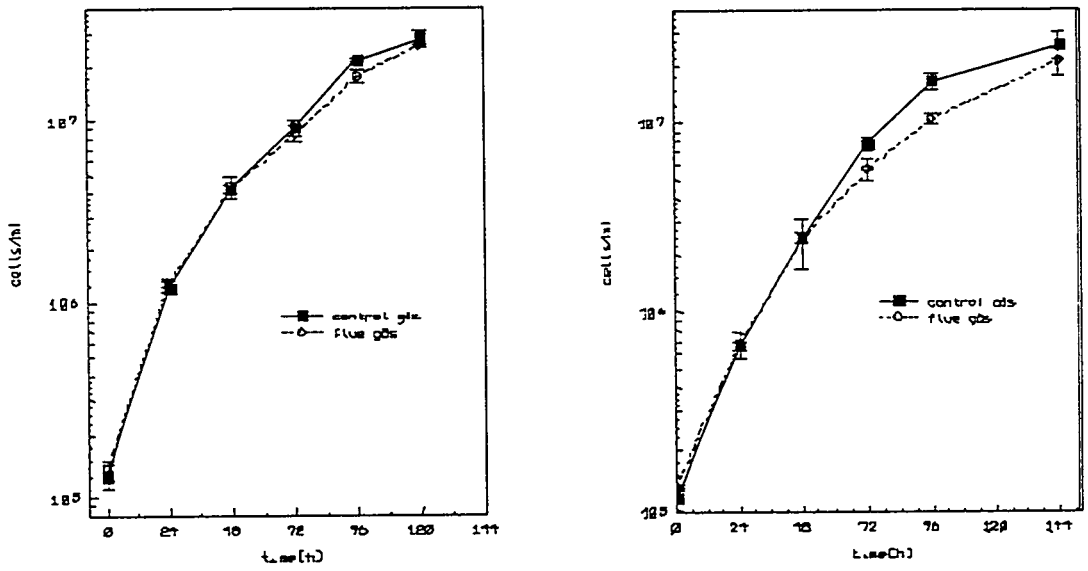

Figure 1. Comparison of cultures exposed to either 1990 CAAA simulated flue gas or control gas at 60 mL/min (at STP) three times per 24 h (left panel) or at 15 mL/min (at STP) 55 times per 24 h (right panel).

There is no significant difference in the rate of growth between cultures exposed to simulated flue gas and those exposed to control gas. These data indicate that 150 ppm NO and 200 ppm SO_2 do not inhibit culture growth under these conditions. Many of these experiments were carried out for as long as two weeks without evidence of inhibition. This is particularly encouraging because an accumulation of acidic sulfur species in the media could inhibit growth. Measurements of pH during the course of the experiment indicate that pH rises as biomass increases (data not shown). Early in the experiments, when biomass is low, the pH-lowering effect of the exposure to the gases is more significant even though the medium is buffered. The pH profile of media (that does not contain biomass) sparged with simulated flue gas or control gas does not exhibit this increase in pH in later time points (data not shown).

In the next series of experiments, the gas delivery and all other experimental conditions were as described above (using the 55 dose-per-day delivery scheme) except that the nitrogen concentration was increased threefold and the phosphorus concentration sixfold. Cell number, biomass and chlorophyll concentration increased dramatically at these higher nutrient levels (see Table 1).

	Low Nutrients 1.76 mM nitrate 36 μM phosphate		**High Nutrients** 5.28 mM nitrate 217 μM phosphate	
Measured Parameter	**Control Gas**	**Flue Gas**	**Control Gas**	**Flue Gas**
Ash-free Dry Weight (g/L)	1.32 ±0.0006	1.25 ±0.031	1.88 ±0.031	1.70 ±0.0474
chlorophyll (ug/mL)	7.40 ±0.087	9.08 ±0.308	39.17 ±0.662	41.39 ±0.345
cell number (x 10^7)	3	3	10	9

Table 1. Comparison of the effect of increased nitrogen and phosphorus on growth, biomass and chlorophyll concentrations for cultures exposed to either simulated flue gas or control gas (sparging was at 15 mL/min for 2 min., 55 times per 24 h).

The impact of these findings is that changes in the culture medium result in highly significant increases in the amount of carbon assimilated as reflected by fixation into biomass. Elemental analysis has shown these cells are approximately 50% C (data not shown). Based on the amount of carbon the cells were exposed to, we can estimate that at least 50% of the carbon supplied to the cultures has been fixed into biomass (data not shown). This is a high efficiency of utilization for a system which has not been optimized for maximum assimilation.

ECONOMIC MODEL - A spreadsheet-based (Microsoft Excel 5.0) economic model was developed for biological trapping of CO_2 from flue gases using microalgae. The rationale behind this approach was that a spreadsheet-based model is compliant and easy to manipulate. Information from the report by Neenan *et al.*[2] was used to develop a design basis for a "base case" process.

The model's consistency was judged to be satisfactory as the $400./t base-case algae cost is within 2% of that reported by Neenan *et al.* for the same "base case.".

The base-case process represents only the current state of technology; the "improved process" illustrates the potential that can be reached with some efforts devoted to research and development. An improved-case design basis was developed based on improvements potentially achievable in the near term. Table 2 provides a comparison of the two cases in terms of process parameters and cost performance in 1994 dollars. Table 3 summarizes the design parameters characterizing the improved process.

Table 2. Comparison of the Base Case Process and Improved Process (1994 $)

	Base Case Process	Improved process
Cell concentration, g/L	0.8	1.2
Lipid content, % wt	30	50
Residence time, d	7	4
Operating season, d/yr	250	300
Productivity, $g/m^2/d$	17.1	45
Photosynthetic efficiency, %	4.9	14.6
Algae cost, $/t	441.6	259.5
Lipid cost, $/bbl, $/gal (unextracted)	205.8 / 4.90	72.5 / 1.73
Lipid cost, $/bbl, $/gal w/ CO_2 credit[1] (unextracted)	170.4 / 4.06	45.2 / 1.08
CO_2 cost, % of annual cost	22.8	49.8
CO_2 mitigation cost[2], $/t CO_2	216.8	45.6

[1]CO_2 credit = $50/t CO_2
[2]Based on credit at the following rate: lipid = $240/t, protein = $120/t, carbohydrate = $120/t

Model Predictions - The updated model allows us to make some observations about the process. This model demonstrates in quantitative terms that our targeted improvements for productivity and lipid content more than double the relative impact of CO_2 collection cost on total annualized cost of the technology (see Table 2). Thus, cost-effective CO_2 collection and efficient delivery and utilization of CO_2 is even more important for the improved process. Accurate estimates for the cost of CO_2 collection are now being developed in order to provide a clearer understanding of this major cost component.

Model predictions were also used to compare the microalgal technology with alternative technologies for CO_2 mitigation costs. For an assumed cost of $66/t for CO_2 collection, the overall CO_2 mitigation cost for microalgal technology is $45.6/t for a targeted lipid content of 50% and a cell productivity of 45 $g/m^2/d$. This cost is competitive with other CO_2 remediation methods being proposed such as absorption with MEA (monoethanolamine).[8] Hence, deployment of this technology for CO_2 mitigation looks attractive if the parameters of the improved process are met. This assumes that there will be a market demand for CO_2 mitigation technology per se, which may not be generally true beyond limited niche situations. For this reason, our long term goal for the technology is to achieve zero cost for CO_2 mitigation. The current model will be used (and expanded) to assess the most effective engineering research directions to pursue towards this goal.

Table 3. Design Parameters for the Improved Process

			Source of Value
Facility Parameters			
Facility size	ha	1000	Neenan, p. 43
Module size	ha	20	Neenan, p. 53
Number of modules		43	Calculated
Total CO_2 processed	mt/yr	178284	Calculated from mass balance
Effective culture area fraction		0.86	Neenan, p. 53
Resource Parameters			
Land cost	$/ha	1420	Adjusted to 1994 (Neenan, p. 53)
Energy cost	$/kwh	0.065	Neenan, p. 53, assumed unchanged
Water cost	$/m^3	0.067	Neenan, p. 53, assumed unchanged
CO_2 cost	$/m^3	0.13	Adjusted to 1994 (Neenan model)
Evaporation rate	m/d	0.0035	Neenan, p. 53
Salinity of source water	g TDS/L	25	Neenan, p. 53
Biological Parameters			
Lipid content	wt. fr. dsb	0.5	Assumed
Protein content	wt. fr. dsb	0.2	Assumed
Carbohydrate content	wt. fr. dsb	0.12	Assumed
Ash content	wt. fr. dsb	0.08	Neenan, p. 54
Intermediate content	wt. fr. dsb	0.10	Neenan, p. 54
Solar radiation	kcal/m^2/d	5000	Neenan model, ref.dat
Photosynthetic efficiency	%	14.6	Calculated, Neenan p. 107
Salinity tolerance	g TDS/L	35	Neenan, p. 54
Operating Parameters			
Operating season	d/yr	300	Assumed
Cell concentration	g dcw/L	1.2	Assumed
Residence time	d	4	Assumed
Productivity	g/m^2/d	45.0	Calculated
Algal production, gross	mt/y	94041	Calculated
Lipid production, gross	mt/y	47021	Calculated
Downstream Processing Parameters			
Concentration factor, 1st stage, microstrainers		10	Neenan, p. 49
Concentration factor, 2nd stage, centrifuges		15	Neenan, p. 49
Concentration factor, overall		150	Calculated
Harvest efficiency, overall		0.95	Neenan model, ref.dat

Sensitivity Analysis - The economic model was used to study the effects of some key parameters on the process. CO_2 collection cost, lipid content, and residence time were selected for the sensitivity analysis due to their potential impact on process economics. Figure 2 shows the sensitivity of CO_2 mitigation cost to lipid content and CO_2 collection costs for the improved process. Utilization of algal biomass determines the economics of algal technology for CO_2 remediation. Algal biomass can be burned with coal or algal lipids can be extracted and converted to biodiesel. The higher specific energy of lipids is a benefit in co-burning. The desirability of higher lipid content is obvious if the algal biomass is to be used as a biodiesel feedstock. Thus, high lipid content confers a significant economic benefit to the process. In this model, credits are assumed for the value of lipids used for biodiesel manufacture and for the value of remaining carbohydrate and protein byproducts.

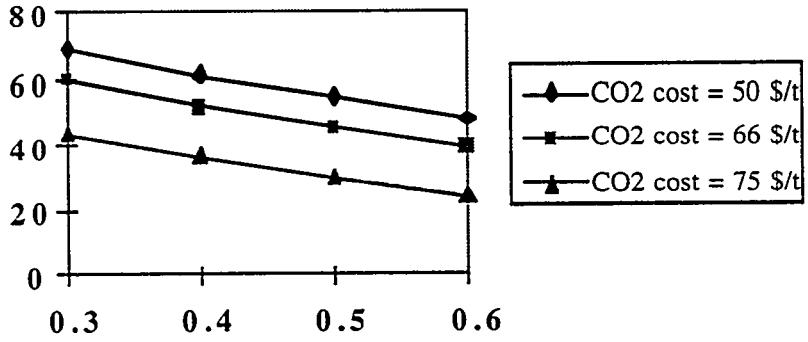

Figure 2. CO_2 mitigation costs ($/mt CO_2) at different lipid fractions and CO_2 Collection Costs.

Figure 3 shows the effect of dilution rate on CO_2 mitigation costs at different lipid fractions. The dilution rate, which is an inverse of the residence time and is directly related to biomass growth rate, determines the throughput at a given pond volume. As is evident from Figure 2, CO_2 mitigation costs rise precipitously at lower dilution rates. Hence, operating at a relatively high growth rate is important for an economical process. While there is an ability to trade off increases in growth rate for increases in lipid content, it is clear that increasing growth rate should be a research priority because of its strong impact on overall cost.

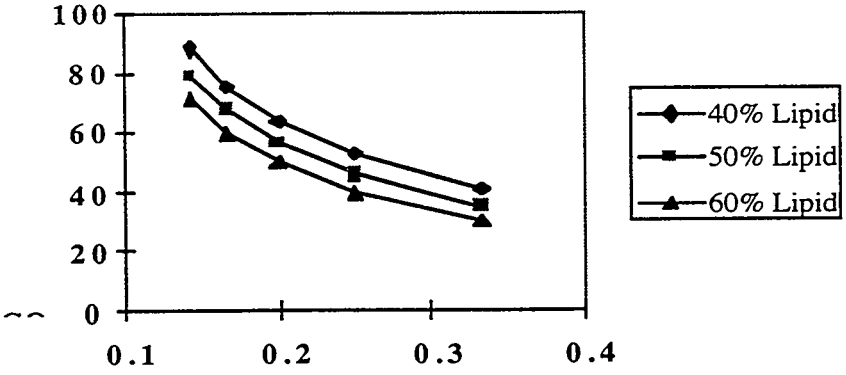

Figure 3. CO_2 mitigation costs ($/mt of CO_2) at different dilution rates and lipid fractions.

FUTURE TECHNICAL WORK - To date, we have identified one strain of green algae with relatively good growth rates, even in the presence of pollutants found in a simulated flue gas. Nutrient levels are also an issue. The two sets of experiments run at different levels of nitrogen and phosphorus demonstrate the effect of nutrient levels on CO_2 assimilation and cell growth. Further studies are needed to optimize nutrient levels based on a balance between nutrient supply costs and improved performance. The combined results of our experimental and economic analysis point toward an immediate need to develop high growth rate algae. We need to expand the range of organisms available for this application, and develop a clearer understanding of how to optimize growth rates of these organisms in order to achieve the goals identified in the economic analysis. In the mean time, efforts to develop genetically engineered strains capable of high lipid production also need to continue. Finally, as part of our effort to reach a long term goal of zero cost, we need to develop new process options beyond those used in the current economic model.

A STRATEGIC PERSPECTIVE - In addition to understanding the steps required for technology improvement, we are continually reassessing the broader, strategic perspective for microalgal technology which considers both internal and external factors that can influence our progress. For the purposes of this discussion, internal factors are the kind of technology-related issues discussed in the first paragraph. External factors are often overlooked in planning research strategies. They run the gamut from political issues to environmental and economic concerns. External factors which present obstacles for the development of microalgal trapping of CO_2 include:

- a utility industry focused almost exclusively on cost competitiveness in light of future increased deregulation
- continued uncertainty about the effects of greenhouse gases
- political pressure against "unfunded federal mandates" and general downsizing of government

On the positive side, opportunities include:

- a long term need for domestic transportation fuels and an increased use of coal
- a developing market for biodiesel in the U.S. as an outlet for microalgal products
- niche opportunities with more forward-thinking companies already exploring options for CO_2 mitigation
- spin-off opportunities in the growing plant biotechnology industry

Our approach, based on this strategic analysis, represents a balance between near term and long term concerns. In the past year, we have initiated R&D support to develop near term higher value niche opportunities for biodiesel, and for possible high value spin-offs from our algal technology development program. We are seeking out strategic partnerships in industry (including utilities, plant biotech companies, biodiesel start-up companies and others) to accelerate research progress and to leverage limited government funds. In the end, we need to balance these activities with our long term goal of providing a "no regrets" option for CO_2 mitigation and for meeting the needs of the transportation sector for domestic, renewable sources of fuels.

ACKNOWLEDGMENTS

The culture studies and economic analysis presented are being funded by the Department of Energy's Pittsburgh Energy Technology Center. Biodiesel and lipid genetics work are being supported by the Department of Energy's Biofuels Systems Division in the Office of

Transportation Technologies. We would like to acknowledge the contributions of Dr. Lewis Brown, formerly of NREL.

REFERENCES

1. C. R. Pauley, The Dow Chemical Co., *Chem. Eng. Prog.* (May 1984).
2. B. Neenan, D. Feinberg, A. Hill, R. McIntosh and K. Terry, **SERI/SP-231-2550**, Solar Energy Research Institute, Golden, CO, 149 (1986).
3. L. M. Brown and K. G. Zeiler, *Energy Convers. Mgmt* Vol. 34, No. 9-11, 1005-1013 (1993).
4. P. L. Chelf, L. M. Brown and C. E. Wyman, *Biomass and Bioenergy* Vol. 4, No. 3, 175-183 (1993).
5. E. A. Laws and J. L. Berning, *Biotech. and Bioengineering*, Vol. 37, 936-947 (1991).
6. J. T. Hauck, G. J. Olson and M. B. Perry, *Proceedings* from Ninth Annual Coal Preparation, Utilization and Environmental Control Contractors Conference, **U.S. DOE**, (1993).
7. L. M. Brown, *Phycologia*, **21**:408-410 (1982).
8. H. J. Herzog, Paper no. 94-RA113.02, Proc. 87th Air & Waste Manage. Assoc. Ann. Mtg. & Exhibit., Cincinnati, Ohio, 1994.

Observations of CO_2 Clathrate Hydrate Formation and Dissolution Under Deep-Ocean Disposal Conditions[1]

Robert P. Warzinski and Anthony V. Cugini
U.S. Department of Energy
Pittsburgh Energy Technology Center
Pittsburgh, PA 15236

Gerald D. Holder
Department of Chemical Engineering
University of Pittsburgh
Pittsburgh, PA 15261

1. INTRODUCTION

Disposal of anthropogenic emissions of CO_2 may be required to mitigate rises in atmospheric levels of this greenhouse gas if other measures are ineffective and the worst global warming scenarios begin to occur. Long-term storage of large quantities of CO_2 has been proposed, but the feasibility of large land and ocean disposal options remains to be established [1].

Determining the fate of liquid CO_2 injected into the ocean at depths greater than 500 m is complicated by uncertainties associated with the physical behavior of CO_2 under these conditions, in particular the possible formation of the ice-like CO_2 clathrate hydrate [1]. Resolving this issue is key to establishing the technical feasibility of this option. Experimental and theoretical work in this area is reported.

2. EXPERIMENTAL

Observations of the CO_2/water system were conducted in a high-pressure, variable-volume view cell. A description of the view-cell system as used in other work at temperatures above ambient has been published [2]. Modifications were made to permit the system to operate at temperatures in the hydrate forming region of interest (0°C to 10°C). The modifications included the incorporation of a cooling coil in the chamber containing the view cell, a small fan for improved air circulation in the chamber, and additional insulation.

Either potable water or water treated by reverse osmosis and deionization was used. CO_2 was obtained as a liquefied gas (99.5%) and used as received. In most experiments, water was first added to the cell then CO_2 was added either directly from the cylinder or from a high-pressure ISCO 260D syringe pump system. The cell was then chilled to the desired temperature and observations initiated. The pressure in the cell was varied during an experiment either by adding or venting CO_2 or by changing the position of a movable piston in the cell. Four phases are possible in this system: liquid water, gaseous CO_2, liquid CO_2, and solid CO_2 clathrate hydrate.

---

[1]This paper has been submitted and accepted for publication by Elsevier Science as part of the Proceedings of the 8th International Conference on Coal Science which is being held in Oviedo, Spain on September 10-15, 1995. Editors are J.A. Pajares and J.M.D. Tascón.

3. RESULTS AND DISCUSSION

Obtaining kinetic data applicable to the formation and decomposition of CO_2 hydrates under conditions that exactly simulate the deep ocean is not possible in the view cell or any similar device owing to contact of the CO_2 with metallic and glass surfaces. These surfaces promote nucleation and conduct heat differently than water and would therefore affect hydrate formation and dissolution. We are in the process of developing a system that precludes these problems. Described below are results obtained from experiments in the view cell that focused primarily on obtaining information that would provide important insights into the general behavior of the CO_2/water system under conditions anticipated for ocean disposal.

3.1 Phase behavior

The phase behavior of the CO_2/water system and the thermodynamic conditions for hydrate equilibrium have been determined [3]. The operation of the view cell was verified with this system by comparing the observed temperatures and pressures associated with hydrate formation and decomposition with the literature values. In these experiments, the conditions in the view cell were adjusted to obtain a lower water phase containing solid hydrates and an upper gaseous CO_2 phase. The presence of hydrates in the water phase provided nucleation sites for further hydrate growth. The amount of CO_2 in the cell and the position of the internal piston were adjusted to place the gas/liquid interface at a position convenient for observation. The pressure in the view cell was brought close to the value at which hydrate formation was anticipated. The pressure was then varied by small movements of the piston to cause additional hydrate to begin to either form or decompose at the CO_2/water interface. Phase changes could be detected with a pressure change of only 7.0 KPa, which was essentially the readability of the Heise gauge in use at this time. The pressures observed at the phase transition were near the literature values. For example, the phase transition occurred in the view cell at 3.06 MPa at 7.4°C to 7.5°C. The literature value was 3.08 MPa at 7.45°C [3].

3.2 Hydrate density

Pure CO_2 hydrates are denser than water or sea water and should sink [4]. Apart from any adverse ecological effects, this would be viewed as a benefit since it could result in very long CO_2 residence times in the ocean. However, some experimental accounts report that CO_2 hydrates float on the surface of water or seawater [5,6]. To help resolve this issue, observations were made of the relative densities of hydrates formed under various conditions in the view cell.

Observations were made on hydrates formed either (1) at the CO_2/water interface with gaseous CO_2, (2) at the CO_2/water interface with liquid CO_2 above the water, (3) in the CO_2 vapor space above a water phase, or (4) in a completely hydrostatic system from liquid CO_2 droplets. In all cases, once hydrate formation started, the hydrates grew rapidly and were snow-like in appearance. The hydrate masses were then broken apart using a magnetic stirring bar in the view cell. The snow-like hydrates were positively buoyant in the water phase. However, with extended time, the hydrates became more ice-like (transparent) in appearance and tended to sink in the view cell. Trapped, unconverted CO_2 may have caused the bulk density of the initially formed hydrates to be less than that of water. With time, this trapped CO_2 could be converted to hydrate, causing the density to increase and the appearance to change. It is interesting to note, that the hydrates sometimes formed a semi-solid mass which occupied the entire water phase. This mass did not impede the movement of the stirring bar but showed no evidence of rising or settling in the cell.

To study hydrate formation from one homogeneous phase, 1.75 g of CO_2 was dissolved in 30.0 g of water in the view cell at 18°C and 14 MPa. This solution would be about 80% saturated at 12°C and 12.662 MPa [7]. The cell was gradually cooled without stirring. Hydrates formed from solution near 5.0°C and 12.40 MPa. At the time of formation, the hydrates were ice-like in appearance and rapidly sank when disturbed by moving the stirring bar. The hydrates were observed for 16 hours under these conditions and appeared to be stable. Later in the experiment, they began to decompose without stirring when the view cell reached 5.4°C. Forming the hydrates from dissolved CO_2 appears to avoid the problem of entrapped CO_2 and results in hydrates that are denser than water.

3.3 Fate of hydrate-coated droplets

The last experiment described above was continued by introducing a liquid CO_2 droplet into the hydrate-containing water phase while the hydrate was still present. It immediately formed a hydrate coating but then exhibited no further change over a period of several hours in a non-agitated system. We have made similar observations in other experiments at different conditions.

When the hydrate coating formed on a CO_2 droplet in water relatively unsaturated with CO_2, the droplet shrank in size as it dissolved. For example, at 6.5°C and 11.1 MPa, a 2.6-mm diameter droplet decreased in radius at a rate of 0.0045 cm/h with slow agitation in the view cell. In the absence of a hydrate coating, a droplet of similar size at 6.1°C and 12.6 MPa decreased in radius at 0.10 cm/h. In comparison, Shindo et al. [8] measured dissolution rates of hydrate-covered CO_2 droplets at 28 MPa to 32 MPa (no temperature given) and found that they decreased in radius at a rate of 0.09 cm/h. The difference in rates may be due to dissimilarities in the experimental procedures and apparatus; however, differences in the thicknesses of the hydrate coating may also have been a factor.

The importance of understanding the kinetics of hydrate formation and dissolution may be illustrated using an earlier model we developed to determine the fate of liquid CO_2 droplets injected into the ocean [4]. At the time, the best kinetic data available for estimating the growth rate for CO_2 hydrates was that obtained from recent vapor phase studies. The above observations indicate these values may not be the most appropriate. Instead of growing in thickness as originally assumed, the hydrate layer on a droplet may remain relatively thin and serve to slow the dissolution rate of the CO_2 into the ocean.

The following illustrates the consequences of both scenarios on ocean disposal of CO_2. The original model predicted that a 1-cm droplet would need to be injected at 1900-m depth to insure effective sequestration if the hydrate shell thickness grew at a steady rate of 0.02 cm/h. In this case, the particle would begin to sink after rising to approximately 500 m owing to the thickening hydrate shell being denser than sea water. If instead of forming more hydrate, the particle dissolved at a rate of 0.09 cm/h, a 1-cm hydrate-coated droplet would still have to be injected at great depth. In this case, a depth of 1500 m would be required for the droplet to be completely dissolved by the time it reached 500 m. For the slower dissolution rate of 0.0045 cm/h, complete dissolution of the rising droplet would not be achieved before 500 m, even if injected at depths approaching those where liquid CO_2 becomes denser than seawater (approximately 2700 m). If injected at depths greater than 2700 m, the CO_2 would sink regardless of hydrate formation. Injection depths greater than 1500 m are not practical at

present [1]; thus understanding and controlling hydrate formation are paramount to successful sequestration of CO_2 in the ocean.

4. CONCLUSION

The observations made in the view cell and the recent observations of others have implications for the effective disposal of CO_2 in the ocean. Simply discharging the CO_2 at great depths may be insufficient if hydrate coatings form on liquid droplets of CO_2. Observations of single droplets indicate that the coating may impede the dissolution and permit the CO_2 droplet to rise to unacceptably shallow depths. Also, the possibility of growth of the hydrate shell cannot be ruled out based on observations of single droplets. In the vicinity of the injection device, the ocean will likely be near saturation owing to the enormous amounts of carbon dioxide being injected. If CO_2 cannot dissolve, then the growth of the hydrate coatings becomes more likely, especially as droplets collide and fresh CO_2 is released.

A better strategy than direct discharge would be to mix the CO_2 and water prior to reaching hydrate-forming depths and then introduce the mixture into some type of confined region that either permits pure hydrates to form under controlled conditions or fosters the growth of the hydrate coatings on CO_2 droplets. Density observations in the view cell indicate that pure hydrates formed in the first case would be negatively buoyant and sink. In the second case, if the hydrate coating contains more than approximately 30% of the CO_2 in the particle, the particle will also sink. Problems with plugging in the event of a flow interruption in such systems may be avoided by operating at slightly undersaturated conditions with respect to CO_2. Observations in the view cell indicate that these conditions favor the formation of a semi-solid mass rather than a solid hydrate plug.

ACKNOWLEDGMENT

The authors would like to thank Richard Hlasnik and Jerry Foster for performing the view cell experiments.

DISCLAIMER

Reference in this report to any specific product, process, or service is to facilitate understanding and does not imply its endorsement or favoring by the United States Department of Energy.

REFERENCES

1. DOE Report DOE/ER-30194, A Research Needs Assessment for the Capture, Utilization and Disposal of Carbon Dioxide from Fossil Fuel-Fired Power Plants, July 1993 (available NTIS).
2. R.P. Warzinski, C.-H. Lee, and G.D. Holder, J. Supercrit. Fluids, 5 (1992) 60.
3. A.T. Bozzo, H.-S. Chen, J.R. Kass, and A.J. Barduhn, Desalination, 16 (1975) 303.
4. G.D. Holder, A.V. Cugini, and R.P. Warzinski, Environ. Sci. Tech., 29 (1995) 276.
5. C.H. Unruh and D.L. Katz, Petroleum Transactions, AIME, (April 1949) 83.
6. S.M. Masutani, C.M. Kinoshita, G.C. Nihous, T. Ho, and L.A. Vega, Energy Convers. Manage., 34 (1993) 865.
7. R. Weibb and V.L. Gaddy, J. Am. Chem. Soc., 60 (1940) 815.
8. Y. Shindo, T. Hakuta, Y. Fujioka, K. Takeuchi, and H. Komiyama, Abstracts Second International Conference on Carbon Dioxide Removal, Kyoto, Japan (1994), 44.

Environmental Impacts of Ocean Disposal of CO_2

Eric Adams
Senior Research Engineer
Department of Civil & Environmental Engineering
Massachusetts Institute of Technology

Howard Herzog
Principal Research Engineer
Energy Laboratory
Massachusetts Institute of Technology

David Auerbach
Graduate Student
Department of Civil & Environmental Engineering
Massachusetts Institute of Technology

Jennifer Caulfield
Graduate Student
Department of Civil & Environmental Engineering
Massachusetts Institute of Technology

Overview

One option to reduce atmospheric CO_2 levels is to capture and sequester power plant CO_2. Commercial CO_2 capture technology, though expensive, exists today. However, the ability to dispose of large quantities of CO_2 is highly uncertain. The deep ocean is one of only a few possible CO_2 disposal options (others are depleted oil and gas wells or deep, confined aquifers) and is a prime candidate because the deep ocean is vast and highly unsaturated in CO_2 . The term disposal is really a misnomer because the atmosphere and ocean eventually equilibrate on a timescale of 1000 years regardless of where the CO_2 is originally discharged. However, peak atmospheric CO_2 concentrations expected to occur in the next few centuries could be significantly reduced by ocean disposal. The magnitude of this reduction will depend upon the quantity of CO_2 injected in the ocean. as well as the depth and location of injection.

Ocean disposal of CO_2 will only make sense if the environmental impacts to the ocean are significantly less than the avoided impacts of atmospheric release. Our project has been examining these ocean impacts through a multi-disciplinary effort designed to summarize the current state of knowledge. The end-product will be a report issued during the summer of 1996 consisting of two volumes: an executive summary (Vol I) and a series of six, individually authored topical reports (Vol II). A workshop with invited participants from the U.S. and abroad will review the draft findings in January 1996.

The six topical reports cover the following subjects:

(1) CO_2 loadings/scenarios

(2) near field perturbations

(3) far field perturbations (performed under subcontract to SAIC, Inc.)

(4) impacts of CO_2 transport (performed under subcontract to UMass-Lowell)

(5) environmental impacts of CO_2 release

(6) policy and legal implications of CO_2 disposal

Each subject area is summarized briefly below with elaboration given to the near field perturbations and environmental impacts of a dry ice release.

CO_2 loadings/Scenarios

A 500 MW_e pulverized coal fired power plant is chosen as a reference. Without capture, this plant will emit CO_2 to the atmosphere at the rate of 115 kg/s (Herzog and Drake, 1993). With ocean disposal we assume 90% CO_2 capture efficiency and a 20% energy penalty. The energy penalty implies that net energy production with capture is reduced by 20% for a given energy input or, alternatively, that the required energy input for a given electrical output is increased by 25%. Considering a net electrical output of 500 MW_e, the effect of ocean disposal on a standard power plant is summarized below:

		Release of Carbon Dioxide	
	Net Power	To Atmosphere	To Ocean
Without Capture	500 MW_e	115 kg/s	0 kg/s
With Capture	500 MW_e	14.4 kg/s	130 kg/s

The emissions loadings are being studied as multiples of the standard power plant. The following matrix summarizes the scenarios that will be investigated:

	Number of 500 MW_e Power Plants (130 kg/s CO_2 per plant)		
Analysis	One	Ten	One Hundred
Near Field (<25 km)	Five injection scenarios with generic ambient conditions	Five injection scenarios with generic ambient conditions	–
Mesoscale (25 km-2500 km)		3-5 specific sites off eastern U.S. with a generic injection at depth of 1000 m.	
Far Field (300 km-global)	–	–	One scenario: 50% injected at 1000 m off Tokyo & 50% injected at 1000 m off New York

One power plant is essentially the lowest level of disposal anticipated while the emissions from ten power plants represent an upper limit on the amount of emissions that are expected to be disposed of at a single point for reasons of economy of transport. One

hundred plants represents a loading of about 1.6% of the world's total anthropogenic CO_2 emissions and, as such, is a lower bound on the global amount of ocean disposal which could "make a difference" to atmospheric CO_2 levels.

For the near field analysis, five injection scenarios are considered:

- a droplet plume injected at 1000 m
- a CO_2 lake on the ocean bottom below 3700 m
- a dense CO_2 seawater plume injected at or below 500 m
- dry ice cubes released from the ocean surface
- a CO_2 hydrate plume injected at or below 500 m

Near Field Perturbations

The five injection scenarios are evaluated using separate models to describe 3-D concentration distributions of excess CO_2 and trace gases such as SO_2 and NO_x. The principal impacts of each scenario - the decrease in pH - are quantified using two criteria. First the spatial distribution of pH change is calculated. Then the range of time-histories of passive organisms traveling through the plume is calculated. Absolute pH is used in order to correlate the experiences with appropriate mortality data.

Far Field Perturbations

Far field perturbations refer to the change in total CO_2 concentration and associated pH at mesoscale and global scale.

Mesoscale simulations are being run for various locations along the eastern U.S.. The mesoscale dispersion model is a stochastic particle model driven by an externally calculated, time-dependent 3-D velocity field. "Particles" of CO_2 are continuously released at an injection site of 1000 m and tracked as they are advected by ocean currents, which include a mean current and turbulent fluctuations. The concentration of CO_2 at any one time can be plotted at a resolution of $1/4 \times 1/4$ degrees latitude and longitude.

A global carbon cycle model is being used to predict far-field long-term pertubations associated with one hundred 500 MW_e powerplants: 50 off of Tokyo and 50 off of New York. Injection depths of 1000 m will be used and simulations will run through the year 2500. The global discharge of anthropogenic CO_2 will be modeled as a simple logistics function of time. The global cycle model is based on the non-biological ocean circulation model of Mairer-Riemer and Hasselmann (1987), with biological carbon cycle components described by Bacastow and Mairer-Riemer (1990).

Environmental Impacts of CO_2 Transport Systems

Enviromental impacts may occur at several stages of transport. The major impact of on-shore pipes occurs during construction when vegetation must be cleared and trenches dug. After construction, land and vegetation needs to be restored. In populated areas, it may be difficult to obtain rights-of-way. There is a remote chance of pipe rupture with the release of vaporized CO_2 . CO_2 is not toxic, but is an asphyxant. Models are being used to estimate the dispersal of this dense vapor and the risk to the surrounding environment.

The major impact of off-shore pipes will also occur during pipe-laying. The first few kilometers will be laid on the continental shelf which may include coral beds, sea vegetation and other marine habitats. Accidental rupture of the pipe would release CO_2

into the seawater, with partial dissolution. The rest of the released CO_2 would rapidly bubble up to the surface and reenter the atmosphere. The dissolved CO_2 will cause acidification of the seawater in the vicinity of the ruptured pipe.

The environmental impacts of tanker transport include (a) accidental releases with possible injury to the tanker crew; (b) release into the atmosphere of fuel combustion gases and particles. Both diesel and steam propelled tankers release into the atmosphere particles (flyash and soot), SO_2 and NO_x, and of course CO_2 .

For pipe transport, on-shore facilities include a pumping station and storage tanks. Construction may require coastal land acquisition and disruption of coastal habitat. There is also a remote risk of accidental release of pressurized, liquid CO_2 . For tanker transport, docking facilities will be required in existing harbors, or specially built ports.

If tanker transport is used for deep sea disposal, floating platforms must be used to unload CO_2 and pump it into a pipe extending from the platform. The floating platforms will cause minimal impact but may be a navigation hazard. The operating crew on the platform will be exposed to storms and other environmental hazards, as well as possible accidental release of pressurized, liquid CO_2 . The vertical pipe should not cause significant impact on the marine environment.

Environmental Impacts of Ocean Disposal of CO_2

Marine life can be classified into four groups: phytoplankton, zooplankton, nekton, and benthos. The groups that will be affected by a CO_2 plume depend on the injection scenario and many scenarios preclude certain types of organisms from harm. The dry ice scenario is discussed below, but the methods and considerations are applicable to other scenarios.

Policy and Legal Implications of CO_2 Disposal

Important considerations relate both to site-specific discharges within or near a country's Exclusive Economic Zone as well as large scale worldwide CO_2 disposal. The Law of the Sea and the United Nations Environment Programme Agenda 21 are tone-setting and establish our committment to curb CO_2 emissions. The London Dumping Convention, as well as other regional treaties, are more specific and classify materials. prohibiting the discharge of some to the ocean.

Worldwide CO_2 disposal would require international cooperation and funding. Presumably it would not be initiated without consensus that avoided impacts/risks of global change outweigh any impacts to the ocean. In opposition to this philosophy, international treaty language is moving toward a precautionary principle and frowns upon end of pipe solutions or solutions which transfer pollution from one medium (air) to another (water). Furthermore, the emotional response of non-governmental organizations (NGOs) can not be discounted.

Analysis for Dry Ice Disposal

The near field perturbations and associated environmental impacts for dry ice injection are considered as an example our methodology. Dry ice cubes must be as large as practical, to insure that only a small fraction of the dissolution occurs near the surface. Cubes with 3 meter sides released from a fixed point were chosen; one standard power plant requires the release of one cube every 320 seconds. CO_2 dissolution to the water column as a function of depth was based on Nakashiki *et al.* (1991).

To obtain a steady state solution the release was approximated as a continuous line source. Turbulence induced by the falling cube was added to a scale-dependent ambient

diffusivity (Okubo, 1973) to obtain the total diffusivity as a function of distance. The solution for the excess total CO_2 concentration is then given by

$$C(x,y,z) = \frac{\dot{M}/u}{\sqrt{2\pi}\sigma} \exp\left(\frac{-y^2}{2\sigma^2}\right)$$

where $\dot{M}(z)$ is the mass flux (kg/m-s) at depth z, u is the current speed (m/s), and $\sigma(x)$ is the lateral standard deviation (m) found from the total diffusivity.

Excess CO_2 concentrations due to the disposal of dry ice were calculated for the one and the ten plant scenarios for $u = 0.02$ and 0.10 m/s. Results for one plant with $u = 0.02$ m/s current are shown in Figure 1. The excess CO_2 was added to the ambient CO_2 to compute new pHs. A map of the change in pH can be seen in Figure 2.

The average ocean CO_2 concentration experienced by an organism passing through the region can be calculated by assuming that the organism is subject to the same diffusivity as the CO_2 . Thus

$$\bar{C}(x,y_o,z) = \frac{C_{max}}{\sqrt{2}} \exp\left(\frac{-y_o^2}{2\sigma^2}\right)$$

where $\bar{C}(x,y_z)$ is the average excess CO_2 concentration experienced at location x and z by an organism that passes through the plume at a lateral distance y_o from the source, and $C_{\max}(x)$ is the concentration at the centerline ($y = 0$) given above. $\bar{C}$ is used to calculate average pH as a function of time. At each depth, several lateral sections are selected and a representative experience is found based on the value of y_o at the middle of each section. Figure 3 shows the experiences at a depth of 900 m for ten power plants in a 0.02 m/s current.

The environmental impact assessment focuses on zooplankton and assumes conservatively that they have no CO_2 avoidance ability. Knowing the volume of water that will experience a given time history of pH, and knowing the population density of organisms in the water is sufficient to estimate the numbers of zooplankton affected by the CO_2 .

Most studies on the effects of pH have been on fish in acidified lakes in response to acid rain concerns. Still, several useful studies have been performed on marine zooplankton in which either the animals were exposed to a constant pH, and mortality assessed at different times, or the animals were exposed to various pHs for a given time and mortality assessed (Grice *et al.*, 1973, Calabrese *et al.*, 1966, Havas and Hutchinson 1982 and Bamber 1987). Results from these studies have been superimposed on Figure 4 to give an approximate map of expected mortality as a function of pH and exposure time. ('Isomortality' curves are drawn for 0%, 50%, and 90% mortality as guides.)

Near field output such as Figure 3 can be discritized to yield the number of hours over which various sections of the plume experience different values of pH. The cumulative impact of a time-varying exposure can be estimated by using the isomortalilty curves to convert exposures into a common metric. For example, on Figure 4, an exposure of 50 hours at pH 6.0 causes roughly the same 10% mortality as an exposure of 15 hours at pH 5.5. Hence we can approximate an exposure of 50 hours at 6.0 plus 10 hours at 5.5 as 25 hours at 5.5. For such an exposure, the graph gives a mortality of 50%. Equivalently, converting the exposures to a metric of hours at 6.0 instead of 5.5, gives a total exposure of 90 hours corresponding to about 40% mortality. The table below illustrates this procedure using data from Figure 3 and compares it with an alternative method (Schubel, 1978).

Section width (m)	hrs. at pH 5.5	hrs. at pH 6.0	hrs. at pH 6.5	hrs. at pH 7.0	mortality % 1	mortality % 2
0-20	.417	2.71	5.97	14.8	0%	2.2%
20-60	0	.90	7.71	15.0	0%	1.3%
60-120	0	0	6.39	16.0	0%	1.0%
120-240	0	0	0	19.4	0%	0.5%

mortality % 1 = mortality using method described above. % 2 = mortality following Schubel (1978).

The section in the first row above is closest to the plume centerline and would experience the greatest effect; these data are plotted in Figure 4. It is clear that even the most severely affected organisms would scarcely be affected (method 2 by design will give non-zero mortalities since it assumes no threshold but these small numbers should be considered artifacts). Thus, we can safely expect little or no harm to pelagic organisms from the scenario of falling dry ice cubes. It should be mentioned that yhe dry ice cube scenario is expected to have the least impact because of the large dilution. We are in the process of studying other injection scenarios using similar methodology.

References

Bacastow, R. and E. Maier-Reimer (1990). "Ocean-circulation model of the carbon cycle" *Clim. Dyn.* 4:95-125.

Bamber, R.N. (1987). "The effects of acidic seawater on young carpet-shell clams Venerupis decussata (ℓ) (Mollusca: Veneracea)" *Journal of Experimental Marine Biology and Ecology*, 108:241-260.

Calabrese, A., and H.C. David (1966). "The pH tolerance of embryos andlLarvae of Mercenaria mercenaria and Crassotrea virginica" *Biological Bulletin*, 131:427-436.

Grice, G.D., E. Hoagland and P.H. Wiebe (1973). "Acid-iron waste as a factor affecting the distribution and abundance of zooplankton in the New York Bight" *Estuarine and Coastal Marine Science* 1:45-50.

Havas, M. and T.C. Hutchinson (1982). "Effects of low pH on the chemical composition of aquatic invertebrates from tundra ponds at the Smoking Hills, N.W.T. Canada" *Canadian Journal of Zoology* 61:241-249.

Herzog, H.J. and E.M. Drake (1993). " Long-Term Advanced CO_2 Capture Options". IEA Greenhouse Gas R&D Programme Report, IEA/93/OE6.

Maier-Reimer, E. and K. Hasselmann (1987). "Transport and storage of CO_2 in the ocean – an inorganic ocean-circulation carbon cycle model" *Clim. Dyn.* 2:63-90.

Nakashiki,N., T. Ohsumi, and K. Shitashima (1991). "Sequestering of CO_2 in the deep-ocean: Fall velocity and dissolution rate of solid CO_2 in the ocean" Central Research Institute of Electric Power Industry, Technical Report EU91003.

Okubo, A. (1971). "Oceanic diffusion diagrams" *Deep-Sea Research* 18:789-802.

Schubel, J. R., C.C. Coutant, and P.M.J. Woodhead (1978). "Thermal effects of entrainment" in *Power Plant Entrainment, A Biological Assessment* (Schubel, J.R. Marcy. B.C. Jr. eds) Academic Press Inc., New York.

Figure 1: Additional CO_2 concentrations due to the addition of the emissions of one standard power plant as 3 meter blocks of dry ice

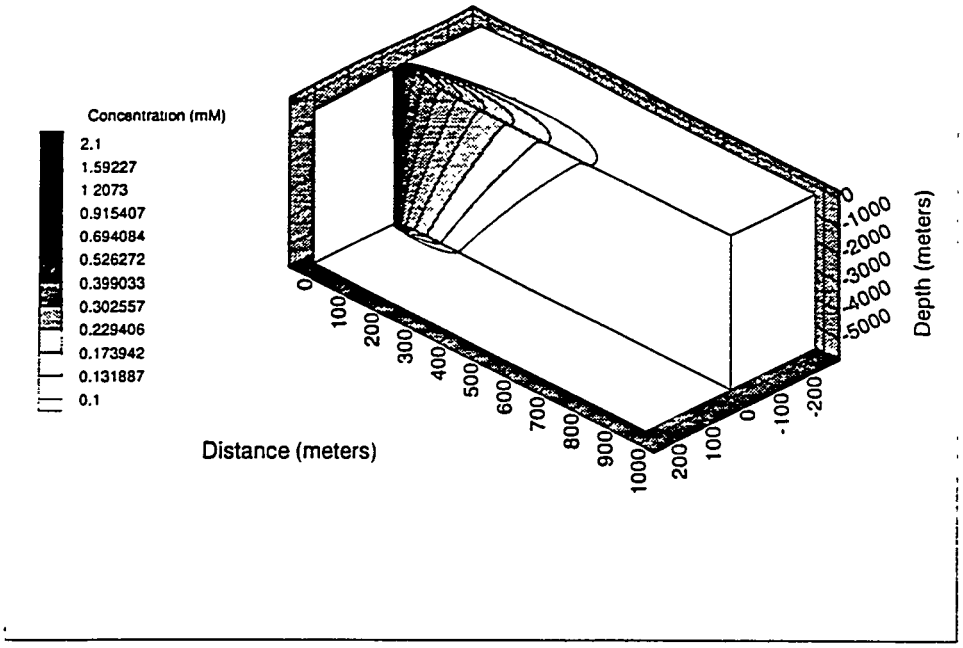

Figure 2: Change in pH resulting from dry ice addition

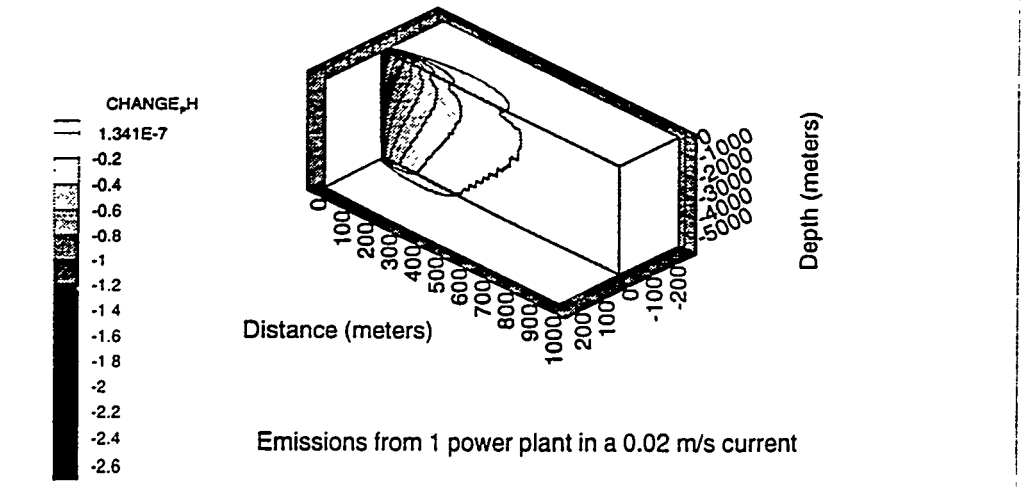

Figure 3: pH-Time experience for organisms at different distances from the plume centerline (conditions at a depth of 900 meters)

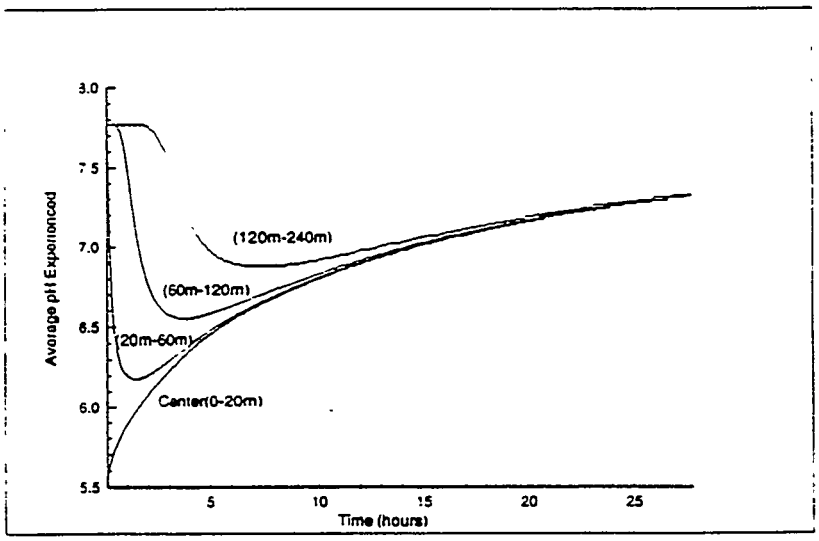

Figure 4: Mortality of zooplankton

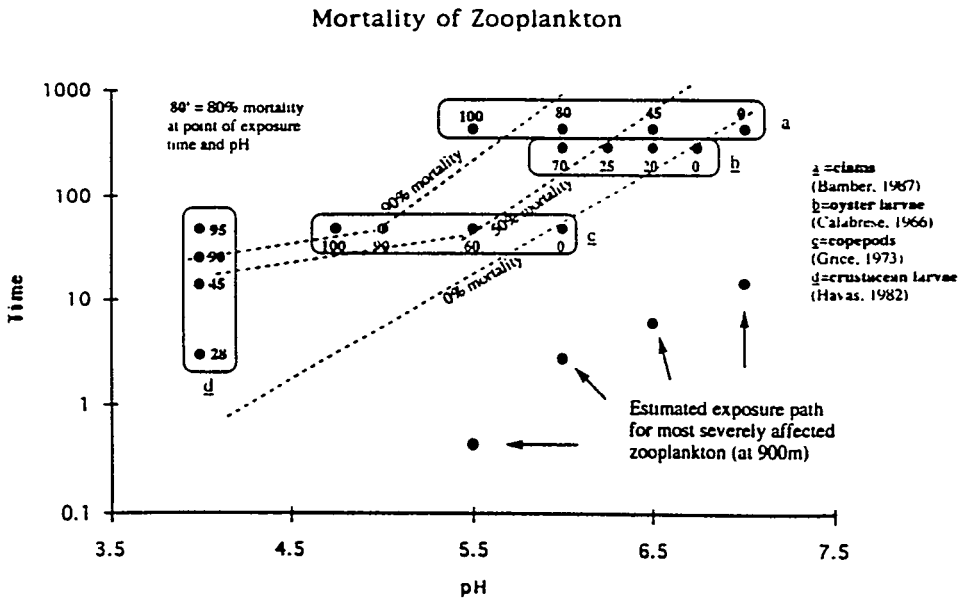

DISPOSAL OF CARBON DIOXIDE IN AQUIFERS IN THE U. S.

EDWARD M. WINTER
BURNS AND ROE SERVICES CORPORATION

PERRY D. BERGMAN
U.S. DEPARTMENT OF ENERGY
PITTSBURGH ENERGY TECHNOLOGY CENTER

ABSTRACT

Deep saline aquifers were investigated as potential disposal sites for CO_2. The capacity of deep aquifers for CO_2 disposal in the U.S. is highly uncertain. A rough estimate, derived from global estimates, is 5-500 Gt of CO_2. Saline aquifers underlie the regions in the U.S. where most utility power plants are situated. Therefore, approximately 65 percent of CO_2 from power plants could possibly be injected directly into deep saline aquifers below these plants, without the need for long pipelines.

INTRODUCTION

One of the options proposed for reducing the buildup of greenhouse gases in the atmosphere is to collect CO_2 from point sources, such as utility power plants, and dispose of the CO_2 by injection into underground structures, such as, abandoned oil and natural gas reservoirs or deep aquifers. This paper describes the the problems associated with locating and evaluating aquifers which are suitable for CO_2 storage in relation to utility power plant emission sources.

The locations of utility power plants and CO_2 emissions from each were taken from a Utility Data Institute (UDI) database. An estimate of aquifer disposal capacity was taken from recent International Energy Agency (IEA) reports. [1,2,3]

POWER PLANT SOURCES OF CO_2

CO_2 emissions from utility power plant CO_2 sources in the United States were calculated by using data on fuel type and annual consumption at each power plant. An average carbon content was used for each fuel type. The CO_2 emissions for 1990 are shown by state in Figure 1. The states with the highest CO_2 emissions are Texas (the largest emitter), Alabama, Georgia, Florida, and a belt of states extending across the upper Midwest from Missouri to New York. These 13 states generate almost 60 percent of U.S. power plant CO_2 emissions. The total CO_2 emissions from all power plants in 1990 was 2.0 Gt (giga tonnes). This estimate compares well with Energy Information Administration (EIA) calculations yielding 1.8 Gt CO_2. [4]

DISPOSAL OF CO_2 IN AQUIFERS

The aquifers most suitable for disposal of CO_2 are the deeper saline aquifers. Figure 2 shows the location of saline aquifers in the U.S. Approximately 65 percent of CO_2 power plant emissions comes from power plants which are situated directly above the aquifers shown in Figure 2. The capacity of saline aquifers for disposal is difficult to estimate because of a dearth of published data.

Figure 3 shows the effect of variations in underground pressure and temperature on storage efficiency. Some formations, mainly at shallow depths, will not be suitable for economical storage simply because low pressures will require much larger volumes of storage capacity per unit mass of CO_2.

The potential aquifer volume available for disposal of CO_2 has been estimated by a number of authors, the range of global totals corresponding to 100-10,000 Gt of CO_2. A recent IEA report discusses these estimates in detail [1] and also gives results of studies in three geographical areas, namely, 1) the Alberta Basin in Western Canada, 2) Senegal in Western Africa, and 3) East Midlands in the UK. The wide range of estimates shows the huge uncertainties involved. Many aquifers in the world are not close to power plants or other sources of CO_2 and cannot be used for storage. The IEA study team concluded that extrapolation of the limited data available to predict global potential was not reasonable at this time.

Prorating the range of capacities above, using relative land areas, gives an estimated disposal capacity in the U.S. of 5-500 Gt of CO_2. Further studies to determine aquifer capacity are obviously required.

By way of comparison, hazardous and nonhazardous industrial wastes in the U.S. are currently being disposed of by underground injection at the rate of approximately 75 million cubic meters per year (20 billion gallons per year). This volume corresponds to about 0.05 Gt of CO_2 or 1/40 the rate of CO_2 emissions from utility power plants.

Unfavorable CO_2 Flow Patterns

Super-critical CO_2, with a density of approximately 0.6 the density of typical brines, would be expected to rise to the top of a formation because of buoyancy. Also, since CO_2 at prevailing underground pressures and temperatures often has a lower viscosity than water, fingering would occur, that is, channeling and accelerated flow of the CO_2 phase relative to the native fluid. The CO_2 would tend to travel along the upper surface of the formation, moving rapidly in a geometry resembling fingers of flow out from the injection well and leaving behind pockets of the brine phase. Only a fraction of the native fluid in the aquifer would be displaced, and only a fraction of the aquifer volume would be filled by CO_2. The CO_2 would be expected to fill any trap (a stagnant pocket above the normal flow path) it might encounter, since the CO_2 is lighter than the formation water. Eventually, the CO_2 would continue on and reach the edge of the formation and escape earlier than the time calculated for the native fluid. It has been

estimated that possibly only 2-4 percent of the total volume of an aquifer would be filled with CO_2 because of these unfavorable properties. [5]

Limitations on Injection Pressure

The permissible injection flow rate depends on the rock permeability in the aquifer. If the permeability is low, the injection rate must be kept low to avoid excessive pressure. A pressure that is too high can cause either fracture of the cap rock and loss of containment or leakage around the injection well, or other wells nearby, within what is termed the cone of influence. The cone of influence is the region surrounding a waste injection well where injection pressure might cause damage to other wells, either operating or plugged and abandoned wells. The radius of this zone is at the discretion of each state but must be at least a quarter mile (0.8 km). In Texas, the cone of influence is taken as 2.5 miles (4 km). Regulations require that modeling of pressure-flow characteristics extend throughout this region when a permit is applied for. Monitoring of well pressure is required after a permit is issued and the well is in operation.

Multiple injection wells will undoubtedly be required. The CO_2 emitted from one moderately sized power plant is too much to be injected into underground storage sites through a single well. Several injection wells might be required, depending on power plant size and the permeability of the rock formation. These wells would have to be spaced a safe distance apart to avoid overpressuring. A network of connecting pipelines could be required, extending outside the boundaries of the power plant property. Or multiple non-vertical wells could be drilled from the same point at the surface at different angles.

Other Limiting Factors

Some authors have stated that geologic traps will be required for CO_2 disposal [1]. If this is the case, only a fraction of the aquifer volume would be available for disposal. Aquifers would be filled much sooner than if the whole aquifer could be used. Traps have not been identified in aquifers to the extent that they have in oil and natural gas containing structures. If traps are required, extensive drilling of test wells could be required to locate them. However, current practice in underground disposal of hazardous and nonhazardous industrial waste in the U.S. does not require injecting into a trap. Obtaining a permit can be based on modeling studies which show that the injected waste will not escape from the confining formation for at least 10,000 years. Very slow movement of the connate fluid in the formation, sometimes as low as a few centimeters per year, would give a retention time long enough to provide confinement for the required period.

The chemistry of some aquifer formations may not allow any disposal of CO_2 in them. Chemical reactions between the injected fluid and the reservoir rock can take place. For example, acid wastes have been known to react with limestone or dolomitic formations, liberating CO_2, which overpressured the formation and caused blowout of the well. If CO_2 is found to react unfavorably with certain types of rock structures, then these formations would not be suitable. The fluid can also chemically combine with the rock material, increasing the

storage capacity of the formation. Disposal capacity could be either reduced or increased depending on circumstances.

Different procedures and policies among various states can affect usable storage capacity. Title 40 of the Code of Federal Regulations, Parts 144-149, contains the regulations for underground injection control (UIC). It establishes minimum requirements for states to set up a UIC program and to obtain primary enforcement authority. Each state can adhere to the federal regulations or impose more stringent rules. Pennsylvania, for example, does not issue permits for underground injection at this time. Other states may have taken this position as well, either because their procedures have not yet been approved by the U.S. Environmental Protection Agency, or because of their policy position. A particular state may allow disposal of wastes in an aquifer, while an adjacent state does not issue permits for the same aquifer. Therefore, the presence of a suitable aquifer may not necessarily lead to approval for CO_2 disposal.

The agency issuing disposal permits is concerned about the fate of the waste material and the time required for the material to travel to the edge of the disposal zone and a number of other issues. What happens to the native brine is also important. The injected waste will displace the brine and may increase its flow velocity, resulting, for example, in increased rate of discharge into a lake or stream, which could handle the previous lower flow safely. Or the higher velocity may cause the brine to discharge along new paths into different zones, for example, mixing into drinking water aquifers that it previously bypassed. If modeling shows that CO_2 injection would accelerate the movement of hazardous and nonhazardous wastes injected in the past, states might limit or prohibit CO_2 injection into these aquifers, further reducing available capacity.

Several state agencies have reported growing resistance from the public to underground disposal of wastes. Permits are becoming harder to obtain. Acceptance of large-scale disposal of CO_2 by underground injection will require much more intensive research to minimize the technical uncertainties and risks.

CONCLUSIONS

The potential for CO_2 disposal in aquifers is very difficult to estimate from the information available. Disposal capacity is probably as great or greater than the capacity in oil and gas reservoirs. Many power plant CO_2 sources are closer to potential aquifer disposal sites than to large oil and gas reservoirs.

Based on this work, additional effort should be directed toward

- Locating and characterizing candidate aquifers to determine their potential for CO_2 disposal.
- Looking at possible chemical reactions between CO_2 and the formation rock.

- Modeling of CO_2 injection and movement into an aquifer to determine its capacity for storage.

REFERENCES

1. Stanley Ind Consultants, Aquifer Disposal of Carbon Dioxide, IEA/93/OE14, Chap. 10, pp. 1,2

2. Hendriks, C.A., Blok, K., "Underground Storage of Carbon Dioxide," Energy Convers. Mgmt. Vol. 34, 1993, pp 949-957.

3. Van der Meer, L.G.H., "The Conditions Limiting CO_2 Storage in Aquifers," Energy Convers. Mgmt., Vol 34, 1993; pp 959-966.

4. Emissions of Greenhouse Gases in the United States, 1985-1990, DOE/EIA-0573, 1993, p 13.

5. Van der Meer, L.G.H., Straaten, R.; Carbon Dioxide Disposal in Depleted Oil & Gas Wells, IEA/93/OE15, 1993; pp 7,66.

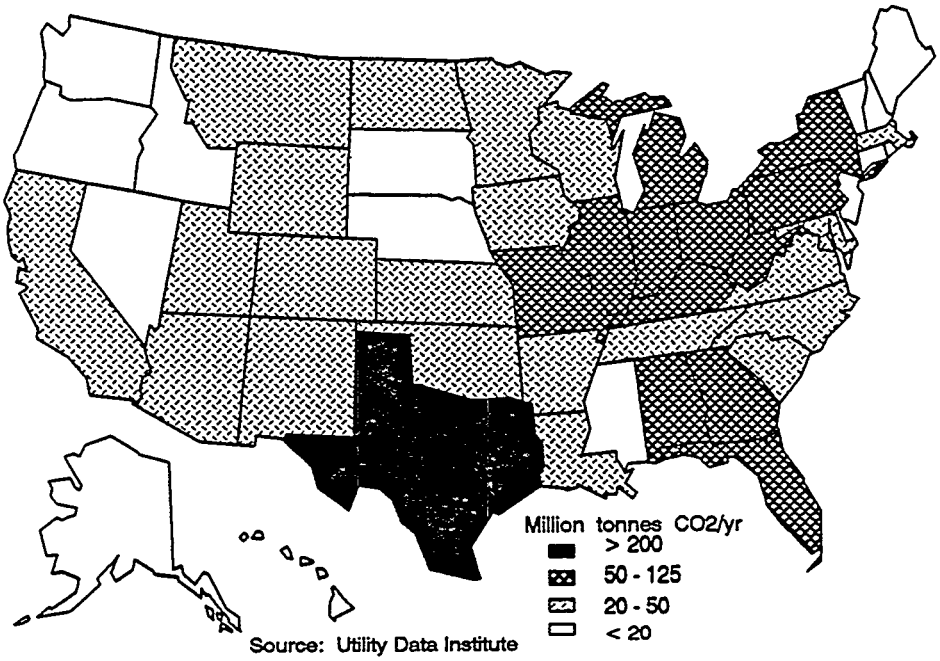

Figure 1. CO2 Emissions from Fossil-Fuel Fired Power Plants

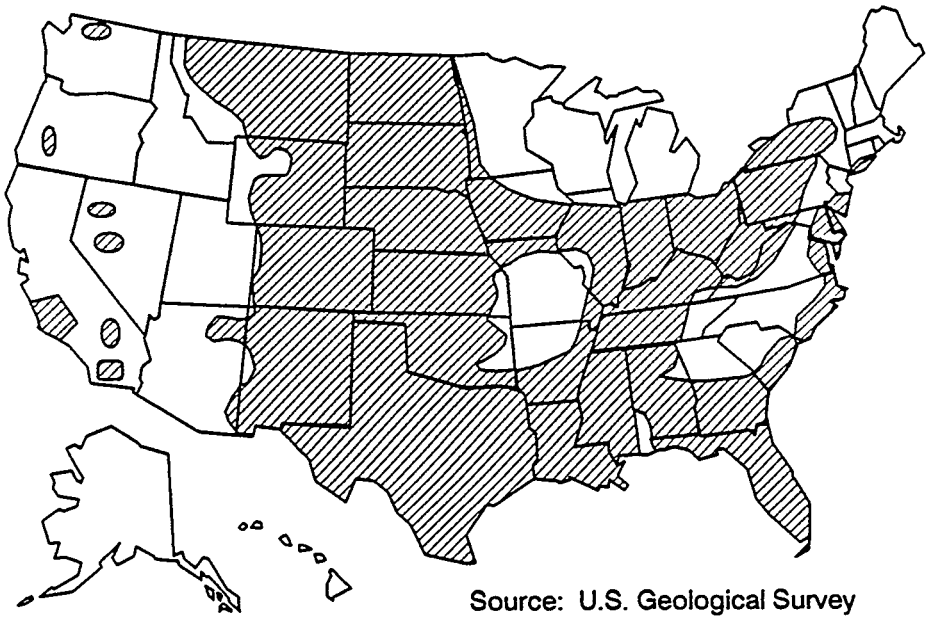

Figure 2. Saline Aquifers in the U. S.

Figure 3. Calculated CO2 Specific Volume at Various Depths
From Texas Natural Gas Reservoirs Atlas

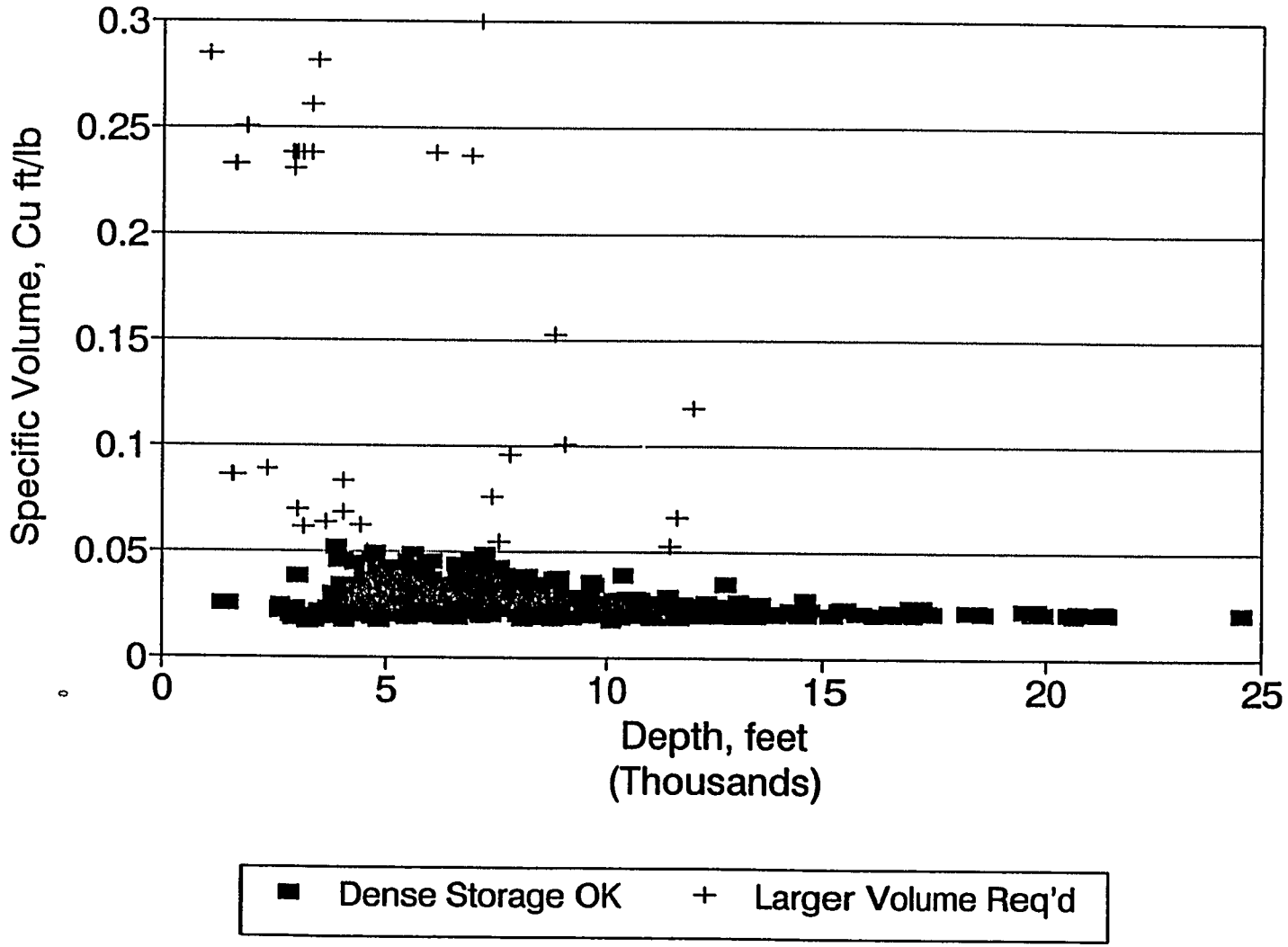

CO_2 CAPTURE AND BIOFUELS PRODUCTION WITH MICROALGAE

John R. Benemann
Department of Civil Engineering
University of California Berkeley
Berkeley, California, 94720

ABSTRACT

Microalgae cultivation in large open ponds is the only biological process capable of directly utilizing power plant flue gas CO_2 for production of renewable fuels, such as biodiesel, thus mitigating the potential for global warming. Past and recent systems studies have concluded that in principle this concept could be economically feasible, but that this technology still requires both fundamental and applied long-term R&D.

INTRODUCTION

The concept of the mass culture of microalgae, for foods, feeds and even renewable fuels production and CO_2 utilization for greenhouse gas mitigation, dates back about half a century (Burlew, 1953; Oswald and Golueke, 1960, see Benemann and Oswald, 1995). Since then the technology for microalgae cultivation has developed from an idea, studied in the laboratory and in very small outdoor systems ($< 10\ m^2$), to large-scale practical applications in wastewater treatment and the production of specialty human foods ("nutriceuticals") and animal feeds.

In wastewater treatment, the first practical application of microalgae culture, no specific algal species are cultivated, and, indeed, even recovery of the biomass is rare. In nutriceuticals production three specific genera of microalgae are being cultivated: Chlorella, Spirulina, and Dunaliella. The latter two are produced commercially in the U.S. (in California and Hawaii), and are also used in animal feeds, along with two recently introduced commercial microalgae being produced fermentatively: Schizochytrium and Spongiococcus. Small photobioreactors ($> 10\ m^2$) of various designs, are being used in the production of specialty aquaculture feeds and diagnostic reagents. Microalgae biotechnology is providing the basis for a growing industry in the U.S. and around the world (Benemann, 1990).

The production of commodities, feeds and fuels, with microalgae cultures has not yet been achieved. Currently microalgae biomass sells for roughly $25,000/ton (dry organic weight basis), while agricultural commodities cost less than $500/ton, and biomass fuels less than half that. The question arises if a two order of magnitude cost reduction could be achieved with current technology, or whether radically new production techniques and fundamental research breakthroughs are required.

The proposition argued herein is that for microalgal fuels production and CO_2 utilization both alternatives apply: Current technology for algal mass culture appears inherently capable of low-cost microalgal production, although only at very favorable sites. However, major technological advances will be required in many aspect of algal culture, in particular the ability to cultivate specific strains, at very high productivities, long-term culture stability, easy harvesting, and a high content of vegetable oils or other desirable compounds.

First the different large-scale microalgae production systems are described, followed by a review of the current state-of-the-art in microalgae culture, and concluding with a discussions of the research and development goals and needs in this field.

MICROALGAE MASS CULTURE SYSTEM DESIGNS

Three major types of systems are used for large-scale practical microalgae cultivation: extensive, intensive, and fermentative.

Extensive microalgae cultivation systems are typically large ponds (from under 1 hectare to up to 100 ha each), relatively deep (>50 cm), without mechanical mixing, or supply of CO_2. Such systems are used for the production of both Spirulina and Dunaliella, and, more widely, in municipal and industrial wastewater treatment. Extensive systems are inexpensive, consisting of simple earthworks with inlet/outlet structures. In extensive wastewater treatment systems no specific algal species are cultivated, and, indeed, may not be feasible to do so. Spirulina and Dunaliella are cultivated in highly alkaline (carbonate) or saline media, respectively, which allows the maintenance of these species as practically unialgal cultures, even in the in the uncontrolled environments of such extensive ponds.

Intensive systems use shallower (<30 cm) ponds, mechanical mixing, CO_2 supply, and hydraulic dilution rates that maintain the algal culture near optimal conditions. Much greater control over the pond environment is possible, and such systems achieve several fold higher productivities than extensive systems and, perhaps most important, can, at least in principle, maintain desired algal species. Of the large-scale intensive system designs, the most prevalent is a raceway ponds design, with ponds up to about 0.5 ha, and mixing typically by paddle wheels. Indeed, this is the basic design used for both Spirulina and one Dunaliella commercial operations in the U.S. Only three municipal wastewater treatment systems in the U.S. (in California) use intensive raceway ponds (mixed by pumps rather than paddle wheels). However, they do not use supplemental CO_2 to maximize algal production, or are specific algal strains cultivated, nor is the algal biomass harvested.

Recently algal production in dark fermenters (using sugars rather than sunlight and CO_2 as energy and C sources) has been developed commercially in the U.S., with two algae being produced: Spongiococcus, high in pigments useful in chicken feed, and Schizochytrium, high in omega-3 fatty acids, similar to fish oils, and useful as an

aquaculture feeds and, potentially, for human food. The price of these products is similar, or even lower, than outdoor pond cultivation costs. In conclusion, currently, microalgae production technology is only feasible for high cost specialty products.

LARGE-SCALE MICROALGAE PRODUCTION

For over three decades engineering cost analysis of increasing sophistication have concluded that it would be possible to produce microalgae at a large scale for the fuel production and utilization of power plant CO_2 (Oswald and Golueke, 1960, Benemann et al., 1982; Reagan and Gartside 1983, Neenan et al., 1986; Weissman and Goebel, 1987; Benemann and Oswald, 1995; see also Benemann, 1994 for a brief review). All these studies were based on similar intensive raceway pond designs, typically paddle wheel mixed. However, these designs also include some characteristics from the extensive systems: large individual growth ponds (10 ha or even larger), no plastic liners (used in most intensive algal production systems) and maximum economics of scale with production systems of 1,000 ha or more. Further, quite favorable assumptions are made about the site, from the cost of land (often negligible), to the low cost availability of water and a nearby power plant for a CO_2 supply. Even with such favorable assumptions and extrapolations, the economics of microalgae culture are still too high for fuel production, by an order of magnitude.

Low cost projections for microalgae production require additional assumptions:

1. The cultivation of genetically selected and improved algal strains in outdoor ponds for long periods with only, occasional, small, inoculations.
2. Achieving very high productivities, near the limits of photosynthetic efficiencies.
3. Production of biomass high in vegetable oils, hydrocarbons, or starches.
4. Harvesting the algal cells by simple sedimentation or other low cost processes.
5. Low cost processing the algal biomass to yield biodiesel and other fuels.

These assumptions represent the major R&D issues, and goals, in the development of a low cost process for fuels production and CO_2 mitigation, and are the main focus of this presentation. However, first some other issues are briefly addressed.

One is the potential of this technology for achieving significant reductions in power plant CO_2 emissions. The joint requirements for favorable climate, land, water, and CO_2 availability, limits this process to a small fraction ($< 5\%$, and probably only 1 - 2%) of U.S. power plant CO_2 emissions. However, even such modest reductions represents tens of millions of tons of CO_2 mitigation. Also, other arguments favor development of this technology, compared to the alternatives (see Conclusions).

Another issue is the technical feasibility of cultivating microalgae using power plant flue gases directly. Recent research in Japan (Hamasaki et al., 1995) and the U.S. (Brown et al., 1994), demonstrated that flue gas is a suitable CO_2 source for algal culture, with NOx, SOx, and other contaminants having little effect on algal growth and productivity. Thus, this is no longer a major uncertainty, and R&D can concentrate on the other, more important, issues, addressed next.

R&D ISSUES IN LARGE-SCALE MICROALGAE PRODUCTION.

Here a brief overview is presented of the issues that must be addressed in any R&D program for developing low-cost algal biomass production technologies. It should be recognized that these problems have, to various degrees, been the subject of much research over the past decades. Thus, one question is why they have, to a large part, not yet been resolved. The answer is that great progress has been made, much more is required. More importantly is the question of how likely they are to be solved in the foreseeable future, and what level of R&D funding would be required.

Cultivation of Selected Microalgal Strains

As stated above, only three algal genera are being commercially cultivated at a large-scale in outdoor ponds. Of these two (Spirulina and Dunaliella) require highly selective media (high bicarbonate and salinity respectively), which allows the maintenance of essentially unialgal cultures, even in extensive systems. However, even in intensive cultures these algal cultures also exhibit low productivities, about 20 to 30 t/ha/y (tons/hectare/year), a third to half of what is achieved by other algae, growing in less restrictive environments. The third microalga grown commercially (only in the Far East), Chlorella, is cultivated with great difficulty, as it has not been possible to maintain the culture for any length (more than a few days to a couple of weeks) in open ponds. Thus, large amounts of inoculum must be produced under highly controlled conditions, at high costs, and the cultures frequently restarted.

This commercial experience might suggest that it is not possible to grow microalgae in outdoor ponds, except for a few species that require unusual conditions and at relatively low productivities, or without inordinate efforts and costs for inoculum production. However, other experience contradict such a conclusion. A green alga, Scenedesmus, was successfully cultivated in simple inorganic freshwater media both in Germany (where this alga first was isolated from growth ponds) and several other countries (Egypt, Peru, Thailand), where commercialization of this technology was attempted. (The commercial failure of these projects, discussed in Benemann and Oswald, 1995, was related in large part to the high costs of harvesting and processing of the algal biomass, compared to its low value as a food and feed).

In intensive wastewater ponds unialgal Microactinium cultures were observed to dominate for many months, even years, over rather large ranges in weather and operating conditions (see review in Benemann and Oswald, 1995). Recently, in Japan, a single strain of Tetraselmis was successfully cultivated in small seawater-fed ponds with actual power plant flue gas for an entire year, under rather unfavorable climatic conditions. And work in New Mexico, sponsored by NREL (National Renewable Energy Laboratory), demonstrated the maintenance of some diatoms in large (1,000 m_2) outdoor ponds (Weissman and Tillett, 1989, 1992), experience that has been successfully applied in commercial bivalve aquaculture production (Weissman, personal communication, 1995).

One common thread in these, and other similar examples, is that the algal strains that successfully dominated such ponds are invading species, that take over from inoculated strains. Thus, making a virtue of necessity, it appears that it is, indeed, possible to cultivate selected strains in open pond cultures even in the absence of strong selective factors, such as high salinity or alkalinity. However, it is also clear that most strains favored by laboratory researchers, are not suitable for outdoor cultures. Thus, the approach to strain improvement should be to move from the outdoor ponds back to the laboratory, not, as has been singularly unsuccessful, to attempt to mass culture strains selected in the laboratory for some particular desired property (e.g. high lipid content, or availability of a genetic system, for example).

Of course, a strain that is relatively well adapted to the pond culture environment, and able to exclude or dominate other algal strains that contaminate the culture, is only a beginning. Successful algal mass culture also requires the control of grazers and other pests. Indeed, this is probably an even greater problem than avoiding the take-over by invading algal strains. Little information is available on this point either in the literature or from commercial operations (where grazer and infestation control generally is held as proprietary information). However, overall, although this is an important practical issue, it does not appear to be a fundamental limitation.

Maximizing Microalgal Biomass Productivities

In microalgae production for fuels and CO_2 mitigation, roughly half of the costs are productivity related. That is, doubling productivity would decrease costs of the final product (e.g. biodiesel) by a quarter. High productivities would also reduce land and water requirements and reduce transportation distances for flue gas, which would make this technology more widely applicable. Maximizing productivities must, thus, be a, if not the, major R&D objective in this field.

Although microalgae cultures have a reputation of very high productivities, this is not correct in actual practice: commercial, intensive, Spirulina production systems have productivities of perhaps only about 25 t/ha/y, which is similar to the gross biomass productivities of many agricultural crops. Of course, as noted above, the chemical environment in these ponds, is not conducive to high productivities. Productivities of algae in wastewater treatment, or of diatoms in brackish and seawater, are over 50 mt/ha/y, and it is likely that 100 mt/ha/y can be achieved at favorable climatic conditions with current technology. This would be similar to record, total biomass yields for the most highly productive higher plants, such as sugar cane, under ideal conditions.

Even higher productivities, 200 mt/ha/y or more should be achievable if the algal cultures are operated near the generally accepted limits of photosynthetic light energy conversion efficiencies, about 10% of solar energy. Indeed, such high conversion efficiencies are routinely obtained in the laboratory, but only at low light intensities. At full sunlight intensities, efficiencies are dramatically reduced,

typically by 50 to 80%, due to the light saturation effect. Essentially, algal cells in a typical culture have more light harvesting pigments (chlorophylls and others) than needed at high light intensities. This results in the algal cells near the surface absorbing more photons than they can readily use, with the excess being lost as heat and fluorescence, rather than being used for CO_2 fixation. The cells a bit further down the water column are shaded, and thus do not get enough light to grow. In theory, it would be relatively simple to use algal strains that have fewer light harvesting pigments. However, such strains are not found in nature (as they would have a competitive disadvantage) and must, thus, be developed by genetic selection and engineering techniques. Of course, such research should, after proof of concept, be carried out with algal strains known to be able to compete in outdoor ponds.

Production of Microalgal Biomass with High Oil Content.

The objective of microalgae cultures for CO_2 utilization is to produce substitutes for fossil fuels, thereby cutting overall CO_2 emissions. Due to the higher value of liquid fuels, compared to solid or even gaseous fuels, these have been the major objective in the microalgae field in recent years. Three types of liquid fuels could be produced from microalgae: ethanol, biodiesel, and liquid hydrocarbons. Ethanol could be fermented from the starch that is accumulated by many types of microalgae. However, the option of producing large quantities of ethanol from lignocellulosic biomass, has focused greater attention on the production of biodiesel from algae. Biodiesel, are the methanol or ethanol esters of fatty acids derived from vegetable oils and animal fats. Considerable work has been carried out on the genetics (Brown, et al., 1994) and physiology of microalgae oils production. In the laboratory biomass with a high (> 50%) lipid content can be produced without reducing productivity (Benemann and Tillett, 1986). Translating such findings to the field is required.

The direct production of hydrocarbon fuels is also possible with microalgae: one species, Botryococcus braunii, is known in the field and laboratory to produce high quantities of relatively large (> C30) hydrocarbons, that could be rather easily cracked to gasoline (see Regan and Gartside, 1983). Relatively little practical culture work has been done with this organism.

Harvesting and Processing of Microalgal Biomass.

Even assuming that culture stability, productivity, and product formation are feasible, there remains the challenge of harvesting (concentrating) the algal biomass, and converting it into a valuable fuel. Harvesting has been the subject of much research over the years, in particular for removal of microalgae from wastewater treatment ponds, a particular challenge due to the heterogeneous, and variable, algal populations present. However, when an essentially unialgal culture are maintained, harvesting is easier. In particular, low cost harvesting based on the settling characteristics of the algae could be used. The conversion of the freshly harvested algal biomass to liquid fuels requires attention, but presents no major challenges.

R&D NEEDS AND RECOMMENDATIONS

The prior feasibility analysis in this field, including the recently completed study sponsored by PETC (Benemann and Oswald, 1995), concluded that it is possible, in principle, to project microalgae derived biofuels costs that are within the range of energy prices forecast for early next century (a moving target, admittedly). This is particularly true if externalities, specifically CO_2 mitigation credits, are considered. Of course, such analysis and projections are, as in related fields (e.g. ethanol production from lignocellulosics), based on a multiplicity of favorable assumptions and extrapolations, whose individual validity appears plausible, at least to the researchers involved, but that have yet to be verified or integrated. Indeed, such feasibility analysis better establish the current state-of-the-art and, most importantly, the required R,D&D (research, development and demonstration), than they project actual costs for systems that still require many years for development and perfection.

It can, however, be projected with some confidence that biomass production costs for microalgae will be on the high side, and could not be justified with current fossil fuel economics without a substantial credit for CO_2 mitigation, much higher than similar projections for alternative biomass fuels, such as wood. Indeed, wood co-firing in coal-fired power plants may have the least cost for direct CO_2 mitigation in the utility industry. Furthermore, as already indicated above, overall impacts from microalgae fuels production will be a small fraction (1-2%) of power plant CO_2 emissions. Other biomass fuels, such as short rotation tree farms, are projected as being able to mitigate well over 10 to 20% of total U.S. CO_2 fossil fuel emissions.

This raises the question of why should such a minor, expensive, and long-range technology as CO_2 utilization with microalgae be developed, when there are other, more promising alternatives. However, there are several arguments that favor microalgae R&D over alternative concepts, specifically wood fuel production:

- **Microalgae R&D is much faster**, over an order of magnitude faster than R&D required to increase wood fuel supplies by means of short rotation forestry.
- **Microalgae R&D is much cheaper**. Most scale-up issues (e.g. culture stability, productivity, harvestability, etc.) can be addressed with appx. 100 to 1,000 m^2 ponds, at a couple of locations. Short rotation tree R&D will require dozens of locations, with hundred of hectares each, studied over several decades.
- **Microalgae R&D is easier to apply** at new sites as there are only two major, uncontrolled, factors: sunlight and temperature. (For trees soil and rainfall are complex additional factors that greatly complicates such extrapolations).
- **Microalgae R&D is specific** to the needs of the "end-of-pipe" CO_2 mitigation program, of particular interest to electric utilities.
- **Microalgae R&D can lead to breakthroughs** both in fundamental and applied fields. For example, increases in productivities achieved with microalgae cultures could potentially find applications in agriculture and forestry.
- **Microalgae R&D will increase U.S. competitiveness** and lead to technology transfer to the private sector, benefiting U.S. industry and export markets.

Of course, these pro arguments must be balanced with con: the undeveloped nature of this technology, the few sites where land/water/sun/CO_2 resources coincide, and the relatively high costs. Overall, the balance favors of a modest, though significant, microalgae R&D effort, that could generate continuing practical applications while proceeding to the long-term goal of a CO_2 mitigation and biofuels capture process. For example, wastewater treatment systems provide a unique opportunity as a sink for CO_2, while also treating and beneficially converting wastewaters to fuels. Seawater is probably the major available water resource for such algal production systems, which can also be used for bivalve aquaculture and other applications. Although eventually such R&D projects should be coupled directly to power plant flue gas utilization, the demonstrated ability of microalgae to grow on actual and simulated flue gases makes makes this a less immediate issue. Demonstration of culture stability, high productivities, easy harvesting and high contents of lipids are more pressing R&D needs. Such an R&D program should closely integrate outdoor pond research (at the 100 to 1,000 m^2 scale) with laboratory studies, including genetic engineering for strain improvement, to achieve rapid progress towards the goal of CO_2 mitigation and biofuels production.

REFERENCES

Benemann, J.R. 1990. "The Future of Microalgae Biotechnology". In R.C. Cresswell, et al., eds., Algal and Cyanobacterial Biotechnology, 317-337 Longman, London.

Benemann, J.R. 1994. "Systems and Economic Analysis of Microalgae Ponds for Conversion of CO_2 to Biomass". In 10th Annual Coal Preparation, Utilization, and Environmental Control Contractors Conf. Proceed. Vol I. pg. 255 (1994).

Benemann, J.R., and D.M. Tillett. 1987. "Microalgae Lipid Production". In D. Klass, ed., Symp. Proc. Energy Biomass Wastes XI, Inst. Gas Tech. Chicago, IL.

Benemann, J.R., R.P. Goebel, J.C. Weissman, D.C. Augenstein. 1982. Microalgae as a Source of Liquid Fuels, Final Report U.S. Department of Energy, pp. 202.

Benemann, J.R. and W.J. Oswald. Systems and Economic Analysis of Microalgae Ponds for Conversion of CO_2 to Biomass. Final Report to PETC (June 1995).

Burlew, J., ed. 1953. Algae Culture: From Laboratory to Pilot Plant, Carnegie Institute, Washington D.C.

Brown, L.M., S. Sprague, E.E. Jarvis, T.G. Dunahay, P.G. Roessler, and K.G. Zeiler, Biodiesel from Aquatic Species Project Report: FY 1993, NREL/TP -442-5726, Golden CO (1994).

Hamasaki, A., et.al., Carbon Dioxide Fixation by Microalgal Photosynthesis Using Actual Flue Gas from a Power Plant", App. Biochem. Biotech. in press (1995)

Neenan, B., et al. 1986. Fuels from Microalgae: Technology Status, Potential, and Research Requirements. Solar Energy Res. Inst, Golden CO,

Oswald, W.J., and C.G. Golueke. Adv. Appl. Microbiol., 11: 223 - 242 (1960).

Regan, D.L., and G. Gartside, Liquid Fuels from Microalgae in Australia, (1983).

Weissman, J. C. and R. P. Goebel. 1987. Design and Analysis of Pond Systems for the Purpose of Producing Fuels, Solar Energy Res. Inst., Golden CO.

Weissman, J.C. and D.T. Tillett, 1989, 1992. "Design and Operation of an Outdoor Microalgae Test Facility". In Aquatic Species Program, Annnual Reports, Solar Energy Res. Inst. (1989) and Natl. Ren. Energy Lab. (1990), Golden, CO.

BIOLOGICAL HYDROGEN PRODUCTION

J. R. Benemann
Department of Civil Engineering
University of California Berkeley
Berkeley, CA 94720

ABSTRACT

Biological hydrogen production can be accomplished by either thermochemical (gasification) conversion of woody biomass and agricultural residues or by microbiological processes that yield hydrogen gas from organic wastes or water.

Biomass gasification is a well established technology; however the synthesis gas produced, a mixture of CO and H_2, requires a shift reaction to convert the CO to H_2. Microbiological processes can carry out this reaction more efficiently than conventional catalysts, and may be more appropriate for the relatively small-scale of biomass gasification processes. Development of a microbial shift reaction may be a near-term practical application of microbial hydrogen production.

Microbial processes for producing hydrogen directly can be classified as fermentations, which require substrates such as organic wastes, and biophotolysis, the production of hydrogen (and oxygen) from water with microalgae. Microbial dark fermentations of organic wastes produce relatively little hydrogen, when compared to microbial methane yields under similar conditions. Development of dark anaerobic fermentations that produce higher yields of H_2 from organic wastes must be a major goal of R&D in this field. Photosynthetic bacteria have been used to boost yields in such waste fermentations, but low solar conversion efficiencies and the complexities of the required photobioreactors limit their potential.

Biophotolysis can result in direct, simultaneous, sustained, and highly efficient, H_2 and O_2 production from water. However, this has been only demonstrated under rather restrictive laboratory conditions. One problem is O_2 inhibition of H_2 evolution. Some microalgae system can overcome such O_2 inhibition by separating the H_2 and O_2 production reactions and coupling them through CO_2 fixation and metabolism. The nitrogen-fixing cyanobacteria (blue-green algae) can be used in such processes, but suffer from low efficiencies. A promising system is a two stage process in which green microalgae are grown in open ponds and then transferred to separate anaerobic reactors for hydrogen evolution, both in the dark and light. A preliminary feasibility analysis suggests that such a process could be competitive with photovoltaic hydrogen production. In the longer-term, the goal should be to overcome the O_2 inhibition in direct biophotolysis to allow the simultaneous production of H_2 and O_2 from water and sunlight. Recent research, supported by PETC, in photosynthesis and H_2 production suggest that the efficiency of photosynthesis in such a reaction can be much higher than previously thought.

INTRODUCTION

Biological processes can be used to produce a variety of biofuels: solid fuels (wood, straw, residues, etc.), alcohols, biodiesel, biogas, synthesis gas, and H_2 (Benemann, 1980). The two major routes for biological H_2 production are:

1. Gasification of woody and other lignocellulosic biomass, followed by the shift reaction to convert the CO in the synthesis gas to H_2, and
2. Microbiological H_2 production from organic wastes and directly from water.

Here these processes are briefly reviewed, with an emphasis on the development of processes for the production of hydrogen from water and sunlight - biophotolysis. A report on this subject was recently completed for PETC (Benemann, 1995).

THE MICROBIAL SHIFT REACTION

The technologies for biomass gasification to produce H_2 (Larson and Katofsky, 1992; Ogden and Nitsch, 1992) are much more advanced than microbial processes, which are mostly still at the laboratory, or even conceptual stage. Biomass gasification is currently the only technologically available process for hydrogen production from biomass, and is being developed with DOE funding. However, the relatively small scale of biomass gasification, imposed by availability and high costs of transportation of biomass, makes even this process relatively uneconomical, at least with current fossil fuel prices and conventional gasification-shift reaction technologies. The use of microbial catalysts to carry out the shift reaction could lower the costs and improve the overall prospects of this technology.

The shift reaction involves the conversion of CO and H_2O to H_2 and CO_2. The fundamental advantage of the microbial shift reaction is that it is carried out at room temperature, where the thermodynamic equilibrium favors H_2 formation. At higher temperatures only a partial conversion takes place and the CO and H_2 have to be separated, and the CO recycled. The microbial shift reaction, first discovered about 20 years ago (Uffen, 1976), is carried out by a number of photosynthetic bacteria that can catalyze this reaction in the dark (where they do not grow). This reaction has most recently been studied by two groups in the U.S. (Klasson et al., 1993; Weaver et al., 1993). The latter isolated over 400 strains of such bacteria and demonstrated rates of H_2 formation of 1.5 mmole H_2/min/gram cell dry weight, about ten times higher than the rates reported from the former study.

A microbial shift reaction process has been demonstrated at the bench-scale, in which the bacteria are grown in a separate reactor, immobilized on a support, and operated as a gas-phase microbial biofilter (Weaver, 1995). Stable operations for several weeks were noted. Large-scale microbial biofilters are used in industry for a variety of air decontamination and gas clean-up applications. Thus, scale-up of this process appears possible. A feasibility analysis would be of interest.

DARK FERMENTATIONS

Hydrogen evolution from organics can be accomplished in the dark by a variety of microbes, through action of well studied anaerobic metabolic pathways and hydrogenase enzymes. In most such systems the H_2 is derived from rather easily metabolizable substrates, such as starches and glucose, in a relatively rapid process. Microbial cultures can even metabolize the more difficult to convert cellulose and hemicelluloses in woody and herbaceous biomass (lignocelullosics), and produce some H_2, although at a much slower rate an with very low yields. Indeed, dark fermentations have generally low yields, only about 10% of stoichiometric, and the H_2 is evolved at typically only relatively low partial pressure (>0.1 atmospheres).

This discouraging state of affairs is due to the thermodynamic limitations of H_2 production: although the anaerobic conversion of glucose (and other substrates) to H_2 is slightly favored thermodynamically, microbes can not obtain sufficient energy for growth from such a process unless the partial pressure of hydrogen is kept very low. Also, in nature, and the laboratory, such fermentation systems can be quickly colonized by methane producing bacteria, that can convert even traces of hydrogen to methane gas. Therefore, fermentative hydrogen evolution is rather rare in nature, being limited to a few restricted microbial populations, for example in termite guts and occasionally even human intestines.

In principle, the thermodynamic limitations to dark, anaerobic, fermentative hydrogen production should not be an insurmountable obstacle to such a process: the energy yielding (catabolic) reactions in cells might be decoupled (chemically, metabolically, or genetically) from the hydrogen producing (anabolic) ones, by decoupling growth from hydrogen evolution, as in the case of the CO shift reaction.

In practice, such a process faces several difficulties. As it must be carried out in "open" systems, as sterilizable bioreactors are much too expensive, contamination by, in particular, methane gas producing bacteria, is a potential problem. This is particularly true for the conversion of the slow to degrade lignocellulosic materials. Thus, conversion of more readily decomposable wastes, such as food processing wastes, would be more likely. Indeed, in Japan a continuous, stable (>2 months), fermentation of sugar mill wastes to hydrogen was demonstrated at the bench-scale, with yields of about 20% H_2 (from what was expected if all fermentable material was dissimilated) at a partial pressure of about 0.5 atmospheres (Morimoto, 1994). In Europe there also has been recent interest in hydrogen fermentations (Solomon et al., 1995).

Due to the above difficulties, both actual and perceived, relatively few studies have been published on hydrogen production by bacterial fermentations, at least when compared to hydrogen production by photosynthetic bacteria and microalgae, discussed next. However, this neglect is perhaps not wholly justified and more research in this area is warranted.

PHOTOFERMENTATIONS

One method for overcoming the limitations of dark fermentations is by adding an exogenous energy source, which can drive the H_2 evolution reaction to completion. The simplest such energy source is light. Almost 50 years ago it was discovered that photosynthetic bacteria can evolve H_2 (Gest and Kamen, 1949). These bacteria grow in the light under anaerobic conditions on a variety of organic substrates. When nitrogen is limiting, they can exhibit relatively high rates of H_2 evolution, completely breaking down a variety of organic substrates to H_2 (and CO_2), at high partial pressures of H_2 (even above 1 atmosphere).

These almost ideal properties suggested H_2 production from organic wastes by photosynthetic bacteria, "photofermentations", as a better choice than the dark fermentation processes discussed above. Indeed, over the past two decades considerable work by over a score of laboratories around the world has been carried out to develop H_2 production by these bacteria (Sasikala et al., 1993).

However, there are several limitations to this concept. The hydrogen production reaction in photosynthetic bacteria is due to a side reaction of the nitrogenase enzyme, and only takes place in the absence of N_2 gas. It is, essentially, an artifact of the laboratory, although that is no detriment per se. The problem is that the nitrogenase reaction requires large amounts of metabolic energy to drive the hydrogen evolution reaction. This metabolic energy must be supplied by the photosynthetic processes in these bacteria.

As light energy is diffuse, relatively large areas must be covered to capture the sunlight required by the process. And to capture the H_2 gas, the photosynthetic bacteria must be contained in a transparent an H_2 impermeable photobioreactor. Such a reactor could only be economically justified if the conversion efficiency of light energy into H_2 is very high. However, the highest reported efficiencies for H_2 evolution by photosynthetic bacteria are only about 5% of light energy converted into H_2 energy. At full solar intensities conversion efficiencies are much lower. And this efficiency calculation does not consider the energy content embodied in the organic substrates, which is similar to that of the H_2 produced.

However, even assuming that the problems of low efficiency could be overcome, the requirement for a cheap (preferably waste), fermentable substrate would be difficult to meet in most situations where small-scale hydrogen production would be desired. Indeed, the use of photofermentative hydrogen production as a method of waste treatment, which has been argued to justify such a process, must be considered speculative at present.

In conclusion, it would appear that the limitations of dark fermentations would be more easily overcome than those of photofermentations, and appear to be a better focus for future research in this area.

BIOPHOTOLYSIS

If H_2 is to be produced by photosynthetic microbes, water, not organics, would be a better substrate. This concept of a biological decomposition of water into H_2 and O_2 by sunlight, also termed biophotolysis, has attracted considerable attention for the past 20 years. Although initially cell-free systems were used (Benemann et al., 1973), such systems are primarily useful as models and for fundamental research, rather than practical approaches to hydrogen production. Using microalgae as the converters of solar into hydrogen energy, has several advantages, primarily the stability and inherently low cost of these self-replicating solar converters.

The field of basic and applied biophotolysis R&D with microalgae has generated hundreds of publications, and consumed tens of millions of dollars over the past two decades (Benemann, 1995). However, little progress has been made in moving this technology from the conceptual to the practical. There are several reasons.

First, the biological processes for hydrogen production are not very efficient. of In the laboratory conversion efficiencies equivalent to a maximum of about 10% of total solar energy can be demonstrated, similar to the efficiencies already achieved by commercial photovoltaic systems outdoors. And such high efficiencies were demonstrated in the laboratory for an algal process that simultaneously produced H_2 and O_2 from water (Greenbaum, 1988). However, these experiments were conducted under low light intensities; under full sunlight, the best conversion solar efficiencies for photosynthesis (microalgae or plants) are only about 3 to 4% of total solar energy, and even such efficiencies have not yet been demonstrated with hydrogen production systems. Although many factors (such as respiration) limit these efficiencies, the most important limitation is the low light intensity at which photosynthesis by algae, and higher plants generally, saturates.

The problem is that microalgae, like other plants, when exposed to full sunlight can use only a fraction, of the absorbed photons, with the remainder (typically about 50 - 80%) being wasted as fluorescence, heat, etc. Fundamentally, this is due to the high levels of light absorbing pigments, which results in more photons absorbed at high sunlight than can be used at high light intensities. The solution to this problem, already recognized several decades ago, is to reduce the "antenna" pigment levels, by genetic or metabolic means. Then solar conversion efficiencies should approach 10% conversion efficiency even in full sunlight (Benemann, 1990).

A second, major, problem is that the O_2 generated during water splitting, is a strong inhibitor of hydrogen evolution. Thus, a direct splitting of water into H_2 and O_2 by microalgae can only be demonstrated for sustained periods when the O_2 tensions are kept very low, as by addition of a chemical absorber or by rapid purging of the reaction vessel with an inert carrier gas (Greenbaum, 1980). Such conditions could not be scaled-up or reproduced outside a laboratory setting. Thus there is great interest in the development of oxygen stable H_2 evolving systems.

As alternatives to oxygen stable hydrogen evolution, indirect processes can be considered: the algae first fix CO_2 into starches (carbohydrates) (while simultaneously generating O_2 from water, in a conventional photosynthetic process), and then these carbohydrates are converted to H_2 gas in a second anaerobic reaction, either temporally or spatially separated from the water splitting reaction, thus avoiding the oxygen inhibition of the reaction.

Probably the single most studied of such systems uses heterocystous cyanobacteria (blue-green algae). These filamentous algae differentiate special cells, the heterocysts, found evenly spaced along the vegetative cells in the filaments, approximately every tenth to twentieth cell. Heterocysts are the site of nitrogen fixation, and protect the oxygen labile nitrogenase reaction from photosynthetically generated O_2. Thus, heterocysts are able to evolve H_2 (in the absence of N_2 gas), and this property can be used to simultaneously produce O_2 and H_2 from water (with CO_2 serving as an intermediate) with these algae (Benemann and Weare, 1974). However, the heterocyst system suffers from significant shortcomings, including low efficiencies (again due in part to the energetic costs of nitrogenase), and the need to separate H_2 from O_2 in the gas phase. Most important, the entire culture system would must be contained in a photobioreactor that allows capture of the H_2 gas. This would appear to be prohibitive at present.

Non-heterocystous cyanobacteria have also been studied extensively for hydrogen production, in a process that as temporally separates the H_2 and O_2 evolution reactions. Such a temporal separation, possibly on a diurnal time scale, would allow pumping the cultures through several stages (bioreactors), of different design, sizes, etc. Unlike the heterocystous algae, the entire surface of the conversion system need not be covered to allow for H_2 recovery: the CO_2 fixation stage could be carried out in open ponds, similar to those already being studied for production of C-containing fuels and CO_2 mitigation (Benemann, 1995, in these Proceedings).

However, even in this case, the reliance on nitrogenase for H_2 evolution would require that a large fraction, approaching half of the total surface area, would still need to be devoted to photobioreactors and H_2 recovery. In short, nitrogenase based H_2 production systems have too low potential solar conversion efficiencies, only about half of H_2 production by reversible hydrogenases, to achieve realistic efficiency and cost goals for such a process.

H_2 production by green algae appears to be inherently the most favorable approach to developing a practical biophotolysis process. In this concept, just as in the case of the non-heterocystous blue-green algae, a temporal, or more likely spatial, separation of the H_2 and O_2 evolution reactions is the case, with these reactions coupled through CO_2 fixation and metabolism.

However, in this case the reversible hydrogenase, rather than nitrogenase, would be responsible for the hydrogen produced. As this enzyme does not require

ATP for H_2 evolution, this greatly reduces the energy requirements, and thus area, for the H_2 production stage. Indeed, it may be possible to extract at least a fraction of the hydrogen in a dark, anaerobic reaction (required, anyway, to induce the hydrogenase activity of the algae). Overall as little as 10% of the total area may be sufficient for the hydrogen production stage, greatly reducing the area (and costs) of the photobioreactors for hydrogen capture and recovery (see Benemann, 1995 for a preliminary feasibility analysis of this concept).

Recently a combined system, based on both green algae and photosynthetic bacteria, was demonstrated in Japan at a small ($< 5\ m^2$) stage (Akano et al., 1995). In this process, two (appx. $2\ m^2$) open ponds were used to cultivate the green alga Chlamydomonas, which accumulates starch. Concentrating and placing the culture under anaerobic conditions resulted in the fermentation of the accumulated starch into various products (acetate, ethanol, etc., including some H_2). After fermentation was complete the algae were recycled to the growth ponds. The fermentation products, after further concentration, were fed to appx. $0.5\ m^2$ photobioreactors containing photosynthetic bacteria, resulting in hydrogen production. Although efficiencies were low ($< 0.3\%$ of total solar), and the process complex, it does demonstrate the feasibility of moving from conceptual and laboratory processes to scale-up and process engineering. The next challenge would be to replace the photosynthetic bacterial stage by a light driven hydrogen production by the green algae themselves.

CONCLUSIONS

This brief overview suggests that photobiological hydrogen production is still in its infancy, at an early stage in development. However, there are several interesting and important research issues, whose resolution could not only significantly improve the prospects for biological hydrogen production but also have applications in other fields. One such problem is the development of dark fermentation that exhibit high yields ($> 50\%$, based on input organics) at high partial pressures ($> 20\%$) of H_2. Another is the demonstration of high solar conversion efficiencies at full solar intensities by microalgae cultures. These objectives might be achieved by genetic and metabolic manipulations.

Indeed, the recent discovery by Greenbaum et al. (1995) that mutants of Chlamydomonas missing photosystem I (one of the two complexes involved in algal and plant photosynthesis) still can evolve H_2 and O_2, and fix CO_2, demonstrates the power of the combined genetic/physiological approach. This major discovery, funded in part by PETC, could provide insights in how to significantly increase overall photosynthetic efficiency, not only in H_2 production but also in CO_2 fixation and plant productivity generally. Indeed, it suggests that despite the inherent difficulties of a simultaneous H_2 and O_2 production process, continued R&D in this area could lead to practical applications.

REFERENCES

Akano, T., et al., "Hydrogen Production by Photosynthetic Microorganisms". 17th Symp.on Biotech. Fuels and Chemicals, May 10, 1995, Vail Colorado.

Benemann, J.R., J.A. Berenson, N.O. Kaplan, and M.D. Kamen. "Hydrogen Evolution by a Chloroplast-Ferredoxin-Hydrogenase System." Proc. Nat. Acad. Sci. USA, System." Proc. Nat. Acad. Sci. USA, 70: 2317-2320 (1973).

Benemann, J.R., and N.M. Weare, "Hydrogen Evolution by Nitrogen-Fixing Anabaena cylindrica Cultures." Science 184, 1917 - 1919 (1974).

Benemann, J.R. "Biomass Energy Economics." Intl. Energy J. 1 107-131 (1980).

Benemann, J.R., "The Future of Microalgae Biotechnology", in R.C. Cresswell, et al., eds., Algal Biotechnology, pp. 317-337 (1990).

Benemann, J.R., Photobiological Hydrogen Production. Report to PETC (May 1995).

Benemann, J.R., "CO_2 Capture and Biofuels Production with Microalgae". These Proceedings (1995).

Gest, H., and M.J. Kamen. "Photoproduction of Molecular Hydrogen by Rhodospirillum rubrum". Science, 109: 558 -559 (1949).

Greenbaum, E. J.W. Lee, C.V. Tevault, S.L Blankinship, and L.J. Mets. "Carbon Dioxide Fixation and Photoevolution of Hydrogen and Oxygen in a Mutant of Chlamydomonas lacking Photosystem I". Nature, in press (1995).

Greenbaum, E., "Simultaneous Photoproduction of Hydrogen and Oxygen by Phtosynthesis" Biotech. Bioeng. Symp. 10: 1-13 (1980)

Greenbaum, E., Energetic Efficiency of Hydrogen Photoevolution by Algalg Water Splitting. Biophys. J., 54: 365 - 368 (1988).

Klasson, K.T., A. Gupta, E.C. Claussen, and J.L. Gaddy, "Evaluation of Mass-Transfer and Kinetic Parameters for Rhodospirillum rubrum in a Continuous Stirred Tank Reactor". App. Biochem. Biotech., 39/40: 549-557 (1993).

Larson, E.D., and R.E. Katofsky, "Production of Hydrogen and Methanol via Biomass Gasification", In Adv. Thermochemical Biomass Conversion (1992).

Morimoto, K. Presentation, 10th World Hydrogen Energy Conf., Cocoa Beach, FL June 23, 1994

Ogden, J.M. and J. Nitsch, "Solar Hydrogen", in T.B. Johansson et al., eds., Renewable Energy, Island Press, Washington D.C., pp. 925-1010 (1992)

Sasikala, K., Ch.V. Ramana, P. R. Rao, and K.L. Kovacs, Anoxygenic Phototrophic Bacteria: Physiology and Advances in Hydrogen Technology", Adv. Appl. Microbiology, 38: 211 295 (1993)

Solomon, B.O., et al., "Comparison of the energetic efficiencies of hydrogen and oxychemicals formation in Klebsiella pneumoniae and Clostridium butyricum during anaerobic growth on glycerol. J. Biotech., 39: 107- 117 (1995).

Uffen, R.L., Proc. Natl. Acad. Sciences, U.S. 73: 7298 (1976).

Weaver, P. "Microbial Hydrogen Production". Annual Review Meet. DOE Office of Utility Technologies Hydrogen Program, Cocoa Beach, April 18-21 (1995).

Weaver, P., P.C. Maness, A. Frank, M. Lange, and J. Blaho, "Photobiological Hydrogen Production Using Whole-Cell or Cell-Free Systems." In Proc. 1993 DOE/NREL Hydrogen Program Review, Cocoa Beach, FL May 4-6 (1993).

CATALYSTS FOR THE REDUCTION OF SO_2 TO ELEMENTAL SULFUR

Y. JIN, Q. Q. YU, and S. G. CHANG
ENERGY & ENVIRONMENT DIVISION
LAWRENCE BERKELEY LABORATORY
BERKELEY, CA 94720

Catalysts have been prepared for the reduction of SO_2 to elemental sulfur by synthesis gas. A catalyst allows to obtain more than 97% yield of elemental sulfur with a single-stage reactor at 540°C. A lifetime test has been successfully performed. The mass balance of sulfur and carbon has been checked. The effect of H_2S, COS, and H_2O has been studied.

INTRODUCTION

Combustion of coal emanates flue gas containing SO_2, a pollutant causing acid rain and visibility reduction in the atmosphere. Several regenerable SO_2 scrubbing system have been developed. In these processes, sulfur dioxide from flue gas is first absorbed into an alkaline solution or adsorbed on a solid substrate, and is subsequently desorbed to produce a stream of high concentration SO_2. It is desirable to convert SO_2 to elemental sulfur for storage, transportation, and/or conversion to valuable chemicals.

Existing technologies for SO_2 conversion to elemental sulfur require multi-stage Claus reactors to achieve desirable yield. Prior to entering the Claus reactors, a proper portion of SO_2 in the gas stream must be reduced to H_2S either catalytically or by the combustion in a hydrocarbon flame under reduced conditions. A simpler process is desirable to convert SO_2 to elemental sulfur.

Sulfur dioxide can be reduced with synthesis gas to produce elemental sulfur at elevated temperatures. The reduction can be facilitated with catalysts. In addition to elemental sulfur, these reactions may produce several undesirable byproducts. These include hydrogen sulfide, carbonyl sulfide, carbon disulfide, and elemental carbon. Numerous research efforts have been carried out to develop catalysts for selective production of elemental sulfur at low temperatures. However, the results [1-4] obtained so far show only limited successes and do not warrant a commercial application. The development of a catalyst capable of obtaining very high yield of sulfur with a high space velocity at low temperatures would be required to warrant a commercial application.

EXPERIMENTAL SECTION

Catalyst Preparation

Catalysts were composed of a combination of several metal oxides supported on Al_2O_3. Two sizes of Al_2O_3 were used: 1. 30-40 mesh particles, and 2. 3mm dia. by 5 mm height granules. By mixing appropriate amounts of metal nitrate solutions with Al_2O_3, the mixture underwent stepwise heating to form the activated catalyst. The ratio of the active catalyst to carrier was about 0.3 by weight.

Apparatus and Procedure

The experimental setup consists of three separate sections: the gas supply section, the main reactor, and the detection and analysis section. Gases are supplied from compressed gas cylinders to flow meters before entering a gas mixer. The tubular reactor is fabricated from a 1.4-cm-o.d. with a 1-mm wall thickness quartz tube. The entire reactor is mounted inside a tubular furnace. A thermocouple, reaching the center of the catalytic reactor, provide measurement of the temperature of catalytic reactions. After the last section of the reactor, the gases pass through a sulfur collector at room temperatures, and then enter into an on-line trap cooled in an ice bath to condense water before entering a six-port sampling valve which is used to inject the products of the catalytic reactions into the gas chromatograph. Finally, the exit gases pass into a scrubber containing concentrated NaOH. The inlet and exit gases are analyzed by using a gas chromatograph

RESULTS AND DISCUSSION

In order to study the kinetics of the reactions and the diffusivity of the reactants, two carrier sizes were used. The smaller size carrier is 30-40 mesh Al_2O_3 particles, which were used typically in laboratory scale experiments to obtain kinetic information. The larger size carrier has a dimension of 3 mm diameter by 5 mm height cylindrical granules, which were used in scale up tests. The parametric studies were conducted on particles and granules for comparison. The lifetime experiments were performed on particles.

Particles (30-40 mesh)

Parametric Studies. The effect of temperatures, space velocity, molar ratios of reductants to SO_2 ($R = F_{(H2 + CO)}/F_{SO2}$), and molar ratios of H_2 to CO ($r = F_{H2}/F_{CO}$) on the activity of the catalyst (Cat-S) were investigated.

Figure 1 shows the results of the temperature dependence study. The experiments were carried out at r= 0.75 and R= 2, and at a space velocity of 10,000 h^{-1} with 1 g of the Cat-S. The Y_{S2} reaches 94.4 % at 480 C.

The effect of space velocity on the activity of Cat-S is shown (Figure 2). The experiments were performed at r= 0.75 and R= 2, and at 480 C with 1 g of the Cat-S. The results indicated that there was little effect on the yield of elemental sulfur over the ranges from 5,000 h^{-1} to 15,000 h^{-1}, this yield lies between 90.0 and 95.9 %. The selectivity of elemental sulfur increases with an increase of space velocity.

The effect of R on the catalyst activity is depicted in Figure 3. The experiments were conducted at r = 0.75, space velocity = 10,000 h^{-1}, and at 480 C. The results show that the optimum operating conditions should be at R = 2, when the Y_{S2} reached 93.5 %. The Y_{S2} and the C_{SO2} decreased when R was less than 2.

Synthesis gas derived from natural gas contains a molar ratio of H_2 to CO approaching 3. Therefore, a separate set of parametric studies was carried out at r = 3. The effect of temperature, space velocity, and R on the conversion of SO_2 and the yield of products was investigated.

Lifetime Tests. The lifetime test was carried out continuously for 1080 h (45 days). The results indicate that the activity of the Cat-S is very stable and does not show any changes during the entire 1080 h of the lifetime test. Figure 4 shows that the yield of elemental sulfur ranges between 93.1 and 96.5 %, which is far superior to results so far reported in the literatures [2,3,4]. These high yields were achieved at a space velocity of 10,000 h^{-1} , compared with a reported result of obtaining 69.3 - 72.8 % yield of elemental sulfur at a space velocity of 2,000 h^{-1}, and a 82.8 % sulfur yield at a space velocity of only 500 h^{-1}.

Mass Balance. The mass balance of the reaction has been performed. The sum of carbon monoxide conversion to carbon dioxide and carbonyl sulfide is $C'_{CO} = Y_{CO2} + Y_{COS}$. The average value of C_{CO} and C'_{CO} from ten experiments are 99.1% and 97.4% respectively, which indicates that carbon monoxide is essentially converted to either carbon dioxide or carbonyl sulfide.

The conversion of sulfur dioxide to hydrogen sulfide, carbonyl sulfide and elemental sulfur was measured to determine the mass balance of sulfur: $C = Y_{H2S} + Y_{COS} + Y_{S2}$. The solid elemental sulfur was collected and weighted, and was found to be about 90% of the theoretical value. It was difficult to obtain a complete recovery of elemental sulfur from the wall of the tubings and vessels. It was likely that the remaining 10% of sulfur stayed on the wall and could not be recovered.

Granules (d. 3 mm x h. 5 mm)

Parametric Studies. The effect of temperature, space velocity, and molar ratio of reactants on the activity and selectivity of the Cat-S catalyst on granules was studied. The yield of sulfur reaches 97.8% at 560 C and a space velocity of 2100 h^{-1} with synthesis gas derived from methane (i.e. r = 3).

The effect of the space velocity on the catalyst for r = 0.4, 0.75, and 3 was studied at three temperatures, 560, 520, and 480°C. The results indicate that C_{SO2}, Y_{H2S}, and Y_{S2} decrease, while Y_{COS} increases along with the increase of the space velocity. S_{S2} remains fairly constant under the experimental conditions employed.

The effect of R on the Cat-S at r = 0.4, 0.75, and 3 was studied at 560, 520, and 480°C respectively. The results indicate that at a given r value, C, Y_{H2S}, and

Y_{COS} show a slight increase along with the increase of R until R reaches 2. Beyond that however, Y_{H2S} exhibits a drastic growth with the increase of R; Y_{COS} also shows some growth with R, but to a much lesser extent than Y_{H2S}. It is obvious that Y_{S2} is the greatest when R is 2 regardless of the ratio of r.

The Effect of Contaminants. Experiments were conducted to determine the effect of contaminants: H_2S, COS, and H_2O. The addition of H_2S and COS does not change the yield of elemental sulfur to any appreciable amount, nor does it increase the yield of the H_2S and COS byproducts. The addition of a large amount of H_2O vapor (15%) results in an increase of the Y_{COS} and thus a decrease of Y_{S2} at low temperatures. The H_2O effect decreases along with the increase of the reaction temepratures; this effect becomes negligible at a temperature of about 440 C when the Y_{S2} is identical.

High Efficiency Recovery. The operating conditions of the Cat-S (granules) to obtain a Y_{S2} of more than 96 % have been determined. Y_{S2} reaches between 96.9% and 97.1% at 520°C and a space velocity from 1,800 h^{-1} to 2,000 h^{-1}; further increase of space velocity to 3,000 h^{-1}, Y_{S2} decreases to 93%. To achieve a Y_{S2} of 96% at a space velocity of 3,000 h^{-1}, the temperature of the catalytic reactions would have to be increased to 580°C.

CONCLUSION

We have developed a catalyst for reduction of SO_2 by synthesis gas. This catalyst is composed of a mixture of inexpensive transition metal oxides supported on alumina. The inventive catalyst can achieve a high conversion efficiency of SO_2 by synthesis gas with a high selectivity to elemental sulfur. Unlike the Claus process, the reaction of SO_2 with synthesis gas to form elemental sulfur is not a reversible process. As a result, a high efficiency recovery of sulfur can be achieved in a single stage reactor.

A lifetime (1080 h) test has been successfully performed. The activity of the catalyst remains very stable during the entire period of the lifetime test. The mass balance of sulfur and carbon has been checked satisfactory.

This catalyst (in granule form) can achieve 97% yield of elemental sulfur at 540 C with a space velocity of 2,000 h^{-1} or at 640 C with a space velocity of 3,000 h^{-1}.

It has been demonstrated that the contaminants, H_2S, COS, and H_2O do not affect the performance of the catalyst to any appreciable extent.

The inventive catalyst possesses very promising properties. As such, it could be utilized as a basis to develop a new process for high efficiency conversion of SO_2 to elemental sulfur by synthesis gas at a more cost effective manner than technologies available currently.

ACKNOWLEDGEMENT

This work was supported by the Assistant Secretary for Fossil Energy, U.S. Department of Energy, under Contract DE-AC03-76SF00098 through the Pittsburgh Energy Technology Center, Pittsburgh, PA.

REFERENCES

(1). Akhmedov, M.M., Shakhtakhtinskii, G. B., Agaev., A.I., Azerb. Khim. Zh. (2) 95 (1983).

(2). Akhmedov, M.M., Gezalov, S.S., Agaev, A.I., Mamedov, R.F., Zh. Prikl. Khim., 61, (1) 16 (1988).

(3). Akhmedov, M.M., Guliev, A.I., Agaev, A.I., Gezalov, S.S., Zh. Prikl. Khim., 61, (8) 1891 (1988).

(4). Akhmedov, M.M., Guliev, A.I., Ibragimov, A.A., Khim. Prom. (1), 37 (1989).

Fig. 1 The effect of temperature on the Cat-S (particles) at H_2/CO=0.75, S.V. =10,000 h^{-1}, $(H_2+CO)/SO_2$=2.

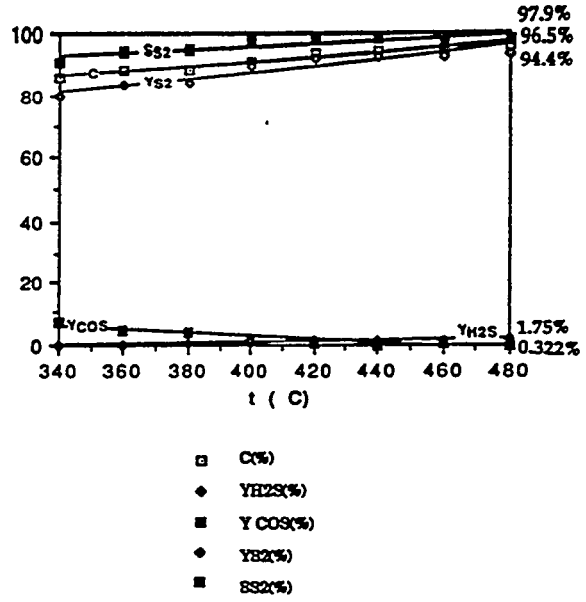

Fig. 2 The effect of space velocity on the Cat-S (particles) at H_2/CO=0.75, $(H_2+CO)/SO_2$=2, 480°C.

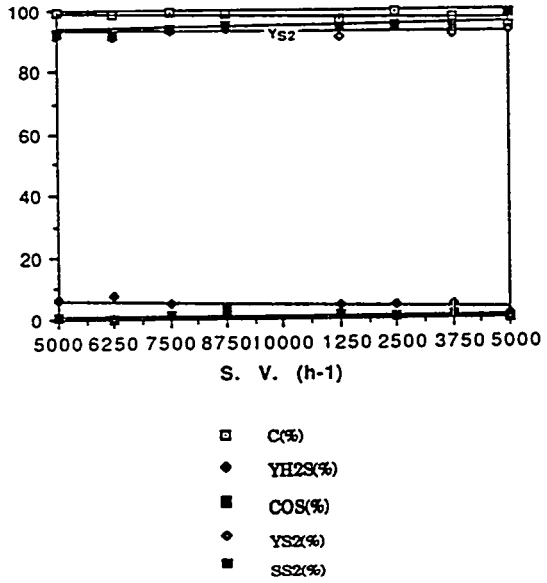

Fig. 3 The effect of molar ratio of reactants on the Cat-S (particles) at H_2/CO=0.75, S.V.=10,000 h^{-1}, 480°C.

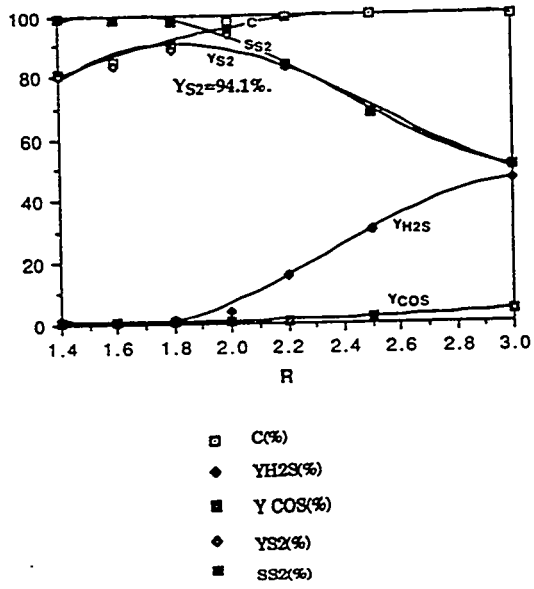

Fig. 4 The yield of sulfur as function of reaction time (H_2/CO)=3, $(H_2+CO)/SO_2$=2, S.V. =10,000 h^{-1}, 480°C.

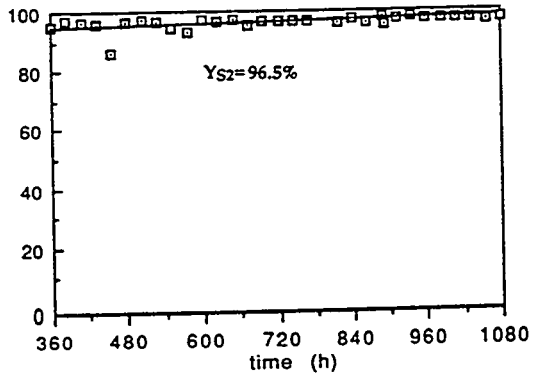

Fig. 5 The effect of 15% H_2O on the Cat-S (particles) at (H_2/CO)=0.75, S.V. =10,000 h^{-1} at varying temperatures.

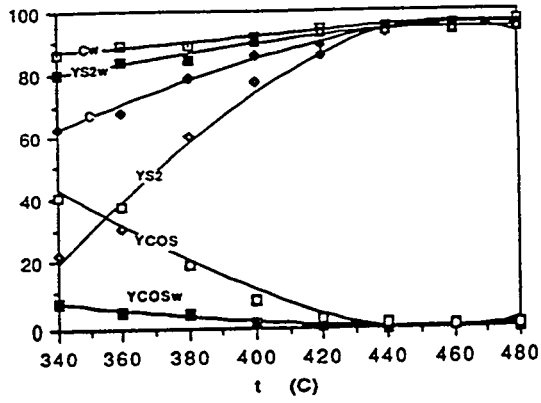

HIGH-EFFICIENCY SO_2 REMOVAL IN UTILITY FGD SYSTEMS

JAMES L. PHILLIPS, SENIOR STAFF ENGINEER
STERLING GRAY, SENIOR ENGINEER
DAVID DEKRAKER, SENIOR ENGINEER
GARY M. BLYTHE, PRINCIPAL ENGINEER
RADIAN CORPORATION, AUSTIN, TEXAS

INTRODUCTION

The U.S. Department of Energy (DOE) and the Electric Power Research Institute (EPRI) have contracted with Radian Corporation to conduct full-scale testing, process modeling, and economic evaluations of six existing utility flue gas desulfurization (FGD) systems. The project objective is to evaluate low capital cost upgrades for achieving up to 98% sulfur dioxide (SO_2) removal efficiency in a variety of FGD system types. The systems include dual-loop, packed absorbers at Tampa Electric Company's Big Bend Station; cocurrent, packed absorbers at Hoosier Energy's Merom Station; dual-loop absorbers with perforated-plate trays at Southwestern Electric Power Company's Pirkey Station; horizontal spray absorbers at PSI Energy's Gibson Station; venturi scrubbers at Duquesne Light's Elrama Station; and open spray absorbers at New York State Electric and Gas Corporation's (NYSEG's) Kintigh Station. All operate in an inhibited-oxidation mode except the system at Big Bend (forced oxidation), and all use limestone reagent except the Elrama system (Mg-lime).

The program was conducted to demonstrate that upgrades such as performance additives and/or mechanical modifications can increase system SO_2 removal at low cost. The cost effectiveness of each upgrade has been evaluated on the basis of test results and/or process model predictions for upgraded performance and utility-specific operating and maintenance costs. Results from this program may lead some utilities to use SO_2 removal upgrades as an approach for compliance with Phase 2 of Title IV of the Clean Air Act Amendments (CAAA) of 1990. This paper summarizes the results of testing, modeling, and economic evaluations that have been completed since July 1994.

EXPERIMENTAL METHODS

The test program at each FGD system has typically consisted of three phases. The first phase is baseline testing where the SO_2 removal performance of a single, representative absorber module is measured at normal operating conditions. The baseline tests also involve measuring SO_2 removal efficiencies over a range of conditions, such as varied slurry pH set points and absorber liquid-to-gas (L/G) ratios, to obtain data to calibrate EPRI's FGDPRISM (FGD Process Integration and Simulation Model) to that system. The calibrated model is then used to predict the SO_2 removal capabilities of the system, including upgrades. Next, the best performance additives and/or upgrades are selected and a parametric test series is run to evaluate the effectiveness of those upgrades for achieving increased SO_2 removal at full scale. Where the selected upgrade includes performance additives, system-wide additive consumption tests are conducted as the third phase of testing. Finally, these results are used to perform economic evaluations of the costs for each

upgrade to achieve high SO_2 removal efficiencies. The cost effectiveness of the upgrades is evaluated by comparing them with the projected market price of SO_2 allowance purchases.

Results for five of the six utility FGD systems included in the program have been presented at previous Contractors Conferences. This paper updates the results for two of these sites: PSI Energy's Gibson Station and Duquesne Light's Elrama Station. For the sixth program site, at NYSEG's Kintigh Station, all of the testing has been conducted since the July 1994 Contractors Conference. Therefore, all of the results for this site are discussed.

RECENT RESULTS FOR PSI ENERGY'S GIBSON STATION

Review of Previous Results for this Site. PSI Energy's Gibson Unit 5 is a 650-MW generating plant that fires coal with a sulfur content ranging from 2.4 to 3.5 wt.%. The unit has a wet limestone reagent FGD system that uses four Kellogg/Weir horizontal-gas-flow absorber modules. The FGD system uses a small amount of dolomitic lime for magnesium enhancement and operates in an inhibited-oxidation mode. Sodium formate and dibasic acid (DBA) additives were considered as upgrade options for this site.

Baseline tests showed that the SO_2 removal efficiency of the FGD system was about 86% at design operating conditions, while the unit was firing a lower-sulfur coal (~2.4 % S). The system operating conditions were three modules and four pumps per module in service (27 ft/sec flue gas velocity, 73 gal/macf L/G ratio), with a pH set point of 5.3.

Just prior to the parametric test series, while the unit was firing a higher-sulfur coal (~3.5 %S), a test was conducted without additive but at an elevated L/G ratio (four modules with four pumps in service) and an elevated pH set point (~5.7). This test showed that the module SO_2 removal efficiency could be increased to 96% without using additional performance additives. However, these operating conditions result in increased power and limestone consumption.

Parametric tests with sodium formate additive showed that, with the higher-sulfur coal, the SO_2 removal efficiency could be increased to 88% at design baseline conditions (three-module/four-pump operation and 5.3 pH), with a formate ion concentration of 2750 ppm. This compares to a predicted SO_2 removal of less than 75% at these same high-sulfur-coal conditions without the additive. By changing the operating conditions to an elevated L/G ratio of 95 gal/macf (four-module, four-pump operation) and 5.7 pH, an SO_2 removal efficiency of 97.5% was observed at a lower formate ion concentration of 1425 ppm.

A long-term sodium formate consumption test was conducted, with the formate ion concentration maintained at 1050 ppm in the reaction tanks. The consumption rate measured was equivalent to 10.6 lb of sodium formate per ton of SO_2 removed by the FGD system. Approximately half of the consumption was due to nonsolution losses from the system, primarily coprecipitation of the additive into the FGD system byproduct solids.

A long-term DBA consumption test was also performed, with DBA being added to the entire FGD system to maintain a concentration of 1150 ppm in the reaction tanks. The consumption rate

measured was equivalent to 9.2 lb of DBA per ton of SO_2 removed by the FGD system. Approximately three-quarters of the consumption was due to nonsolution losses, with that equally split between coprecipitation and oxidative degradation of the additive.

Sodium formate appeared to have a detrimental effect on byproduct solids dewatering properties at this site. After formate was added to the FGD system, the settling rate of the slurry solids and the filter cake solids content measured by laboratory tests each decreased. However, there was no apparent change in crystal size or shape, based on scanning electron microscope (SEM) photographs of solids samples with and without sodium formate present. In contrast, DBA appeared to have a beneficial effect on solids dewatering properties. After DBA was added, the settling rate of the slurry solids and the filter cake solids content measured by laboratory tests both increased. However, as with the sodium formate test results, there was no apparent change in crystal size or shape based on SEM photos of solids samples with and without DBA.

Economic Evaluation Results. Since the 1994 Contractors Conference, results of the baseline and parametric tests were used to calibrate EPRI's FGDPRISM model to the Gibson Station FGD system. Because the baseline and parametric test series were conducted at significantly different inlet SO_2 levels, FGDPRISM model simulations were used to perform technical and economic evaluations of the various upgrade options at a consistent coal sulfur content of 3.0 wt.%. The options evaluated with the model include operating at high L/G ratio (four-module/four-pump operation), decreasing reagent utilization (higher recycle slurry pH), using sodium formate additive, and using DBA additive.

The results for these upgrade options were compared to the design baseline operating conditions. These include three-module and four-pump operation, 85% limestone utilization, 9500 ppm dissolved magnesium concentration, and no flue gas bypass, all at a boiler load of 620 MW. For these conditions, the baseline SO_2 removal efficiency is approximately 80%.

Increasing the L/G ratio by operating with all four modules in service resulted in the largest removal increase at the lowest cost. Increasing the L/G ratio in this manner increases the SO_2 removal efficiency to 93% at an average cost of $48 per additional ton of SO_2 removed. As a result, an additional 13,200 tons of SO_2 can be captured. The other options, when considered individually, resulted in smaller increases in SO_2 removal and at higher costs. No individual upgrade option was capable of increasing the SO_2 removal to 95% or greater, so operation at a high L/G ratio was evaluated in combination with the other options. For high L/G operation, 95% SO_2 removal could be achieved either with a higher pH set point, which would decrease reagent utilization to about 80%, or by using either sodium formate or DBA additive at a concentration of about 500 ppm. The average costs for achieving 95% SO_2 removal with these options ranged from about $58 per ton (80% utilization or 500 ppm DBA) to $64 per ton of additional SO_2 removed (500 ppm formate). At 95% removal, a total of 15,000 additional tons of SO_2 can be removed relative to design baseline performance.

The net annual values of the upgrade options vary as a function of the SO_2 removal level achieved. The net annual value of achieving 93% SO_2 removal by operating at high L/G with all four modules in service is approximately $2.6 million, assuming an SO_2 allowance value of $250/ton, or $1.3

million assuming a value of $150/ton. When combined with other upgrade options, a maximum net annual value of approximately $3.0 million is achieved at 96% removal based on a $250/ton allowance value. At an allowance value of only $150/ton, a maximum net annual value of $1.4 million is achieved at a slightly lower removal of about 95%.

A sensitivity analysis was also performed to examine the impact of operation at a higher unit load (650 MW), a minimum level of flue gas bypass (5%), and a higher coal sulfur content (3.4%). At these conditions, four-module, four-pump operation is required to achieve the overall SO_2 removal efficiency of 82% necessary for compliance, although this would allow a 12.5% flue gas bypass rate. Upgrades considered involved reducing the flue gas bypass rate to the specified minimum of 5% and using either sodium formate or DBA additives, still with four-module, four-pump operation. The analysis shows that an overall SO_2 removal of 90 to 91% can be achieved with 1000 to 1500 ppm of either additive. The maximum net annual value of $1.5 million is achieved with DBA additive if allowances are valued at $250/ton. For a lower allowance value of only $150/ton, the maximum annual value achieved is $0.7 million.

RECENT RESULTS FOR DUQUESNE LIGHT'S ELRAMA STATION

Review of Previous Results for this Site. The first step in identifying low-cost upgrades for the Elrama FGD system was to conduct baseline tests to measure the performance of the magnesium-lime reagent venturi scrubbers as they normally operate. The FGDPRISM model was calibrated to the Elrama scrubber performance using these data, then used to predict how the scrubber would perform with a variety of potential upgrade options. After modeling the candidate upgrade options, a cursory economic evaluation of each option was performed. The options that appeared to be most cost effective were further evaluated in the parametric test series. Parametric test results were then used to conduct a second round of economic evaluations based on measured rather than modeled performance.

The two most promising options, which were subsequently tested during the parametric tests, involved operating at elevated thiosulfate concentrations and at increased venturi pressure drop, respectively. In the parametric tests, sodium thiosulfate concentrations were varied from the normal level of 170 ppm to as high as 2800 ppm. Tests were performed at two venturi pressure drops: the normal value of 10 inwc and a higher value of 12 inwc. Each condition was also tested at two pH values: the normal value of 7.2 and a lower value of 6.5.

The baseline SO_2 removal for the parametric series was about 89%. With elevated thiosulfate levels, improved SO_2 removal was obtained for three scenarios: pH 6.5 and 12 inwc venturi pressure drop, pH 7.2 and 10 inwc venturi pressure drop, and pH 7.2 and 12 inwc venturi pressure drop. These results are summarized in Table 1. The highest SO_2 removal efficiencies were measured at the pH 7.2 and 12 inwc venturi pressure drop conditions; a maximum of 93% removal was obtained at sodium thiosulfate concentrations of 1600 to 2700 ppm.

The results summarized above were reported in preliminary form at the July 1994 Contractors Conference. The following is a discussion of the results of the second round of upgrade economic evaluations, which were based on the full-scale parametric test results.

Economic Evaluation Results. The costs associated with operating at each test condition are also summarized in Table 1. At the highest SO_2 removal conditions of pH 7.2 and 12 inwc venturi pressure drop, the costs were estimated to range from $105 to $149/additional ton of SO_2 removed, depending on the thiosulfate concentration. Assuming an SO_2 credit value of $150/ton, the overall net value of operating at the elevated venturi pressure drop ranges from $3,000 per year to $65,000 per year, depending on the thiosulfate concentration. The costs or savings associated with improved SO_2 removal are compared to the base case parametric test, where 89.1% SO_2 removal efficiency was achieved at a pH of 7.2, a venturi pressure drop of 10 inwc, and a thiosulfate concentration of 170 ppm.

The lowest cost operating scenario was for the pH 6.5, 12 inwc venturi pressure drop conditions. The results in Table 1 show that for elevated thiosulfate concentrations, it is possible to improve the SO_2 removal efficiency while achieving an overall savings in operating costs. The savings come from improved lime utilization at the lower operating pH. At an assumed SO_2 allowance value of $150/ton, the value of operating at the pH 6.5, 12 inwc pressure drop conditions (compared to the base case) can be as much as $360,000 per year.

Laboratory settling tests indicated that the settling rate of the scrubber solids improved at the higher thiosulfate concentrations. This suggests that the thickeners would be able to better concentrate the scrubber liquor solids and lower the moisture content of the waste solids. This could result in substantial savings in waste disposal costs, a benefit that was not considered in these economics. However, because the parametric tests were performed on a single tower, it was not possible to determine what effect would occur in the full-scale thickeners if all of the towers were operated in this mode. System-wide testing at high thiosulfate concentrations would be required to determine if Elrama could realize further cost savings through reduced waste solids moisture.

RESULTS FROM NYSEG'S KINTIGH STATION

System Description. The NYSEG Kintigh Station is a 700-MW facility located near Barker, New York, that typically fires a 2.0 to 2.8 % sulfur coal. The unit is equipped with a limestone FGD system employing six open spray absorber modules. Each absorber has five recycle pumps independently feeding five spray header levels. At design conditions, only four modules and four spray headers per module are required to be in operation. The FGD system operates in an inhibited oxidation mode. Sodium formate additive was the only upgrade option tested at this site.

Summary of Test Results. Baseline tests showed that the SO_2 removal efficiency of the test module at normal full-load operating conditions (pH 5.6, flue gas velocity of 9 ft/s, four recycle pumps in service) was about 86%. Parametric tests with sodium formate additive showed that with a formate ion concentration of 3800 ppm in the recycle slurry liquor, the test module's SO_2 removal efficiency could be increased to 99.4%. The project target of 95% removal could be achieved with a formate ion concentration of only 500 ppm.

In a subsequent long-term additive consumption test, sodium formate was added to the entire FGD system to maintain an average formate ion concentration of 1080 ppm in the recycle slurry liquor. At this formate concentration, the FGD system SO_2 removal efficiency averaged about 97%. The

total sodium formate consumption rate was measured to be equivalent to 16.6 lb/ton of SO_2 removed. Of the total consumed, 12% was solution loss with the moist filter cake, 32% was lost by precipitation into the filter cake solids, 6% was lost by vaporization into the flue gas, and the remaining 50% was attributed (by difference) to degradation. The sodium formate additive had no measurable effect on the process chemistry or on the dewatering properties of the calcium sulfite byproduct solids.

Results of Economic Analyses. The economics of sodium formate addition were evaluated based on a capital cost of $300,000 for a 100 lb/hr additive storage and delivery system, using operating cost data provided by NYSEG. These results show that by using sodium formate additive at 1000 ppm (as formate ion) in the recycle slurry to raise the module SO_2 removal efficiency to nearly 98%, the Kintigh FGD system could remove more than 10,000 additional tons per year of SO_2 at an average additional cost of only $76/ton. Depending on the assumed value of SO_2 allowances, the estimated net annual value of the additional SO_2 removal for this optimum case ranged from $800,000 (assuming a value of $150/ton) to $1.8 million (assuming $250/ton).

Further analysis based on performance predictions with the calibrated FGDPRISM model suggested that approximately 97% removal could be obtained by operating with a finer limestone grind. This was predicted to remove an additional 9800 tons of SO_2 per year (relative to baseline performance) at an average cost of only $53 per additional ton removed. This finer grinding might be done by operating the reagent preparation system at a lower throughput for two shifts per day instead of the current one shift per day. Some modifications to the ball mill classifier would also be required. Additional tests would be required to verify the results of these FGDPRISM predictions.

CONCLUSIONS

The results from this program show that upgrades to existing FGD systems can be a very cost-effective component of a utility's strategy for complying with the CAAA of 1990. Table 2 provides a summary of results for all six sites included in the program. For five sites, the goal of cost-effectively achieving 95 to 98% overall SO_2 removal has been met. Two sites have exceeded this goal, with 99% overall SO_2 removal appearing to be very cost effective. At the sixth site, the goal was nearly met, with a maximum of 93% SO_2 removal being attained.

The costs for achieving these high SO_2 removal levels appear to be very attractive. The estimated incremental costs for the five sites that achieved 95% or greater SO_2 removal range from $39/ton to $76/ton of additional SO_2 removed. For the sixth site, the most cost-effective option actually showed a predicted reduction in FGD system operating costs, although this case resulted in an increase in SO_2 removal of only 3 percentage points above the baseline level. To put these estimated costs (or savings) into perspective, in the first EPA auction for SO_2 allowances, the average successful bid price was $150/ton. EPRI estimates that at the beginning of Phase 2 for the CAAA (the years 2000 through 2005), SO_2 allowance market prices will range from $250/ton to $500/ton of SO_2 in 1992 dollars.[1] Furthermore, we estimate that the cost of generating SO_2 allowances by installing new FGD systems on units firing medium- to high-sulfur coal would be at the upper end of this range. SO_2 allowances generated at $76/ton or less in existing FGD systems should be very desirable.

The amount of SO_2 allowances that can be generated by upgrading existing FGD systems can be substantial. At the Pirkey Station, more than 21,000 tons/yr of additional allowances can be generated, which would be sufficient to completely offset the Phase 2 SO_2 emissions from a 250-MW unit with no FGD system firing a medium-sulfur coal.

These results are very encouraging. Several of the six utilities plan to implement upgrade options tested at their site. The results from these sites may be applicable to a number of other existing FGD systems. Furthermore, the methodology applied in this program can be applied to any FGD system to evaluate the potential for cost-effectively upgrading its performance.

REFERENCES

1. Torrens, I. and J. Platt. "Update on Electric Utility Response to the CAAA." ECS Update, No. 30, p.3, Fall 1993.

Table 1. Parametric Test Economics for the Duquesne Light Elrama Station

	Measured SO_2 Removal %	Net Increase in SO_2 Removal ton/hour	Thiosulfate Concen-tration ppm	Total Cost $/ton SO_2	Net Annual Value @ $150/ton $1000/yr	Net Annual Value @ $250/ton $1000/yr
Base Case	89.1		170			
Case 1 - pH 7.2, 10 inwc						
Test 3	90.1	509	454	125	13	64
Test 7	91.1	993	1021	135	15	114
Test 11	91.5	1197	1579	147	4	124
Test 15	90.9	891	2705	205	(49)	40
Case 2 - pH 7.2, 12 inwc						
Test 2	92.0	1451	170	105	65	210
Test 4	92.2	1578	454	111	61	219
Test 8	92.5	1731	1021	122	48	221
Test 12	93.0	1986	1579	130	39	238
Test 16	93.2	2062	2705	149	3	209
Case 3 - pH 6.5, 12 inwc						
Test 6	87.3	(916)	437	453	277	186
Test 10	90.7	815	1135	(272)	344	426
Test 14	92.0	1477	1667	(94)	360	508
Test 18	91.8	1375	2836	(79)	315	452

Table 2. Summary of SO_2 Removal Upgrade Project Results

Utility	Station (Unit)	Absorber Type	Reagent	Oxidation Mode	Observed Base SO_2 Removal	Upgrade Options	Optimum SO_2 Removal	Est. Incremental Cost of Add'l SO_2 Removed, $/ton	Additional SO_2 Removed, tons/yr
Tampa Electric	Big Bend (#4)	Dual-loop, Packed	Limestone	Forced	94	DBA Additive	99	65	4,400
Hoosier Energy	Merom (#1 and #2)	Co-current, Packed	Limestone	Inhibited	83[1]	DBA Additive	97	61	15,100
SWEPCo	Pirkey	Dual-loop, Tray	Limestone	Inhibited	80[2]	DBA Additive	99	39	21,200
PSI Energy	Gibson (#5)	Horizontal Spray Tower	Limestone	Inhibited	80[3]	Sodium Formate, DBA Additive	95	63	15,100
Duquesne Light	Elrama	Venturi	Mg-Lime	Inhibited	86 to 89	Increase in Thiosulfate Level, Venturi Pressure Drop	92	-94[4]	1,500
NYSEG	Kintigh	Vertical Spray Tower	Limestone	Inhibited	86[5]	Sodium Formate Additive	98[5]	76	10,600

[1] Includes the effects of flue gas bypass; SO_2 removal across the test module was measured at 86 to 90%.
[2] Includes the effects of flue gas bypass; SO_2 removal across the test module was measured at 97%.
[3] Includes the effects of flue gas bypass; SO_2 removal across the test module was measured at 86%.
[4] The most cost effective upgrade option actually resulted in a net decrease in system operating costs, with a modest increase in SO_2 removal capability.
[5] Assumes no flue gas bypass.

Portions of the data obtained at Hoosier Energy's Merom Station are the result of an effort that has been jointly sponsored by the Rural Electric Research Program of the National Rural Electric Cooperative Association and EPRI. Funding for the FGDPRISM portion of this program was provided by EPRI.

FUNDAMENTAL MECHANISMS IN FLUE GAS CONDITIONING

Todd R. Snyder
Research Environmental Engineer
Principal Investigator

P. Vann Bush
Manager, Particulate Science and Engineering Group
Program Manager

Southern Research Institute
2000 Ninth Avenue, South
Birmingham, AL 35205

Contract DE-AC22-91PC90365
June 1991 to July 1995

OBJECTIVES

The overall goal of this research project has been to formulate a model describing effects of flue gas conditioning on particulate properties. By flue gas conditioning we mean any process by which solids, gases, or liquids are added to the combustor and/or the exhaust stream to the extent that flue gas and particulate properties may be altered. Our modeling efforts, which are included in our Final Report, are based on an understanding of how ash properties, such as cohesivity and resistivity, are changed by conditioning. Flue gas conditioning involves the modification of one or more of the parameters that determine the magnitude of forces acting on the fly ash particles, and can take place through many different methods. Modification of particulate properties can alter ash resistivity or ash cohesivity and result in improved or degraded control device performance. Changes to the flue gas, addition of particulate matter such as flue gas desulfurization (FGD) sorbents, or the addition of reactive gases or liquids can modify these properties. If we can better understand how conditioning agents react with fly ash particles, application of appropriate conditioning agents or processes may result in significantly improved fine particle collection at lower capital and operating costs.

LITERATURE REVIEW

We began this project with an extensive literature search to assess current knowledge of interparticle forces, sorbent and ash interactions, and flue gas conditioning. We summarized the findings of our review in two Topical Reports published in the first year of the contract. The Topical Reports emphasize the crucial roles water plays in bulk fly ash behavior and fly ash collection. Adsorbed water is an almost universal factor in the interaction of particles, even in cases of very low relative humidities. Water can be present as adsorbed monolayers or multiple layers on particle surfaces, or as "free" mobile water on the surface of the particles. The form of the water depends on the relative humidity (RH) of the gas, the morphology of the particles, the geometry of the contact points, and the surface chemistry of the particles. Agents can be applied to particles to alter the affinity of their surfaces to water, and thereby affect the adhesion.

Adsorbed water will form liquid bridges between particles when relative humidity exceeds some critical level for condensation to occur at contact points. A meniscus forms around the point of contact between particles, and the surface tension of the liquid exerts a capillary force between particles. If the particle surfaces dry after liquid bridges have been formed, residual solid bridges between particles can be formed. Any water-soluble salt can act as an adhesive in this way. Solid bridges are the strongest

of interparticle bonds. ESPs and fabric filters typically operate in such a way as to systematically, or occasionally, create liquid and consequential solid bridges between collected particles.

Effects of Particle Bonding Strength on ESP Operation

In electrostatic precipitation, cohesivity and electrical resistivity are two major properties of the particulate matter that affect performance. (Particle size is a third major property but unlike cohesivity and resistivity it can not be modified by flue gas conditioning.) Electrical resistivity of the collected material dictates the allowable current density that can be imposed on the material without causing electrical breakdown. Electrical breakdown in the collected particulate layer is the source of back corona (ionization within and from the collected layer) that can degrade particle charging and collection by spewing neutralizing ions into the interelectrode region and by forcing operation at reduced voltages and corona currents. If the electrical resistivity of a layer of particles is high enough ($\gg 10^{11}$ Ω-cm), the imposition that it makes on operating voltages and currents can dramatically lower ESP collection efficiency. If electrical resistivity is too low ($\ll 10^{8}$ Ω-cm), the charge on the particles and the applied electric field are insufficient to hold the particles on the collecting electrodes. The resulting phenomenon is called non-rapping, or electrostatic, reentrainment and can also dramatically lower ESP collection efficiency. Below about 400 °F the electrical resistivity of particulate matter can be decreased by lowering the temperature, or by adding some agent to the surface of the particles that enhances conduction of charge (water and SO_3 vapor are the most common additives that are used). Flue gas desulfurization systems that lower the gas temperature through cooling by evaporation of water, either as a constituent of a sorbent slurry or water spray, can produce conditions in ESPs at which the resistivity of the particulate matter is very low. Southern Research Institute (SRI) and others have documented cases of substantial non-rapping reentrainment in ESPs downstream of FGD systems.

Ash dislodged from the collection electrodes by rapping must fall off as large agglomerates in order to reach the hopper. If ash cohesivity is too low, a substantial portion of this ash may be redispersed into individual particles (or very small agglomerates). These ash particles and small agglomerates are consequently reentrained in the flue gas stream, placing an increased load on the ESP. When particles collected in the last ESP field are reentrained, outlet mass concentrations can increase significantly.

Liquid Bridges and Fabric Filtration

Ash characteristics affect three main facets of fabric filtration: filtering pressure drop, the removal of collected ash during cleaning cycles, and, in some cases, the overall collection efficiency of the fabric filter. Once stable operation (with constantly increasing filtering pressure drop) has been reached during a filtration cycle, the rate of increase of the pressure drop is entirely dependent on the concentration and characteristics of the particles being collected and the strength of the bonds between them. Darcy's Law, which describes the resistance to gas flow through a porous medium, indicates that particle morphology, specifically surface area, has a strong effect on pressure drop. (Resistance increases as the size of the particles decreases, or as the particles become rougher.) In general, flue gas conditioning has not been shown to significantly alter these aspects of particle morphology.

Conditioning has been shown to be quite effective in altering filter cake porosity, the other main characteristic of the cake that controls flow resistance. Porosity of a filter cake can be increased by the deposition of a liquid layer on the surfaces of the ash particles prior to their collection on the cake. The liquid layer increases the bonding strength between ash particles, and causes the particles to form an agglomerate with an increased porosity. Filtering pressure drop can be substantially reduced if filter cake porosity can be increased.

After each filtration cycle, cleaning energy is used to dislodge the recently collected ash so it can fall into the hopper for ultimate disposal. If the particle-to-particle bonds in the filter cake are too strong, the cleaning energy may not be sufficient to dislodge the cake. During cleaning the ash dislodged from the filter cake must fall off as large agglomerates if it can be expected to reach the hopper. If the

bonding forces between particles are too low, a substantial portion of ash dislodged during cleaning may be redispersed into individual particles (or very small agglomerates). This ash does not fall quickly enough into the hopper, and it is consequently recaptured during the next filtration cycle. This recollection of ash places an excessively high load on the baghouse.

PARAMETRIC TESTS OF FLY ASHES AND POWDERS

Following our literature review, we investigated fly ash conditioning and interparticle bonding forces in the laboratory. Because of the importance of liquid bridges in ash particle bonding, and because many of the various types of conditioning currently in use rely on liquid bridges to provide increased bonding strength, we concentrated on understanding and measuring liquid bridges on fly ashes and other powders. Since the material most commonly responsible for these adsorbed layers and liquid bridges is water, relative humidity was a key experimental parameter. The strength of interparticle attraction and bonding is controlled by such factors as particle morphology, total contact area, and other surface characteristics of the particles (chemical compounds, adsorbed water, etc.) By varying these factors and performing selected analyses of bulk samples of fly ashes and fine powders, we related relative humidity to surface chemistry, particle morphology, and consequently, bulk ash cohesivity and resistivity. As suggested by our literature review, increased amounts of adsorbed water increased the cohesivity of the ash. We also verified adsorbed water reduces bulk ash resistivity. As the amount of water adsorbed onto ash samples increased, the tensile strengths of the samples also increased. This trend was noted for relative humidities above about 20 to 40 % for most samples. At very low humidities the tensile strengths of many of the samples we tested were also relatively high. (Detailed summaries of our laboratory analyses and results are included in the various Quarterly Technical Progress Reports issued under this contract.)

PILOT-SCALE TESTS TO VERIFY THE ROLES OF ADSORBED LIQUID

In order to verify the relationships we identified in our literature review and laboratory analyses, we conducted three pilot-scale tests on a slipstream taken from SRI's 6 million Btu/hr Coal Combustion Facility (CCF). We designed these tests to determine the effects that adsorbed water (induced by flue gas humidification) had on the permeability of filter cakes, and to determine the conditions and factors that control electrostatic reentrainment of previously collected ash layers in an ESP. The first and second pilot-scale tests have been discussed in earlier papers and reports prepared under this project. In this paper, we compare the results of this earlier testing with the results from our third and final test. In each test we withdrew and conditioned a slipstream of flue gas and entrained fly ash particles from the CCF process stream. For our third test, the CCF burned Powder River Basin (PRB) coal. Since we evaluated PRB coal fly ash in our laboratory studies, CCF tests of this coal provided an excellent opportunity for the comparison of the results of our pilot-scale tests to our laboratory results.

Flue gas temperature and water content were the primary independent variables in our test matrix. The normal relative humidity in the CCF flue gas was around 1.7 % (at 300 °F). Our laboratory data and our review of field experiences indicated that the most likely conditions for electrostatic reentrainment would be high relative humidity and relatively cool flue gas. We also expected that the strongest liquid bridges that we could form in the dust cake in our Fabric Filter Sampling System (FFSS) would result from relatively moist conditions.

In our third test, water and/or steam were injected directly into various points in the CCF, upstream of our slipstream system which consisted of a small ESP and our FFSS. This injection scheme allowed us, within certain constraints, to control both duct moisture and temperature in our slipstream system. The heat exchangers in the CCF ductwork were used to vary the temperature of the flue gas without modifying its water content. Because of its configuration in the slipstream system, the temperature of the FFSS was controlled independently of the rest of the system. Our FFSS withdrew about 2.5 acfm of flue gas from this conditioned stream. The remainder of the slipstream flow passed through the ESP and a venturi, and into the CCF pulse-jet baghouse. The CCF was operated so the pressure drop

between points where we accessed the CCF process stream induced the desired flow of 280 acfm through the ESP.

Our slipstream ESP was a relatively small, single field, single flow passage unit with a specific collection area of 62 ft^2/kacfm, and was < 90 % efficient. These factors aided in our characterizations of reentrainment. We installed continuous monitors upstream and downstream of the ESP to measure total mass concentrations in the flue gas and monitored temperature at critical points throughout the system. We installed a wet-bulb thermocouple at the outlet of the ESP to use with dry thermocouple readings from the same location to derive moisture contents of the flue gas from a standard psychrometric chart. We used two different means for identifying the onset of electrostatic reentrainment. Because the ESP we used had windows at both ends that allowed illumination and viewing of the wires and plates, we were able to visually inspect the collected ash layer on the plates as the conditions in the ESP were varied. We also observed the outlet mass monitor output as we attempted to induce reentrainment.

In order to analyze the effects that duct humidification had on the filtration characteristics of the ash collected in the FFSS, we observed two main parameters: the rate of pressure drop increase across the filtering fabric, and the amount of ash entering the FFSS. We measured the mass concentration entering the FFSS by periodically placing an absolute filter upstream of the FFSS. This allowed us to normalize the rate of filtering pressure drop increase by the mass concentration entering the FFSS. (The mass of ash reaching the filter cake cannot be directly measured because of the near-continuous operation of the FFSS, and the influence that the geometry of the FFSS transform has on selective particle settling.)

Several attempts were made to induce electrostatic reentrainment in the ESP. Our general approach was to establish a stable condition (moisture and temperature) in the ESP and then to build an ash layer (without rapping the plates) at these conditions. The ESP was typically operated at an applied voltage of 38 - 41 kV and current densities ranging between 0.8 and 3 nA/cm^2. (Higher voltage and current settings were avoided due to the possibility of high-voltage sparks and corresponding damage to the data acquisition system and/or optical mass monitors.) Once the layer was formed, we would alter the flue gas moisture and/or temperature while we observed the ash layer. During our second pilot-scale test our visual observations of the ash layers deposited on the ESP plates indicated that the appearance of the layer depended on the relative humidity in the ESP during deposition. When ash layers were deposited at around 275 °F (1.2 % RH) the ash layer looked smooth, with many large craters in its surface. In contrast, the ash layers deposited under high humidity conditions (22 % RH at about 165 °F) appeared fluffy, and the surface of the layer seemed to be composed of small (1/32 inch diameter) agglomerates of ash particles. Since the major reentrainment phenomena we observed (at about 193 °F and 17 to 20 % RH) were from these fluffy ash layers, the characteristics (porosity and tensile strength) of the layer may be key factors in inducing reentrainment.

In our third test, our initial attempt at inducing reentrainment in the ESP was with an ash layer we formed at around 200 °F and with flue gas having about 22 % H_2O by volume (27 % RH). We used water and steam injection into the CCF duct to create and hold these conditions. The ash layer on the ESP plates was formed into plateaus up to 0.25 inch thick. We began a gradual increase in ESP temperature by adjusting the CCF's heat exchangers while attempting to hold the water content constant at about 22 % by volume. During this ramp up in temperature, the steam generator malfunctioned and over the two hours we ramped the ESP temperature up to about 220 °F, the water content of the flue gas dropped to about 15 % H_2O by volume. During this period we did not observe any significant non-rapping reentrainment.

For our next attempt at inducing electrostatic reentrainment, we built an ash layer at about 200 °F and about 30 % H_2O by volume (37 % RH). We then observed the layer as we decreased the water content of the flue gas while holding gas temperature constant. We continued this trial until the water content had been reduced to 15 % H_2O by volume (18 % RH). As before, we observed no

electrostatic reentrainment of the ash layer. We continued to observe the layer as we increased the flue gas temperature in the ESP up to about 265 °F and gradually decreased the water content to about 8 % by volume (3 % RH). This trial also failed to induce reentrainment. We then rapped the plates and built a new ash layer at 210 °F and 24.5 H_2O by volume (24 % RH). Once the ash layer had matured, we discontinued all water and steam injection and observed the ash layer as it dried out gradually while the CCF used its heat exchangers to hold the temperature constant. As before, no electrostatic reentrainment was observed during this transition period. Our final attempt to induce reentrainment began with the formation of a new ash layer at about 200 °F and 10.5 % H_2O by volume (13 % RH). No water or steam were injected into the CCF duct during this period. After the ash layer had been collected at these conditions, we ramped the ESP temperature up to 270 °F. By the end of this period of rising temperatures, the relative humidity in the flue gas was 3.5 %. No reentrainment was generated during this procedure.

The data we obtained with the FFSS during our second and third pilot-scale tests are summarized in Table 1. The final column in this table normalizes the rate of pressure drop increase by the mass we collected in the mass train thimble filters we periodically placed upstream of the FFSS. This normalized value should provide a fair indication of relative changes in K_2 at different flue gas conditions. The relative humidity values presented in Table 1 are based on the moisture measured in the ESP inlet duct during the FFSS filtration test periods.

Table 1
Summary of FFSS Operation

test/run	FFSS fabric temperature, °F	$\delta\Delta P/\delta t$, in. H_2O/ hr (a)	inlet mass load rate, g/hr	approximate RH in FFSS, %	$\delta\Delta P/M$, in. H_2O/g
2/1	300	0.23	7.6	1.3	0.030
2/2	300	0.22	7.6	1.3	0.029
2/3	300	0.40	11	1.2	0.037
2/4	260	0.30	6.8	2.5	0.044
2/5	220	0.11	4.9	6.1	0.022
2/6	190	0.00	--	--	--
2/7	165	0.01	2.5	22	0.0040
2/8	165	0.01	3.0	23	0.0034
3/1	225	0.375	1.720	5.2	0.218
3/2	220	0.394	--	9.1	--
3/3	217	0.449	--	15.1	--
3/4	231	0.325	--	16.3	--
3/5	231	0.259	0.834	7.7	0.310
3/6	229	0.293	1.501	7.3	0.195
3/7	281	0.218	0.672	3.0	0.324
3/8	343	0.442	1.180	1.2	0.375

(a) ΔP is the pressure drop across the dust cake and fabric, δt is the time interval.

With two exceptions, the values in Table 1 indicate that the normalized rate of pressure drop increase falls as humidity increases. (The data obtained for tests/runs 2/4 and 3/5 vary from this trend.) As discussed above, we attribute this reduction in the accumulation of pressure drop at higher relative humidities to increased porosity induced by liquid bridging between particles. Like the filtration results we obtained with an eastern, bituminous low-sulfur coal ash (test 2), the results of the third test seem to indicate that the PRB ash can also be conditioned with water to improve filtration characteristics by increasing dust cake porosity. For liquid bridges to be able to increase dust cake porosity above the characteristic value associated with an ash, free, mobile water must exist on the

surfaces of the particles which comprise the dust cake. Once the cake is formed at an elevated porosity, that porosity should remain intact even if the adsorbed surface water is subsequently immobilized. In our laboratory studies, we related the high calcium content of PRB ash to the immobilization of adsorbed water. We believe that the calcium and the silica present in the ash undergo a pozzalonic reaction with water that adsorbs on the surface of the ash particles to form hydrocalcium silicates. In the dust cake, additional water is continuously adsorbed on the particle surfaces in the dust cake because fresh flue gas is continuously passing through the cake and over the surfaces of the collected particles. Therefore, we postulate that free water is always available for the formation of liquid bridges between the particles on the surface of the dust cake and the newly arriving particles as they are captured by the cake.

For adsorbed water to affect tensile strength and cohesivity, it must exist and remain as free water on the surfaces of the ash particles. If the water originally adsorbed on the particle surfaces becomes strongly bound up as hydrocalcium silicates (or possibly other compounds), it is no longer available to form or maintain liquid bridges. With respect to ash resistivity, the inclusion of hydrated water in the chemical matrix of the ash particles does affect volume conduction through the ash layer collected in an ESP; however, continuously present free surface water is needed for improved surface conduction.

Two factors tend to hold previously collected ash on the ESP plate. In most cases, the electrical clamping force derived from the applied electric field across the ash layer and the resistance to current flow through the layer is sufficient to hold the collected ash on the plate. However, this clamping force will diminish and possibly even become a repelling force as the resistivity of the ash decreases due to a decrease in ash temperature and/or the adsorption of water onto the surfaces of the particles. The magnitude of the effects of temperature and adsorbed water on ash resistivity and clamping force depend on the particular characteristics of the ash and the structure of the ash layer.

Over the wide range of conditions we created in the ESP, we could not modify resistivity, cohesivity, and/or tensile strength sufficiently to induce electrostatic reentrainment of the PRB ash. To help understand this behavior, we measured the tensile strength of this ash as a function of relative humidity. As with other ashes we have characterized in this way, the PRB coal ash exhibited a relative minimum in tensile strength. For this ash, this minimum tensile strength exists between 22 and 50 % RH. Figure 1 compares the tensile strength of this ash with measured values for the eastern, bituminous low-sulfur coal ash that did reentrain during our second pilot-scale test.

Figure 2 shows the dependence of resistivity on temperature for the two ashes described above. This figure includes data showing the effects that water vapor conditioning has on the laboratory-measured resistivity of the PRB coal ash. (Similar behavior has been noted for the other ashes we have characterized.) Because in many of our pilot-scale trials we increased the relative humidity and lowered the ash temperature concurrently (as would occur with simple water injection), the reduction in clamping force can be linked to an increase in relative humidity. The overall tensile strength of the ash layer provides the second factor that holds the collected ash layer on the ESP plate. Although we observed that the magnitude of this tensile strength varies as a function of the amount of adsorbed water on the ash particles (Figure 1), its overall contribution to holding the ash on the plate is always positive.

Because of the dependence of the electrical clamping force and the tensile strength on ash temperature and adsorbed water, the overall force adhering the ash to the plate can change significantly as temperature and humidity change. Figure 3 demonstrates how relative humidity affects the way these two factors combine with the characteristics of the collected ash to either hold the ash on the plate or cause electrostatic reentrainment. Figure 3(a) shows for two ashes how the electrical clamping force becomes negative after enough water is adsorbed on the surfaces of the ash particles. (As mentioned above, this increase in adsorbed water is usually accompanied by decreases in ash temperature and subsequent reductions in the resistivity of ash.) Figure 3(b) presents a generalized relationship between tensile strength and relative humidity for these same two hypothetical ashes. In Figure 3(c),

the electrical clamping force has been added to the adhering force due to the tensile strengths of the ashes to demonstrate that for an ash with the proper characteristics, electrostatic reentrainment can occur over a finite range of conditions.

ACKNOWLEDGMENTS

This work was sponsored by the U.S. Department of Energy, Pittsburgh Energy Technology Center under Contract No. DE-AC22-91PC90365. Mr. Tom Brown is the Project Manager.

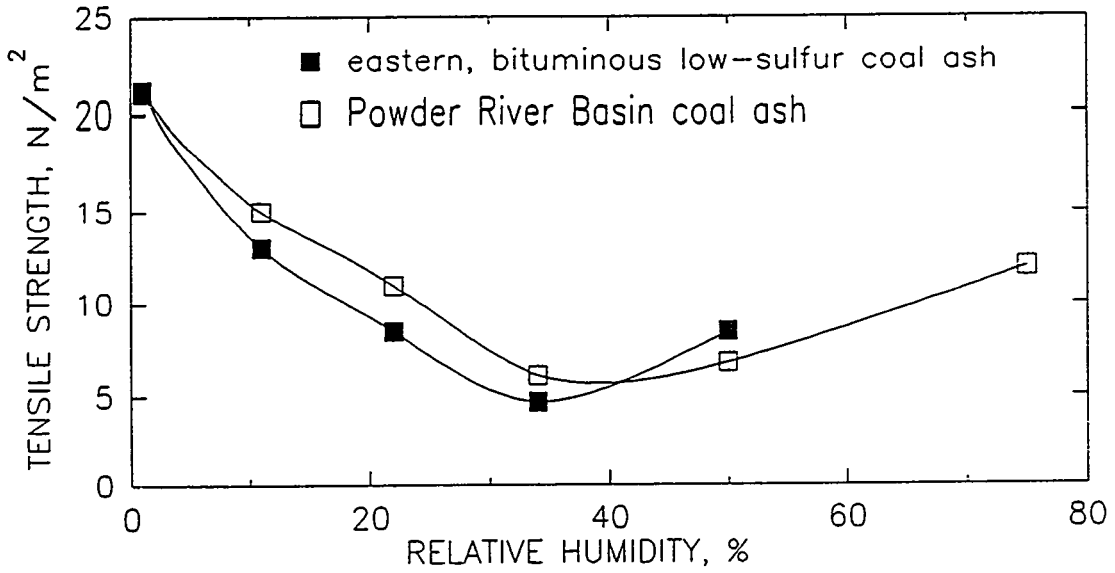

Figure 1. Tensile strength as a function of relative humidity for PRB coal ash and eastern, bituminous low-sulfur coal ash.

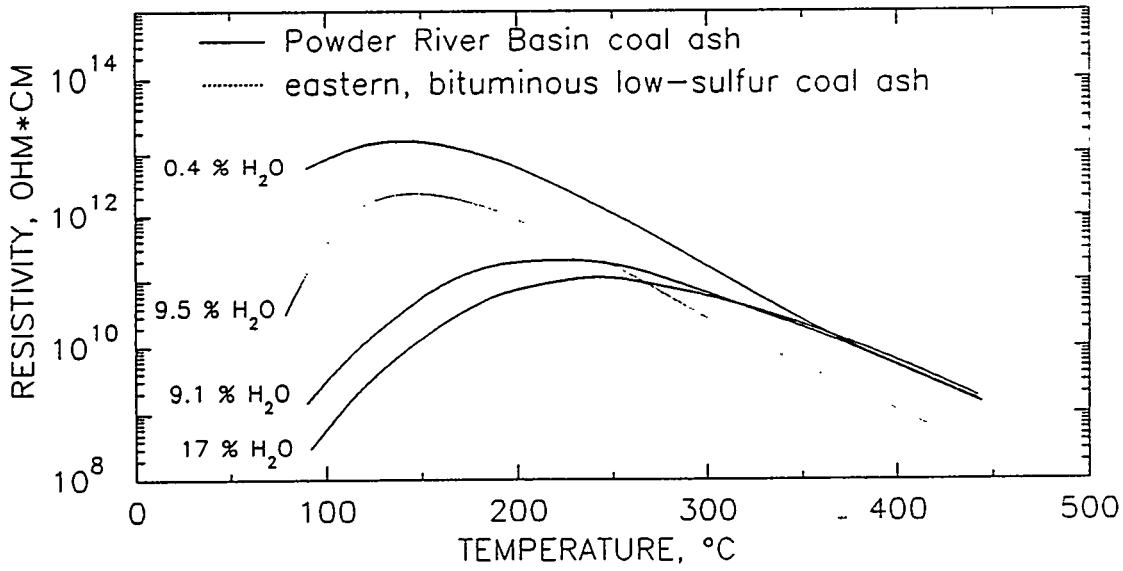

Figure 2. Resistivity as a function of temperature for PRB coal ash measured for ash samples conditioned at three different moisture contents, and eastern, bituminous low-sulfur coal ash measured for an ash sample conditioned at 9.5 % water by volume.

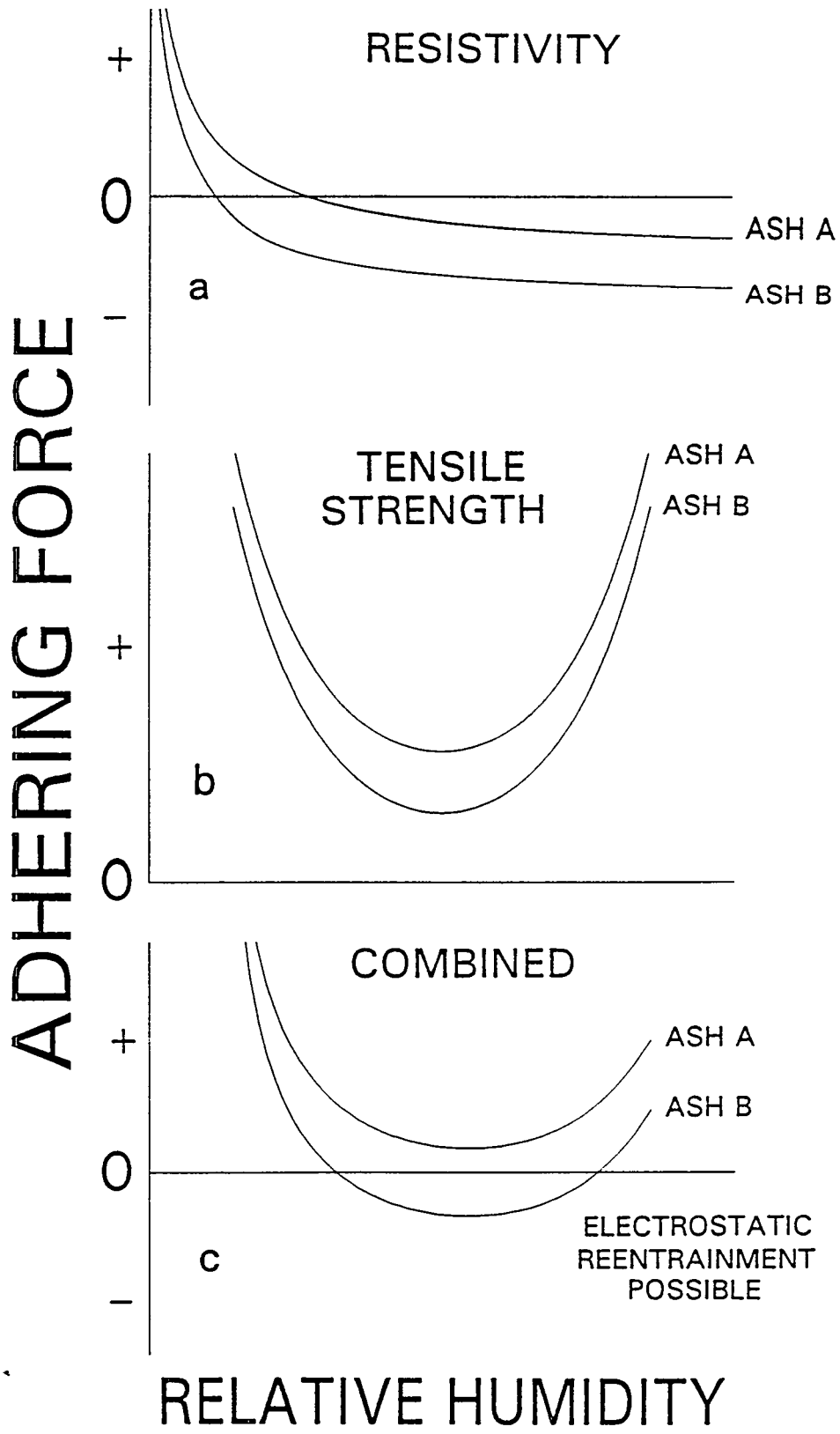

Figure 3. This figure demonstrates how relative humidity affects the way the electrical clamping force and tensile strength combine to yield conditions that can be conducive to electrostatic reentrainment.

ENHANCED PERFORMANCE OF ELECTROSTATIC PRECIPITATORS THROUGH CHEMICAL MODIFICATION OF PARTICLE RESISTIVITY AND COHESION

Michael D. Durham, Ph.D., Kenneth E. Baldrey, C. Jean Bustard, Timothy G. Ebner, Sharon M. Sjostrom, and Richard H. Slye

ADA Technologies, Inc.
304 Inverness Way So.
Englewood, CO 80112
(303) 792-5615

Introduction

Control of fine particles, including particulate air toxics, from utility boilers is required near-term by state and federal air regulations. Electrostatic precipitators (ESP) serve as the primary air pollution control device for the majority of coal-fired utility boilers in the Eastern and Midwestern United States. Cost-effective retrofit technologies for fine particle control, including flue gas conditioning, are needed for the large base of existing ESPs. Flue gas conditioning is an attractive option because it requires minimal structural changes and lower capital costs. For flue gas conditioning to be effective for fine particle control, cohesive and particle agglomerating agents are needed to reduce reentrainment losses, since a large percentage of particulate emissions from well-performing ESPs are due to erosion, rapping, and non-rapping reentrainment.

A related and somewhat ironic development is that emissions reductions of SO_2 from utility boilers, as required by the Title IV acid rain program of the 1990 Clean Air Act amendments, has the potential to substantially increase particulate air toxics from existing ESPs. The switch to low-sulfur coals as an SO_2 control strategy by many utilities has exacerbated ESP performance problems associated with high resistivity flyash. The use of flue gas conditioning has increased in the past several years to maintain adequate performance in ESPs which were not designed for high resistivity ash. However, commercially available flue gas conditioning systems, including NH_3/SO_3 dual gas conditioning systems, have problems and inherent drawbacks which create a need for alternative conditioning agents. In particular, NH_3/SO_3 systems can create odor and ash disposal problems due to ammonia outgassing. In addition, there are concerns over chemical handling safety and the potential for accidental releases.

Program Objectives

The purpose of this program funded by the Department of Energy Pittsburgh Energy Technology Center (PETC) is to identify, evaluate, and develop cost-effective ESP conditioning agents to improve removal of fine particle air toxics from coal-fired combustion flue gas streams. This goal can be met by reduction of reentrainment losses of collected ash and by control of ash resistivity.

The project has focused on the development of cohesive agents to overcome reentrainment problems associated with low particle holding force. This effort has encompassed an extensive laboratory screening, followed by bench-scale and pilot-scale tests. Discovery of a promising cohesivity agent and resistivity modifier in August, 1994, led to a further round of laboratory and pilot-scale field testing in late 1994. Because of the commercial potential for this additive, its chemical composition is being kept confidential; it has been designated ADA-23 in the following discussion of test results. It meets cost and toxicity selection criteria for the overall project in that it is a common food additive.

Laboratory Evaluation of ADA-23

ADA-23 was first tested in the laboratory as an additive for ADA's fabric filter flue gas conditioning project. On this project, screening tests with many conditioning agents were conducted using a laboratory flue gas generator and a portable filter test device. ADA-23 was one of several agents which were found to modify filter dust cake properties for flyash from a Texas lignite coal, resulting in reduced particle emissions and lower filter pressure drop. This finding led to an evaluation of the performance of ADA-23 as an ESP conditioning agent, beginning with the investigation of its effect on flyash resistivity as measured in the ADA resistivity apparatus.

The additive was injected into the ADA laboratory test fixture, where a simulated flue gas stream is passed through an additives injection chamber and then through the resistivity measurement chamber. In this system, both flyash and gas constituents are added dynamically to create specific gas composition and ash content. Moisture of the flue gas is controlled with a temperature-controlled humidifier upstream of the additives chamber. In the chamber the additive under test is sprayed into the flow with a fine mist atomizer. Additive volume to the injection nozzle is controlled with a precision peristaltic pump.

The simulated flue gas stream contains flyash that is added to the flow by a screw feeder; the injection rate is controlled by a variable speed motor. Entrained flyash is collected downstream of the additive injection chamber in the ADA resistivity apparatus, a modified point-plane electrostatic precipitator. In the resistivity cell, a dust layer is collected by either electrical precipitation or by filtering across an electrically isolated metal frit. Following precipitation, the thickness of the collected flyash layer is measured, and then the resistivity of the dust layer is determined from the measured voltage and current across the dust layer at a uniform field strength of 4 kV/cm.

Tests at Cold-Side ESP Conditions

Redispersed flyash was obtained from a generating station that fires a Texas lignite coal. Sulfur content of the lignite coal is approximately 0.6% and the flyash is low in alkali metals, sodium and potassium. The combination of low sodium and low sulfur content is associated with high-resistivity ash at cold-side ESP temperatures for a variety of coals. This ash resistivity was more than 10^{13} ohm-cm at 300 °F. It should be noted that the simulated flue gas mixture did

not contain free SO_3 vapor, which also contributed to the high resistivity of the unconditioned ash.

Two parameters were varied to determine the impact of additive ADA-23 on flyash resistivity. Tests were run over an extended flue gas temperature range of 200 to 450 °F. The concentration of additive was tested over a range comparable to that for SO_3 conditioning systems. The additive, ADA-23, demonstrated dramatic reductions in resistivity of the lignite flyash over the entire temperature range tested, as shown in Figure 1. At all temperatures tested, the resistivity could be decreased to the optimal 10^{10} ohm-cm range. Increasing the concentration of the additive at a constant temperature of 310 °F caused a reduction in flyash resistivity from about two to over four orders of magnitude. It should be noted that the liquid injection rate was identical for all test cases. The concentration of additive in the injected solution was varied to meet the target additive-to-flyash mass ratio. For tests without additive, water was injected at the same liquid feed rate.

For both baseline and conditioned samples, the ash layer was collected via point-plane electrostatic precipitation. Figure 2 plots the rate of ash layer precipitation in the resistivity apparatus; it is seen to increase with increasing additive concentration. This result is in part due to resistivity improvement, but it is also indicative of ash layer cohesivity. When collecting an unconditioned high-resistivity ash, the resistivity measurement cell typically exhibits increased blow-off for dust layers more than 1 mm thick. Conditioning with ADA-23 produced dust layers up to 4.1 mm thick without significant reentrainment.

Based on results to date using aqueous spray injection, the new additive has definite commercial potential as a conditioning agent for cold-side ESPs. The most important driver affecting the commercialization of the additive will likely be the chemical amounts required to achieve optimal conditioning. Tests have indicated that at the injection rates which work successfully in a spray chamber, conditioning with the additive in a liquid spray delivery system will certainly be cost-competitive with commercial systems. Further testing is needed at full-scale to optimize additive injection in a full size duct and to demonstrate the technology for cold-side applications.

Tests at Hot-Side ESP Conditions

All of the test data for ADA-23 has indicated that flue gas conditioning for resistivity modification is applicable to a wider temperature range than for conventional SO_3 conditioning. Based on our experimental results and on knowledge of the additive's chemistry and physical properties, it appeared that conditioning could extend the ash surface conduction mode to temperatures normally dominated by volume (bulk) conduction. If so, conditioning with ADA-23 could alleviate ESP performance problems associated with sodium ion depletion in ash layers of hot-side ESPs.

To test whether ADA-23 could be used to condition hot-side ESPs, laboratory resistivity tests were recently conducted using ADA's flue gas simulator and additive injection chamber. Tests were first run at 700 °F with an ash sample from a hot-side ESP at a plant firing a western

subbituminous coal. This ESP has historically exhibited severe performance problems associated with a low sodium content in the coal. Resistivity of fresh ash at hot-side operating temperatures has typically been measured in the 10^{10} - 10^{11} ohm-cm range; it is expected that the resistivity increases significantly for an aged ash layer. For this test, the additive and ash were injected at 700 °F in a 10% moisture, air environment. As seen in Figure 3, the additive reduced resistivity at 700 °F by up to two orders of magnitude. The amount of the resistivity reduction can be controlled by the concentration of the additive. This demonstrates that conditioning can be effective at hot-side temperatures.

Further laboratory resistivity tests were conducted using a mixture of 75% SiO_2 and 25% Al_2O_3 powder. This synthetic "flyash" mix was created to entirely eliminate alkali ion charge carriers from the dust layer and thereby present a worst-case ash to condition. The mixture of refractory powders was redispersed on the resistivity measurement frit and was heated to 700 °F in a 10% moisture gas stream. The powder layer was conditioned by injecting liquid additive as an aqueous spray in the spray additive chamber upstream of the resistivity measurement cell at 700 °F. Additive was brought into contact with the powder layer by drawing sample gas through the powder layer and the porous sample frit. Baseline tests were also conducted with no flue gas conditioning by injecting a water spray rather than an additive solution. Resistivity of the baseline powder sample was 4 x 10^9 ohm-cm; conditioning with the additive successfully lowered resistivity by an order to magnitude to 4 x 10^8 ohm-cm. While the unconditioned powder layer at this temperature exhibited only moderate resistivity, the test demonstrated that the additive can effectively reduce resistivity independent of sodium or lithium ion charge carriers at hot-side conditions.

SRI Coal Combustion Facility Test

Pilot-scale tests were conducted on a 300 acfm slipstream at the Southern Research Institute Coal Combustion Facility (SRI CCF) during a trial burn of a Powder River Basin coal (Bell Ayr). The tests reconfirmed the previous laboratory results that ADA-23 injected as an aqueous spray is effective as a conditioner for high resistivity flyash. Additionally, ESP performance of a single field, 9" wire-plate ESP was improved by conditioning with ADA-23, as measured by both increased electrical field strength and by decreased outlet particulate emissions. Importantly, the additive worked successfully in an actual flue gas environment.

The ESP was instrumented to continuously monitor voltage, current, flow rate, temperatures, and outlet particulate. In addition, at each test condition, both a "clean plate" and a "dirty plate" V/I curve was taken manually. Resistivity was measured continuously at the ESP inlet with a measurement cycle of less than 30 minutes. Resistivity samples were collected by filtering across an electrically isolated metal frit, rather than by point-plane precipitation. This modification reduced the required sample time and it improved test repeatability. Dust layers collected by this method were approximately 0.2 to 1 mm thick.

The test began with a baseline condition at an ESP inlet temperature of 300 °F, without spray conditioning. Flue gas moisture content was 9.5%. Baseline flyash resistivity was 5 x 10^{11} ohm-cm. At this condition, the pilot-scale ESP was operating poorly, with an electrical field

strength of only 0.5 nA/cm^2. Throughout the test, ESP secondary voltage was maintained at 40 kV to avoid sparking to avoid disruption of the data acquisition and computer control system.

Conditioning with ADA-23 reduced the ash resistivity to 9 x 10^9 ohm-cm. Electrical field strength improved to 2 nA/cm^2 with the baseline unconditioned layer still on the plates. The plates were rapped clean and conditioning with ADA-23 continued at the same rate. Once a layer had built up, ESP field strength increased to 8 nA/cm^2. Spray injection was then switched to water at the same flow rate. Resistivity returned to 4 x 10^{11} ohm-cm, essentially a repeat of baseline. ESP electrical conditions also began to degrade. This confirmed that the improved electrical conditions during additive injection were not a result of water spray cooling. The improved electrical conditions resulted in lower particle emissions from the ESP as measured by a real-time optical mass monitor.

Additional Pilot-Scale Tests

The performance tests with ADA-23 first in the laboratory and then at SRI's CCF were conducted with spray injected in special additives spray chambers at low gas velocity. Once the additive was shown to work predictably under these conditions, the next step was to evaluate spray conditioning at typical duct conditions. For this, a further test was conducted at a Colorado power plant firing a Powder River Basin coal.

Flue gas was extracted isokinetically from an 18 inch diameter duct that supplies a particulate control pilot plant in operation at the power plant. The slipstream is extracted from the plant duct downstream of the air heater and upstream of a reverse gas baghouse. An atomizing spray nozzle manifold was inserted into the slipstream duct approximately 40 ft. and a 90 degree bend upstream of a sample probe. Liquid feed to the nozzle manifold was controlled with a peristaltic pump. The sample probe drew flue gas isokinetically to a portable ESP at a flow rate of approximately 60 acfm. In all, sample residence time from injection to the ESP inlet was less than 2 seconds. Velocity in the duct was 50 - 60 ft/second and the gas temperature was 250 °F. The sample was reheated to a constant 300 °F at the ESP inlet.

The portable ESP was configured as a single channel wire/plate at a 9" plate spacing with standard 0.1" diameter bare wires. This configuration was intended to approximate the performance characteristics of a typical full-scale ESP. Special teflon baffles were installed around and beneath the collection plates to minimize sneakage. The flow rate was set to provide an SCA of 180 ft^2/kacfm. The high voltage power supply was spark limited with an industry-standard power controller.

ESP voltage and current were monitored continuously and V/I curves were taken to sparking for each test condition. Multiple resistivity measurements were taken at the ESP inlet for each test condition. Outlet particulate concentrations were monitored by a Triboflow monitor, which produces a response proportional to the number of charged particles contacting the probe. Conditioning reduced the ash resistivity from a baseline of mid 10^{11} ohm-cm to 10^9 ohm-cm. The ESP conditions also improved and the triboflow monitor response was also

reduced during conditioning periods. Based on these results, the following conclusions were reached:

- Aqueous additives solutions can be successfully injected into a turbulent flue gas stream at 40-60 ft/second gas velocity;
- Liquid droplet size for the nozzle array was less than 40 μm Sauter mean diameter based on manufacturer's specifications for the nozzle;
- A residence time of 1 - 2 seconds between injection and control device is adequate for conditioning;
- Flue gas spray cooling is 5 - 10 °F for the conditioning rates required with ADA-23;
- Effective spray distribution will be critical to the success of conditioning. This must be tested at full-scale.

Ash Characteristics

Based on tests that ADA has conducted to date, additive conditioning with ADA-23 at effective concentrations does not alter fly ash chemical and handling characteristics. During this test, samples of ash from a pilot particulate control device were taken during a baseline period with no conditioning and during additive injection. The samples were submitted to an independent testing laboratory for elemental analysis and for TCLP analysis for leachable metals. The TCLP analysis indicates that the conditioned flyash is not enriched in any of the leachable metals, including the volatile metals, mercury and selenium. Conditioning with ADA-23 should produce a non-hazardous waste suitable for commercial sale or conventional landfilling.

Conclusions

Following are the conclusions reached from the laboratory and field performance tests with ADA-23:

- Cohesivity effects due to ADA-23 are evident from observations of high tensile strength ash layers developed in the resistivity device;
- ADA-23 is an effective resistivity modifier for low-sulfur high-resistivity western coals;
- Surface conduction mode through ash layers is extended to a higher temperature range of cold-side ESP operation (>350 °F).ADA 23 is effective at hot-side ESP temperatures;
- ESP electrical characteristics and particulate collection can be significantly improved by conditioning;
- Conditioned ash should be suitable for commercial use (TCLP tests indicate no enrichment in volatile metals);
- Ash handling is not impaired at conditioning levels required for resistivity control.

Further testing is needed at full-scale at both cold-side and hot-side ESP conditions with a high-resistivity, subbituminous coal. This is necessary to develop additive delivery systems, optimize and define the additive concentration, and to demonstrate the technology. Tests at the pilot-scale provide ample evidence of performance to justify this step.

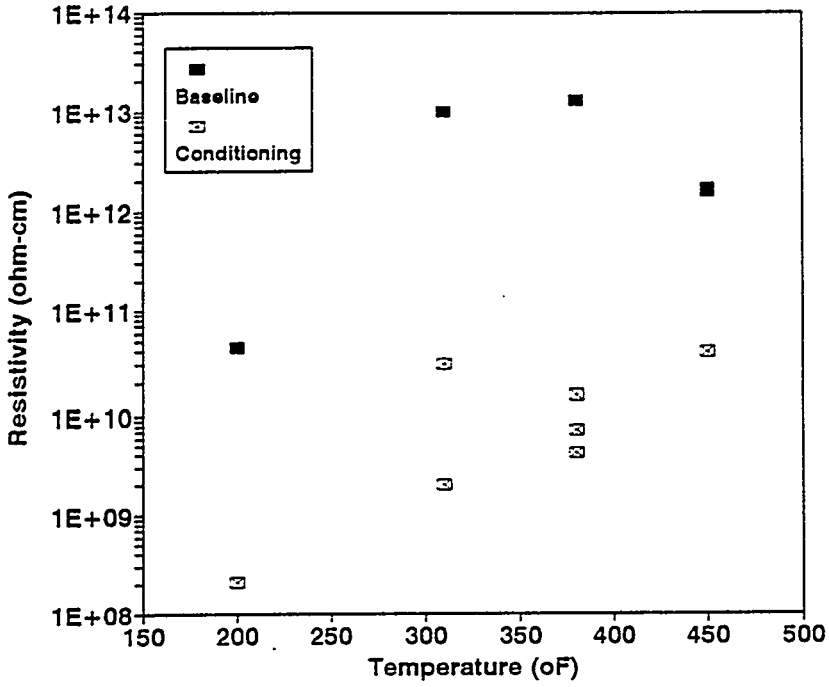

Figure 1. Additive ADA-23 Effect on Flyash Resistivity as a Function of Temperature.

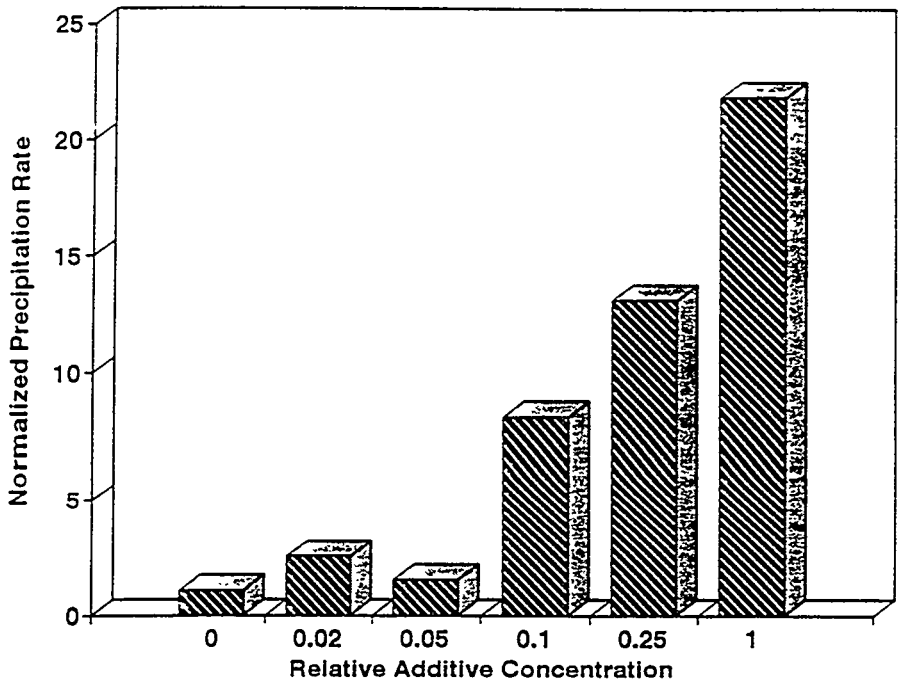

Figure 2. Flyash Precipitation Rate as a Function of Relative Additive Concentration.

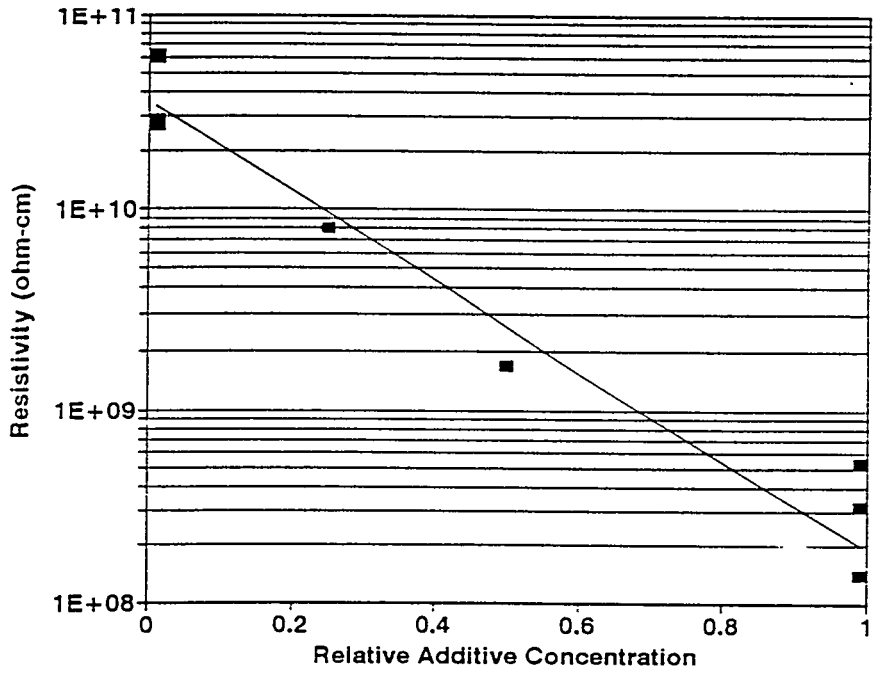

Figure 3. Resistivity versus Additive Concentration for a Hot-Side ESP Flyash at 700 °F.

NON TOXIC ADDITIVES FOR IMPROVED FABRIC FILTER PERFORMANCE

C. JEAN BUSTARD
Scientist

KENNETH E. BALDREY
Senior Research Engineer

TIMOTHY G. EBNER, SHARON M. SJOSTROM
Research Engineers

RICHARD H. SLYE
Senior Research Technician

ADA Technologies, Inc.
304 Inverness Way South, Suite 110
Englewood, CO 80112
(303) 792-5615

Introduction

The overall objective of this three-phase Small Business Innovative Research (SBIR) program funded by the Department of Energy Pittsburgh Energy Technology Center (PETC) is to commercialize a technology based upon the use of non-toxic, novel flue gas conditioning agents to improve particulate air toxic control and overall fabric filter performance. The ultimate objective of the Phase II program currently in progress is to demonstrate that the candidate additives are successful at full-scale on flue gas from a coal-fired utility boiler. This paper covers bench-scale field tests conducted during the period February through May, 1995.

The bench-scale additives testing was conducted on a flue gas slipstream taken upstream of the existing particulate control device at a utility power plant firing a Texas lignite coal. These tests were preceded by extensive testing with additives in the laboratory using a simulated flue gas stream and re-dispersed flyash from the same power plant. The bench-scale field testing was undertaken to demonstrate the performance with actual flue gas of the best candidate additives previously identified in the laboratory. Results from the bench-scale tests will be used to establish operating parameters for a larger-scale demonstration on either a single baghouse compartment or a full baghouse at the same site.

The bench-scale field test matrix included four separate phases that were scheduled over a three month period. The phases included 1) set-up, mechanical checkout and baseline testing, 2) screening tests, 3) optimization tests, and 4) long-term operation. Nine additives were screened

during the bench-scale field tests. Of these, six decreased outlet emissions; one of these also reduced the number of bag cleans per hour. The additive that reduced both the number of bag cleans per hour and the outlet emissions was further optimized and tested for a one-week longer-term test. This additive reduced the outlet emissions by an order of magnitude and reduced the number of cleans required by a factor of 2 to 8.

Experimental Apparatus

The test equipment consisted of an isokinetic sample probe, an additive contact chamber, an additive injection assembly, and the ADA Filter Test Device (FTD), as shown in Figure 1. In the additives contact chamber, a small, dual-fluid nozzle atomizes and injects an aqueous solution of diluted additive into the flue gas stream. Additive liquid flowrate is metered and controlled with a precision peristaltic pump. The liquid injection rates were set to minimize flue gas spray cooling due to water evaporation to less than 45°F below duct temperatures for the initial bench-scale screening, and to a maximum of 15°F below duct temperature during the later optimization tests.

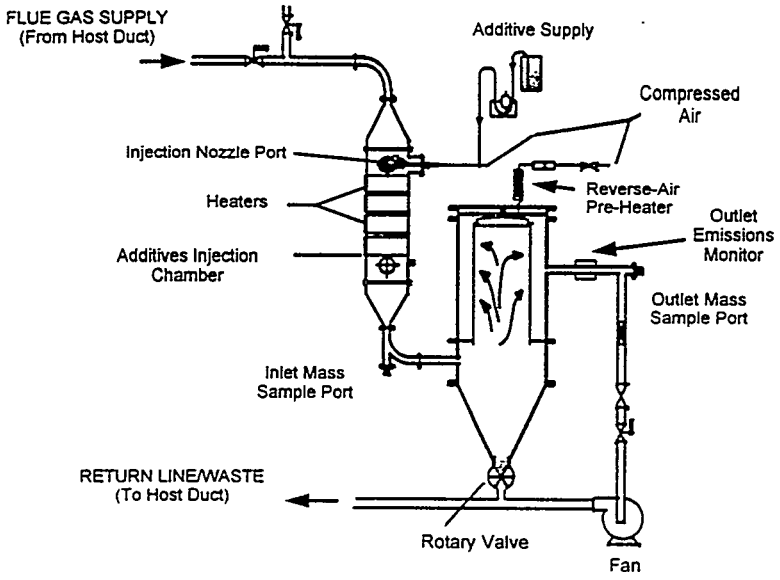

Figure 1. Sketch of the ADA bench-scale Filter Test Device (FTD), configured for reverse-gas cleaning, and the upstream additives injection chamber.

For the bench-scale additives tests, the FTD was configured for reverse-gas cleaning with an 8-inch diameter fiberglass bag of a weight and weave to match the bags currently in use in the shake/deflate baghouse of the host power plant. Relative outlet particulate emissions were measured using a Triboflow™ monitor installed downstream of the FTD filter chamber. The Triboflow™ instrument measures particle concentration via detection of the electric charge on

particles which impact a sensor in the gas stream. Outlet emissions measured by the Triboflow™ monitor were confirmed periodically by particulate mass measurements via EPA Method-17.

A primary parameter of interest for fabric filter performance is the cleaning frequency required to maintain a baghouse at a given average pressure drop. Cleaning frequency and pressure drop are interdependent; some baghouses are operated on a fixed cleaning schedule and the average pressure drop is monitored to gauge performance. Other baghouses are operated by initiating the cleaning sequence at a maximum pressure drop with the cleaning frequency as the dependent variable. The latter approach was used during the bench-scale testing; the FTD control logic was configured such that the bag was cleaned when the pressure drop across the filter bag reached 5-inches H_2O. A pressure initiate of 5-inches H_2O across the tubesheet was chosen based on previous experience with the FTD and with pilot-scale and full-scale baghouse operation. This value represents a pressure drop within an acceptable range for baghouse fans and it provides meaningful data for comparison to other baghouses when using new filter bags.

At an operating power plant, flue gas temperatures, flyash concentration, and gas composition change with normal variations in plant operations (load, coal composition, and combustion conditions). These data were collected during the bench-scale tests for two reasons: 1) the performance of the FTD is affected by variations in flue gas conditions and 2) a full-scale additive injection system may need to control with respect to either a specific process parameter or a combination of parameters.

Site Description

The particulate control equipment at the host plant includes an electrostatic precipitator operating in parallel with a shake/deflate baghouse. Flue gas conditioning with ammonia is used to maintain performance of the particulate control equipment. The ammonia injection location for the host system is located downstream of the sample ports where the FTD was installed. The operating air-to-cloth ratio for the baghouse was nominally 2.5 ft/min; this was chosen as the target air-to-cloth ratio for the FTD for the screening tests. The bag fabric for the FTD testing was also chosen to match the weight and weave of the fiberglass bags currently used in the host plant baghouses. Thus, the FTD test conditions matched those in the full-scale shake/deflate baghouses as closely as possible.

Set-up, Mechanical Checkout and Baseline Testing

During this phase of the testing, the FTD was installed on the host duct in a reverse gas configuration (Figure 1). Following mechanical checkout to verify proper operation, the FTD was operated unattended for eight days to establish a stable baseline. This baseline test was performed without any additive or water injection. Baseline particulate mass tests were conducted at the FTD inlet scoop location to determine mass loading, flue gas moisture content, and stack velocity. Mass concentration measurements in the FTD inlet line during the baseline tests indicated a loading of 11 gr/acf entering the FTD. This loading is at the upper limit of what

can be considered representative at this site, however, it is unusually high for power plants in general. The host duct temperature at the inlet extraction location ranged from 360 to 400°F. The FTD chamber temperature and the additives contact chamber were maintained at nominally 400°F for all tests. At the end of baseline testing, the cleaning frequency was 3 cleans per hour with a clean initiate set-point at a tubesheet pressure drop of 5 inches H_2O. The Triboflow™ monitor registered an average signal of 35% at the FTD outlet.

Additive Screening

A re-evaluation of laboratory results in an actual flue gas environment was identified as an essential first step in the bench-scale field tests. It is difficult to accurately simulate particle size distribution in the laboratory due to inherent limitations in collecting and re-dispersing a representative ash sample. The laboratory ash sample was probably biased to larger particles (as compared to the size distribution in the flue gas). The ash was valuable in comparing the effectiveness of the additives, however, small particles (less than 3 μm), which are present in disproportionately low levels in laboratory testing, are more challenging for a baghouse to filter. A further potential bias, in this instance, was the effect of residual ammonia in the laboratory ash sample. Also, fluctuations in actual flue gas conditions could not be duplicated in the laboratory.

Screening tests were conducted for the best-performing additives identified in previous laboratory tests. The same bag used during initial baseline tests was left in place for the screening tests. Water was injected following the initial baseline to determine the effect, if any, of water alone. Once the operation stabilized with water injection, short additive injection runs were conducted (3-5 cleaning cycles) to document short-term changes in performance. The system was then returned to baseline with water injection. After re-establishing water-only baseline conditions, the next additive was injected and the procedure repeated. Additives were injected at the rates previously determined in the laboratory trials.

Screening tests were completed for nine candidate additives. Of these nine candidates, two were identified for optimization and long-term testing at the bench-scale. The results for the screening tests as compared to baseline are shown in Table 1. Data is presented in terms of percent reduction in outlet emissions and percent change in cleaning frequency. ADA-6 and ADA-14 were initially selected for optimization and longer-term testing because they significantly reduced outlet emissions and reduced the number of cleans required to maintain the tubesheet pressure drop at a given level. ADA-9 and ADA-10 were considered secondary options because they significantly reduced outlet emissions without increasing the number of cleans required to maintain the tubesheet pressure drop.

A screening test was repeated for ADA-14 using plant make-up water to prepare the additive solution. This test was conducted to identify potential problems with additive delivery components (spray nozzle, pump) or with solution chemistry when plant water is used to mix additives (it would be an advantage at this site if plant water could be used as the carrier liquid). The performance results were similar to those presented in Table 1 for ADA-14. There was also no indication of nozzle pluggage. If further tests with plant make-up water are conducted, it will

be important to monitor total suspended solids and if necessary, make modifications to prevent possible nozzle plugging.

Table 1. Bench-Scale Screening Test Results

Additive	Cleaning Frequency change to baseline	Reduction in Emissions % change to baseline
ADA-7	33% increase	78
ADA-6	78% decrease	98
ADA-9	0	70
ADA-10	0	96
ADA-14	20% decrease	90
ADA-18	0	0
ADA-19	112% increase	90
ADA-20	0	0
ADA-21	0	0

A final screening test was conducted to better simulate flue gas conditions which will likely be present during a full-scale test. Since ammonia will probably be injected during compartment or full-scale testing, but was not present in the FTD flue gas slipstream, it was necessary to document the effect of ammonia on the additives performance. Ammonia was injected into the inlet of the FTD at a rate of 25 ppm. After 8 hours of ammonia-only injection there was no noticeable effect on outlet emissions or cleaning frequency. Previous testing with ammonia showed that the beneficial effect of ammonia is very sensitive to SO_3 levels in the flue gas. Because no effect was seen, it was assumed that the SO_3 level was probably very low (SO_3 measurements were not made). ADA-14 was then injected at the previous screening test concentration simultaneously with the ammonia. Again performance results were similar to those presented in Table 1 and it was therefore concluded that ammonia did not negatively impact the effect of ADA-14.

Optimization Tests

Based on the results from the screening tests, additive optimization was scheduled to be performed on ADA-6 and ADA-14. Initial optimization of ADA-6 revealed that this additive did not perform as indicated in the screening tests. Boiler load had decreased significantly during screening of ADA-6. It was initially believed that this contributed only partially to the ADA-6 success during screening. Apparently, the grain loading to the inlet of the FTD plummeted with boiler load and, subsequently, the caused time between cleans to increase. It was concluded based on the additional optimization test data that ADA-6 was not a viable candidate.

As an alternative to ADA-6, ADA-10 was tested. ADA-10 decreased outlet emissions; however, the time between cleans also decreased significantly, even at very low concentrations.

This behavior indicated that this additive was forming an overly cohesive ash and was not acceptable for further testing.

A full series of optimization tests was performed on ADA-14. These results are presented in Table 2. The additive-to-ash concentration is presented as normalized to a value identified as the optimized concentration. Concentration rate was increased incrementally, while the effect on performance was noted for at least 4 hours. At very low concentrations a 60% decrease in outlet particle loading was measured. As the concentration was increased, the cleaning frequency decreased and further reductions in outlet emissions occurred. At two times the screening test concentration, the time between cleans was 5 times greater and the outlet emissions were 99% less that baseline conditions. These tests were very encouraging for several reasons: 1) performance improvement was directly proportional to additive concentration, 2) beneficial performance occurred at very low injected concentrations, and 3) response times to additive concentration changes were nearly immediate. After observing the effect on performance from the additives, it is believed that relatively low concentrations can be used and that the effect will improve over time.

Table 2. ADA-14 Bench-Scale Optimization Test Results

Normalized Concentrations	Cleaning Frequency decrease to baseline	Reduction in Emissions % change to baseline
0.25	No Change	No Change
0.5	No Change	60%
0.75	50-75%	60-99%
1.0	100%	60-99%
1.5	200%	80-90%
2.0	400%	99%

A new bag was used for step two in the optimization process. Additive injection was begun immediately at startup to document if improved performance could be realized on new bags. The injection rate was the normalized concentration of 1. The additive did not appear to have a detrimental effect on start-up performance, and this was considered the beginning of the long-term test. If additive injection at startup had appeared to cause problems, the bag would have been changed out and a baseline established before beginning the long-term tests.

Long Term Tests

Longer-term (one week) tests were run at the optimized conditions identified from the optimization tests. The objective of these tests were to observe the impact of continuous operation and flue gas fluctuations on additive performance. During the long-term tests, inlet and outlet mass tests were completed to quantify particulate collection efficiency. One additive was evaluated during the long-term test.

Long-term tests were performed using ADA-14 at a normalized additive-to-ash ratio of 1. The beginning of optimization step two marked the beginning of the long-term test. Additive injection was started within the first hour of exposure of the bag to flue gas. Figure 2 graphically compares the results from the long-term test to a baseline test in terms of time between cleans, post-clean pressure drop, Triboflow™ signal, and duct temperature. A total of 140 hours operation were obtained. An interpretation of these results follows:

- In general, the time between cleans was at least 2 times longer with additive injection. This value fluctuated with host boiler load conditions and when the injection nozzle plugged. For example, around 120 hours the load decreased significantly. This can be seen as a decrease in temperature. The time between cleans increased to nearly 8 times the baseline values. There are two phenomena occurring. First, the ash loading decreased (as documented earlier) thus reducing time between cleans. In addition, when the ash loading decreased the additive-to-ash ratio increased because the injection concentration was not changed. As shown in the optimization tests, improvement in baghouse performance is directly proportional to additive concentration.
- Outlet emissions, as measured by the Triboflow™ meter, were significantly lower when ADA-14 was injected. In general, the signal was 70% lower compared to baseline. Comparing Method 17 mass tests conducted during baseline testing and ADA-14 injection to the Triboflow™ signal resulted in a correlation factor of 0.92. Therefore, ADA-14 reduced outlet emissions by nearly an order of magnitude.
- During additive injection, the post-clean pressure drop quickly increased to 3.0 inches H_2O and appeared to stabilize below 4.0 inches H_2O. In comparison, the baseline data show that without additive injection the post-clean pressure drop increased more gradually at first, but continued to increase to a level nearly an inch greater than that with additives. This shows that the additive is forming a dustcake that has better cleaning properties. This lower post-clean pressure drop contributes to the increase in time between cleans with additive injection.
- Host duct temperature is presented because it was the only continuously monitored parameter that followed boiler load. This plot shows that boiler load was fairly similar between the baseline and long-term tests. This is important, because it would be difficult, if not impossible, to compare the two test periods if boiler load had been significantly different.

Conclusions

Bench-scale tests were performed on actual flue gas from an operating power plant with nine additives. The results from these tests showed that one additive, ADA-14, significantly improved baghouse performance by reducing both outlet emissions and cleaning frequency. Repeatable results were obtained through screening, optimization, and long-term tests. Testing also showed that plant make-up water (pond water) could be used as the carrier fluid and that ammonia injection did not interfere with ADA-14's beneficial properties.

Based on the excellent results with ADA-14, arrangements for a larger scale test, nominally 10 MW(e), are being pursued.

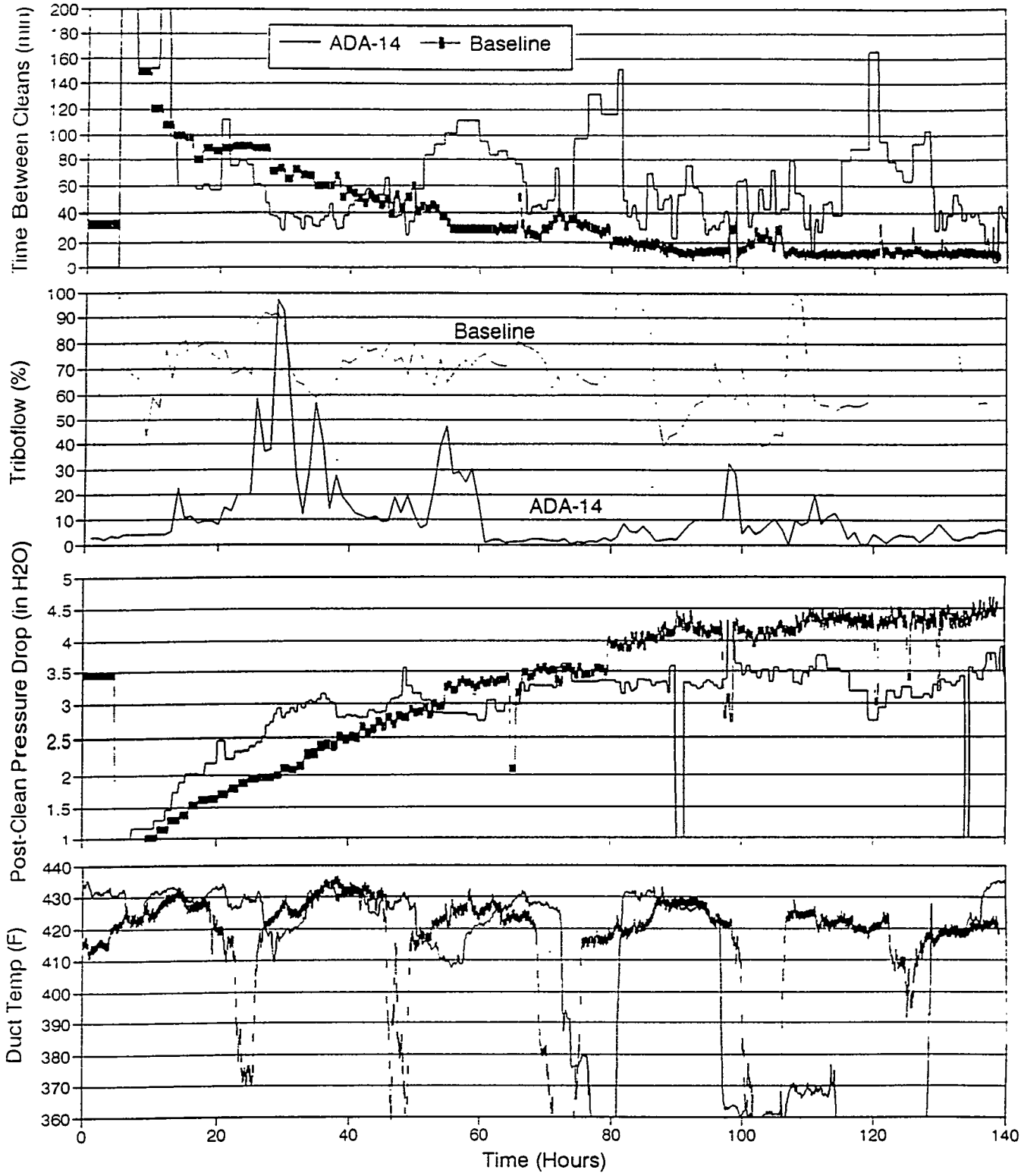

Figure 2. History of FTD performance during baseline and ADA-14 injection. All plots are trends of 5 minute averages except Triboflow™, which is a trend of 1 hour averages.